# Understanding the chitinolytic system of *Paenibacillus* sp. LS1 and advancing chitooligosaccharide bioproduction

Thesis submitted for the degree of **DOCTOR OF PHILOSOPHY (Ph.D.)** 

by **Saumashish Mukherjee**(Regd. No. 17LPPH08)



Department of Plant Sciences, School of Life Sciences, University of Hyderabad Hyderabad – 500046 India

September, 2024



### University of Hyderabad

(A Central University established in 1974 by an act of parliament) Hyderabad – 500046, India



#### **CERTIFICATE**

This is to certify that the thesis entitled "Understanding the chitinolytic system of *Paenibacillus* sp. LS1 and advancing chitooligosaccharide bioproduction" submitted by Saumashish Mukherjee bearing registration number 17LPPH08 in partial fulfilment of the requirements for the award of Doctor of Philosophy (Ph.D.) in the Department of Plant Sciences, School of Life Sciences, is a bonafide work carried out by him under my supervision and guidance.

This thesis is free from plagiarism and has not been submitted previously in part or in full to this or any other University or Institution for the award of any degree or diploma.

The student has the following publication(s) before submission of the thesis for adjudication and has produced evidence for the same in the form of acceptance letter or the reprint in the relevant area of his research:

- 1) **Mukherjee, S.**, Sarma, S. S., Rao, T. N. & Madhuprakash, J. (2024) The first evidence of cryo-milling improving enzymatic production of chitooligosaccharides from chitin biomass. *ChemRxiv*. <a href="https://doi.org/10.26434/chemrxiv-2024-q2g1v">https://doi.org/10.26434/chemrxiv-2024-q2g1v</a> (Preprint).
- 2) Yao, R. A., Reyre, J.-L., Tamburrini, K. C., Haon, M., Tranquet, O., Nalubothula, A., **Mukherjee, S.**, .... & Berrin, J.-G. (2023) The *Ustilago maydis* AA10 LPMO is active on fungal cell wall chitin, *Applied and Environmental Microbiology*. 89, e00573-23. <a href="https://doi.org/10.1128/aem.00573-23">https://doi.org/10.1128/aem.00573-23</a>
- 3) **Mukherjee, S.**, Lodha, T. D. & Madhuprakash, J. (2023) Comprehensive Genome Analysis of Cellulose and Xylan-Active CAZymes from the Genus *Paenibacillus*: Special Emphasis on the Novel Xylanolytic *Paenibacillus* sp. LS1, *Microbiology Spectrum*. 11, e05028-22. <a href="https://doi.org/10.1128/spectrum.05028-22">https://doi.org/10.1128/spectrum.05028-22</a>
- 4) Duhsaki, L., **Mukherjee, S.** & Madhuprakash, J. (2023) Improving the efficiency and sustainability of chitin bioconversion through a combination of *Streptomyces* chitinactive-secretomes and mechanical-milling, *Green Chemistry*. 25, 6832-6844. https://doi.org/10.1039/D3GC01084H
- 5) Duhsaki, L., **Mukherjee, S.**, Rani, T. S. & Madhuprakash, J. (2022) Genome analysis of *Streptomyces* sp. UH6 revealed the presence of potential chitinolytic machinery crucial for chitosan production, *Environmental Microbiology Reports*. 14, 431-442. https://doi.org/10.1111/1758-2229.12986 (equal first author)

6) **Mukherjee, S.**, Behera, P. K. & Madhuprakash, J. (2020) Efficient conversion of crystalline chitin to *N*-acetylglucosamine and *N*, *N*'-diacetylchitobiose by the enzyme cocktail produced by *Paenibacillus* sp. LS1, *Carbohydrate Polymers*. 250, 116889. <a href="https://doi.org/10.1016/j.carbpol.2020.116889">https://doi.org/10.1016/j.carbpol.2020.116889</a>

The student also has presented his work in the following conferences:

#### **Oral Presentations:**

- 1) **Mukherjee, S.** & Madhuprakash, J. The multi-modular chitinase-5 from *Paenibacillus* sp. LS1 effectively degrades crystalline chitin into *N*-acetyl-*D*-glucosamine and *N*,*N*-diacetylchitobiose. *12<sup>th</sup> Asian Community of Glycoscience and Glycotechnology* (*ACGG*) *Conference*, jointly organized by School of Life Sciences and School of Chemistry, University of Hyderabad from 8<sup>th</sup> Nov 11<sup>th</sup> Nov, 2023.
- 2) **Mukherjee, S.** & Madhuprakash, J. Efficient conversion of crystalline chitin to *N*-acetylglucosamine and *N*, *N'*-diacetylchitobiose by the enzyme cocktail produced by *Paenibacillus* sp. LS1. Invited *Mahesh Award lecture* at the *13<sup>th</sup> Plant Sciences Colloquium*, organized by Department of Plant Sciences, School of Life Sciences, University of Hyderabad on 29<sup>th</sup> Oct, 2021.
- 3) **Mukherjee, S.** & Madhuprakash, J. Insights into the chitin valorization by *Paenibacillus* sp. LS1. *National Conference on Frontiers in Plant Biology* (*NCFIPB*), organized by Department of Plant Sciences, School of Life Sciences, University of Hyderabad from 31st Jan 1st Feb, 2020.

#### Poster Presentations:

- 1) **Mukherjee, S.** & Madhuprakash, J. The multi-modular Chitinase-5 from *Paenibacillus* sp. LS1 efficiently converts crystalline chitin to chitooligosaccharides. *International Conference on Current Trends and Future Prospects of Plant Biology (CTFPPB)*, organized by Department of Plant Sciences, School of Life Sciences, University of Hyderabad from 23<sup>rd</sup> Feb 25<sup>th</sup> Feb, 2023.
- 2) **Mukherjee, S.** & Madhuprakash, J. Insights into the chitin-active repertoire of *Paenibacillus* sp. LS1 and its implication in chitooligosaccharides production. *International Conference on Frontier Areas of Science and Technology (ICFAST*), organized by Indian JSPS Alumni Association (IJAA) and School of Physics, University of Hyderabad from 09<sup>th</sup> Sept. 10<sup>th</sup> Sept, 2022.
- 3) **Mukherjee, S.,** Behera, P.K., Rani, T.S., & Madhuprakash, J. *Paenibacillus* sp. JM-1: A potential target for chitin valorization. *8<sup>th</sup> Indian Chitin and Chitosan Society* (*ICCS*) *Symposium*, organized by Institute of Chemical Technology, Mumbai from 19<sup>th</sup> Sept 20<sup>th</sup> Sept, 2019.
- 4) **Mukherjee, S.,** Behera, P.K., Rani, T.S., & Madhuprakash, J. Chitin valorization using the enzyme-cocktail produced by *Paenibacillus* sp. JM-1. *59th Annual Conference of Association of Microbiologists of India (AMI) and International Symposium on Host-Pathogen Interactions*, organized by Department of Plant Sciences, School of Life Sciences, University of Hyderabad from 9<sup>th</sup> Dec. 12<sup>th</sup> Dec, 2018.

Further, the student has passed the following courses towards fulfilment of coursework requirement for Ph.D.:

<b>Course Code</b>	Name	<b>Credits</b>	Result
PL801	Research Methodology/Analytical Techniques	4.0	Pass
PL802	Research Ethics, Biosafety, Data Analysis and Biostatistics	4.0	Pass
PL803	Scientific Writing and Research Proposal	4.0	Pass

**Supervisor** 

Dr. J. Madhuprakash
Assistant Professor
Dept. of Plant Sciences
School of Life Sciences
University of Hyderabad
Hyderabad-500 046, INDIA

Head of the Department

Dept. of Plant Sciences School of Life Sciences University of Hyderabad Hyderabad-500 046. INDIA Dean of School

संकाय अध्यक्ष / Dean जीव विज्ञान संकाय / School of Life Sciences हैदराबाद विश्वविद्यालय / University of Hyderabad हैदराबाद / Hyderabad-500 046.



### University of Hyderabad

(A Central University established in 1974 by an act of parliament) Hyderabad – 500046, India



#### **DECLARATION**

I, Saumashish Mukherjee, hereby declare that this thesis entitled "Understanding the chitinolytic system of Paenibacillus sp. LS1 and advancing chitooligosaccharide bioproduction" submitted by me under the supervision and guidance of Dr. Jogi Madhuprakash is a bonafide research work and is plagiarism free. I also declare that it has not been submitted previously in part or in full to this University or any other University or Institution for the award of any degree or diploma.

Supervisor

Dr. J. Madhuprakash Assistant Professor Dept. of Plant Sciences School of Life Sciences University of Hyderabad Hyderabad-500 046, INDIA Saumashish Mukherjee Regd. No. 17LPPH08

Date: 23.09.24

I am grateful to every individual who has helped me and/or stayed by my side in this journey. This achievement of my life would never have been possible without them.

At the outset, I would like to extend my gratitude to my supervisor, *Dr. Jogi Madhuprakash* for his rigorous training, strong support and constant motivation towards achieving my research objectives. I am a better and focussed individual today, all thanks to him. It was challenging being his first student as there were so many responsibilities to take care of, but his strong belief in me was the fuel to keep me going. His zeal and love towards science (particularly in his areas of research interest) has always been my motivation throughout my Ph.D. journey and I hope that I can keep working with the same zeal and interest towards my future endeavours.

I am grateful to *Prof. Santosh R. Kanade*, our lab's in-charge during *Dr. Madhuprakash's* sabbatical leave, for his kindness and support in all possible ways, whenever it was required.

I thank the former Deans of School of Life Sciences, *Prof. N. Sivakumar*, *Prof. S. Dayananda*, *Prof. K.V.A. Ramaiah*, *Prof. M.N.V. Prasad* and *Prof. P. Reddanna* and the present Dean, *Prof. Anand K. Kondapi* and former Heads of the Department of Plant Sciences, *Prof. G. Padmaja* and *Prof. Ch. Venkata Ramana*, and the present Head, *Prof. S. Rajagopal*, for allowing me to use the school as well as departmental facilities for my research work.

I thank my doctoral research committee members, *Prof. Ch. Venkata Ramana* and *Dr. K. Gopinath*, for their encouragement, support and valuable suggestions towards my research work.

My heartfelt gratitude goes to all those faculty members of University of Hyderabad (UoH), who extended their lab facilities to me for my research work. I am extremely thankful to *Prof. Appa Rao Podile*, *Dr. K. Gopinath* and *Prof. Rahul Kumar* (Department of Plant Sciences, School of Life Sciences, UoH), *Prof. R. Koteswararao* (SEST, UoH) and *Dr. T. Saravanan* (School of Chemistry, UoH) for allowing me to use their lab facilities.

Special thanks to *Prof. Ch. Venkata Ramana* for providing environmental samples to our lab for the screening of chitinolytic bacteria. I thank *Dr. Pavel Kerchev* and *Dr. Martin Černý* from Mendel University in Brno, Czechia for helping us obtaining the secretome data for *Paenibacillus* sp. LS1. I am grateful to *Prof. Dr. Bruno Moerschbacher* and *Dr. Stefan Cord-Landwehr* from University of Münster, Münster, Germany for helping us with F<sub>A</sub> analysis of the chitin samples. I thank *Prof. Tushar Jana* from School of Chemistry, UoH, for allowing access to the BET facility. I am grateful to *Dr. Tushar D. Lodha* for his help with the genome sequencing of *Paenibacillus* sp. LS1 at the NCCS-National Centre for Microbial Resource, Pune, India. I am indebted to *Dr. T. Swaroopa Rani* for her support and valuable suggestions towards my research work. I thank *Dr. Tata Narasinga Rao* and *Mr. S. Sudhakara Sarma* for their help with cryo-milling of chitin.

My sincere gratitude to all the non-teaching staff of the Department of Plant Sciences and School of Life Sciences, UoH.

I thank the instrumentation facilities at both the Department and School level for their assistance in my research. I also extend my gratitude towards the XRD facility at School of Physics, the FT-IR facility at the DRDO Industry Academia - Centre of Excellence (DIA-CoE; formerly, ACRHEM) and the BET facility at School of Chemistry, UoH, for their assistance with substrate characterisation of the chitin samples.

I thank DST-INSPIRE, SERB-CRG, CSIR-HRDG and UoH-IoE for funding to our lab. I also thank UGC-SAP, DST-PURSE, DST-FIST and DBT-SAHAJ for funding to the Department of Plant Sciences. I am grateful to UoH-BBL and SERB-CRG for providing my fellowship.

Words fail to express my gratitude and love for my labmates, Ms. Koyel Bardhan, Ms. Vandhana TM, Ms. Lalduhsaki and Mr. N. Akshay. They have been my strongest support in the lab and beyond. They were always there for me at my highest as well as my lowest. Koyel and Vandhana are my sisters, with whom I share a deep, unbreakable bond on a personal level. I cannot count the endless memories that we have together, which might become a book in itself if I start writing about them. When it comes to work, Vandhana has helped me intensively with crystallization of Chi3 (I cannot even count the number of plates that she has setup for the same!!), while Koyel and I, have worked together on a different project. Akshay is my brother, who has been by my side since his M.Sc. project days. Be it admin work or my research work, he was always there. Despite being a beginner, he gave his best for the knockouts work for Paenibacillus sp. LS1 and I always acknowledge him for that. We also had several conflicts over these years, but those had only made our bond stronger. Last but not the least, a few words for *Lalduhsaki*, or simply *Saki* for us. She is a perfect example of a researcher, who is quick and efficient, which I believe is a rare trait. She is someone who I looked up to during my Ph.D. tenure, when it comes to efficiency while handling multiple projects. All of my labmates have the potential to do excellent in life, if given suitable opportunities. All I have for them, are best wishes.

I am deeply grateful to my senior and former labmate, *Mrs. Bhavana Karlapudi*. She not taught only me the basic techniques in lab, but was also my strongest support and shield. Further, I would also convey my heartfelt gratitude to all the former project students of the lab: *Mr. Prashanta Kumar Behera*, *Ms. N. Mounika*, *Ms. Sreya Ghosal*, *Mrs. M. Hemanjali*, *Mrs. G. Haritha*, *Mr. Arkaprabha Adhikari*, *Ms. Stuti Srivastava*, *Mr. Nitya Nandan Sharma*, *Ms. Prajakta M. Tarnekar*, *Ms. Shweta Pathak* and *Mr. Aditya Raj*. All of them were unique in their own respect and it was great knowing and working with them.

I am indebted to my friends, who are family to me: *Mr. Supriya Laha*, *Mr. Arpan Chatterjee*, *Mr. Ayon Chatterjee*, *Mr. Prodosh Gupta* and *Mr. Abhishek Roychowdhury*. Surviving Ph.D. at UoH would have been very difficult without them. They laughed with me at times of joy, shared my sorrows during hard times, took care of me when I was sick, loved me from the core of their hearts and criticised me when needed. In short, they are my lifelines. *Supriya* and I have known each other

for 9 years now, but we became soul-brothers only after coming to UoH. He is my brother, roommate and local guardian, and I cannot imagine a life without him at UoH. Ayon and Arpan, the twins, are two of the most important characters of my Ph.D. journey. They have always taught me to be thoughtful towards the different decisions that I take in life. Not only that, they always ensured that I actually execute those decisions into reality. Prodosh da, my big brother, is my partner in crime in many things. I have always admired him for his ability to keep himself normal, even in highly stressful situations. To me, he is the great example of "patience my friend!! your hard work will not go in vain". Last but not the least, Abhishek, our youngest brother. The only word that comes to my mind when I take his name, is "balance". He has this amazing ability to balance his work and personal life extremely well, which to me, is a great thing to learn for anybody, particularly in the world of academia. Proudly, all my friends are excellent budding researchers in their own fields, with the capability of becoming the absolute best in future.

I also extend my love and gratitude to *Mr. Arkaprabha Adhikari (Bulu)*, my younger brother at UoH. I am thankful to him for making me understand the role of discipline in every aspect of life, for motivating me and for making me believe that I too can be a role model to someone. He is one of the best minds that I have ever met in my life and I believe he is destined to go long distances in the field of cancer biology or wherever he gives his heart into. I am also thankful to my sister and *Arkaprabha's* partner, *Ms. Anupriya Shekhar* for her constant support and love. My love and gratitude also go to *Mr. Amrit Chattopadhyay*, *Mr. Arnab Das*, *Mr. Ankur Chatterjee* and *Mr. Suvajit Basu*, for their love, support and belief in me.

I always say that I might not have earned good amount of money during my Ph.D., but I have certainly earned people, who I call my friends. I am thankful to my friends from SLS: *Dr. Rajat Srivastava*, *Dr. Akash*, *Dr. Dushyant Kumar Gautam*, *Ms. Akanksha Tripathi*, *Dr. Surabhi Lata*, *Mrs. Sumi Rana*, *Mrs. Baby Kumari*, *Ms. Sruchytha Kalali*, *Mr. Satyajit Mukherji*, *Mr. Shrey Trehan*, *Ms. Dipanita Biswas* and *Ms. Sujata Mishra*. SLS has also given me my sisters, *Ms. Ritwika Mohinta*, *Ms. Debanjana Roy* and *Ms. Kritika Chauhan* and I am grateful to them for their love and support. I am also grateful to my senior, *Dr. Mouboni Dutta* for her support whenever I approached her for suggestions or advice.

A small dedication to my beloved dogs in the campus (my four-legged wonders). Thank you for loving me unconditionally and letting me love you all. I used to forget all my stress just by looking at their faces. They are my saviours, my wingless angels.

I believe that no matter what we do in life, we can never ever repay our parents for their love, cooperation, motivation and sacrifices. You don't say thank you to your parents, but stay eternally grateful to them. My mother, *Mrs. Mita Mukherjee*, had dreamt of seeing me successful in life. Even though, she is not there with me physically today, her soul is always there by my side. I wish she is proud of me today and I seek her blessings for the future. When it comes to my father, *Mr. Sambhu* 

*Nath Mukherjee*, nothing can compare to the sacrifices that he has made for me. He is my biggest support and my biggest critic. He is someone that I have been looking up to since my childhood and I still look up to him to this date. Without his support, my Ph.D. journey might have ended long ago. Making him proud and happy, is my greatest achievement and my ultimate goal.

I am extremely grateful to my partner and would-be fiancée, *Ms. Sangjukta Roy*. I always say, any other woman might have left me long ago, if it wasn't her. She has been by my side from the beginning of my Ph.D. journey. She has seen it all and never left me stranded in my worst times. She too has sacrificed a lot and compromised for me on several situations. My journey would be incomplete without her love and dedication, and her belief and support.

I also extend my gratitude to my friends and family back home. I am extremely thankful to my sister, *Mrs. Sayani Bandyopadhyay* for her love and support.

Last but not the least, I believe nothing in this world happens without god's will. My sincere prayers to *Mahadev*, *Maa Kali*, *Lokenath Baba* and *Hanuman ji* for their blessings. I am indebted to them and shall always be.

Saumashish Mukherjee



Dedicated to my grandparents, parents, Sangjukţa and my dogs

# **Table of Contents**

Contents	Page Number
List of Abbreviations	i-iv
List of Figures	v-viii
List of Tables	ix
Chapter-1: Introduction	1-15
Chapter-2: Deciphering the genomic and proteomic insights of chitin degradation by <i>Paenibacillus</i> sp. LS1	16-38
Chapter-3: Molecular characterization of selected chitinases from <i>Paenibacillus</i> sp. LS1	39-67
Chapter-4: Development of a bioprocess for efficient and selective production of GlcNAc and (GlcNAc) <sub>2</sub> directly from chitin	68-87
Chapter-5: Summary and Conclusion	88-92
References	93-100

**Abbreviation Full Form** Å

ANI Average Nucleotide Identity

Angstrom

Bicinchoninic acid **BCA** 

**BET** Brunauer-Emmett-Teller

bp Base pair(s)

**BMIA** 1-butyl 3-methyl imidazolium acetate ([BMIm]Ac)

°C degree Celsius

CAZy/CAZymes Carbohydrate Active enZymes Carbohydrate Binding Module **CBM** 

CCColloidal chitin

**CDS** Coding sequence(s)

**CGC** CAZyme gene cluster(s)

CHOS or NA-CHOS Chitooligosaccharides or N-acetyl chitooligosaccharides

CE Carbohydrate Esterase

Centimetre(s) cm CM Cryo-milled

CM-cellulose Carboxymethyl-cellulose

Copper amine oxidase-like N-terminal domain CuAO

CVColumn volume

DA Degree of acetylation

Database for automated Carbohydrate-active enzyme and substrate

dbCAN

**ANnotation** 

**DDA** Degree of deacetylation **DDBJ** DNA Databank of Japan DDH **DNA-DNA** Hybridization **DNA** Deoxyribonucleic acid

DP Degree of Polymerization

dsDNA Double-stranded deoxyribonucleic acid

DTT Dithiothreitol

EC **Enzyme Commission number EDTA** Ethylenediaminetetraacetic acid

1-ethyl-3-methylimidazolium acetate ([EMIm]Ac) **EMIA** 

ENA European Nucleotide Archive

ESI-MS Electrospray Ionization-Mass Spectrometry

 $F_A$  Fraction of acetylation

FAIMS High field asymmetric waveform ion mobility spectrometry

FE-SEM Field emission-scanning electron microscopy

g Gram(s)

g/L Grams per litre

GGDC Genome-to-Genome Distance Calculator

GH Glycoside Hydrolase

GlcN Glucosamine

GlcNAc N-acetyl-D-glucosamine

(GlcNAc)<sub>2</sub> N,N-diacetylchitobiose

(GlcNAc)<sub>3</sub> N,N,N-triacetylchitotriose

 $(GlcNAc)_4$  N,N,N,N-tetraacetylchitotetraose

(GlcNAc)<sub>5</sub> *N,N,N,N,N*-pentaacetylchitopentaose

(GlcNAc)<sub>6</sub> N,N,N,N,N-hexaacetylchitohexaose

GT Glycosyl Transferase

h Hour(s)

HILIC Hydrophilic Liquid Interaction Chromatography

HPLC High-Performance Liquid Chromatography

I<sub>CR</sub> Crystallinity Index

IL Ionic Liquid
IL-6 Interleukin-6

IPTG Isopropyl β- d-1-thiogalactopyranoside

K Kelvin

kDa Kilodalton(s)

kV Kilovolt
L Litre(s)

LB Luria Bertani

LFQ Label Free Quantification

m/z Mass per charge number of ions

M Molar

Mb Megabase

mg/g Milligram(s) per gram

min Minute(s)
mL Millilitre

mL/min Millilitre(s) per minute

mMMillimolar Millimetre mm Microgram μg Microlitre μL Micromolar  $\mu$ M Micrometre μm Micromole μmol N Normal

NCBI National Center for Biotechnology Information

ncRNA Non-coding ribonucleic acid

nm Nanometre

NO Nitric Oxide

OD Optical density

PAGE Polyacrylamide gel electrophoresis

PCR Polymerase chain reaction

PDB Protein Data Bank
PF Periplasmic fraction
PL Polysaccharide Lyase

pM picomolar

PMSF Phenylmethylsulfonyl fluoride

PUL Polysaccharide Utilization Locus (Loci)

pXRD Powder X-ray diffraction

RAST Rapid Annotations using Subsystems Technology

RefSeq Reference Sequence Database

RNA Ribonucleic acid

ROS Reactive Oxygen Species

rpm Revolutions per min

rRNA Ribosomal ribonucleic acid

s Second(s)

S<sub>BET</sub> BET surface area

SDS Sodium dodecyl sulphate

SDS-PAGE Sodium dodecyl sulphate-polyacrylamide gel electrophoresis

SEM Scanning electron microscopy

SLH S-layer homology domain

1-sulfobutyl 3-methyl imidazolium hydrosulfate

SMIH ([BHSO<sub>3</sub>MIm]HSO<sub>4</sub>)

SPE Solid phase extraction

TCA Trichloroacetic acid

TIM Triosephosphate Isomerase

TNF-α Tumor Necrosis Factor - Alpha

tRNA Transfer ribonucleic acid

U Enzyme Units

UM Unmilled

UPLC Ultra Performance Liquid Chromatography

V Volts

v/v Volume by volume w/v Weight by volume

Chapter Number	Figure Number	Figure Legend	Page Number
Chapter 1	Figure 1	Chitin structure and its sources	2
	Figure 2	Chain orientation in polymorphs of chitin and hydrogen bond structure in $\alpha$ -chitin.	4
	Figure 3	Diversity and functionalities of GH18 chitinases across the tree of life.	9
	Figure 4	The general catalytic mechanism of a GH18 chitinase ( <i>Sm</i> ChiB in this case).	11
	Figure 5	Morphology of and chitin degradation by <i>Paenibacillus</i> sp. LS1.	14
	Figure 6	Phylogenetic analysis of <i>Paenibacillus</i> sp. LS1.	14-15
Chapter 2	Figure 7	Growth of <i>Paenibacillus</i> sp. LS1 on various chitin substrates.	25
	Figure 8	Cell growth and chitinase activity analysis.	26
	Figure 9	Detection of chitinase isozymes by semi-native PAGE.	27
	Figure 10	FE-SEM analysis of $\alpha$ -chitin treated with <i>Paenibacillus</i> sp. LS1.	28
	Figure 11	FE-SEM analysis of $\beta$ -chitin treated with <i>Paenibacillus</i> sp. LS1.	28
	Figure 12	Distribution of genes among 26 subsystem categories in the annotated of genome of <i>Paenibacillus</i> sp. LS1 by the Rapid Annotation using Subsystem Technology (RAST) server.	29
	Figure 13	Family-wise distribution of different CAZyme classes in the genome of <i>Paenibacillus</i> sp. LS1.	31
	Figure 14	Arrangement of the chitinase genes in the genome of <i>Paenibacillus</i> sp. LS1.	32
	Figure 15	Schematic representation of the domain organization of the predicted GH18 family proteins in <i>Paenibacillus</i> sp. LS1.	34
	Figure 16	Heatmap of secreted CAZymes from <i>Paenibacillus</i> sp. LS1.	36

	Figure 17	Heatmap of secreted substrate-binding proteins of the different transporter systems encoded by <i>Paenibacillus</i> sp. LS1.	38
Chapter 3	Figure 18	Structure-based sequence alignment of the GH18 family proteins from <i>Paenibacillus</i> sp. LS1.	47
	Figure 19	Cloning and over-expression of GH18 family proteins of <i>Paenibacillus</i> sp. LS1.	50
	Figure 20	Optimal conditions for activity and steady-state kinetics of Chi3.	52
	Figure 21	Substrate specificity of Chi3 on different chitin and non-chitin substrates.	52
	Figure 22	Optimal conditions for the activity of Chi5.	54
	Figure 23	Michaelis-Menten kinetics for Chi5 on CC (A) and $\beta$ -chitin (B).	55
	Figure 24	Substrate specificity of Chi5 on different chitin and non-chitin substrates.	56
	Figure 25	Hydrolytic activity of Chi3 on CHOS.	58
	Figure 26	Schematic representation depicting the mode of action of Chi3 on (GlcNAc) <sub>3</sub> (A), (GlcNAc) <sub>4</sub> (B), (GlcNAc) <sub>5</sub> (C) and (GlcNAc) <sub>6</sub> (D) as the substrate.	59-60
	Figure 27	Hydrolytic activity of Chi5 on CHOS.	61
	Figure 28	Schematic representation depicting the mode of action of Chi5 on (GlcNAc) <sub>4</sub> (A), (GlcNAc) <sub>5</sub> (B) and (GlcNAc) <sub>6</sub> (C) as the substrate.	63
	Figure 29	Hydrolytic activity of Chi3 on crystalline chitin substrates.	64
	Figure 30	Hydrolytic activity of Chi5 on various crystalline chitin substrates.	66
Chapter 4	Figure 31	Crude $\alpha$ -chitin used in the present study.	74
	Figure 32	Characterization of cryo-milled (CM) and IL-treated un-milled (UM) α-chitin substrates.	75

Figure 33	pXRD analysis of cryo-milled $\alpha$ -chitin substrates treated with ionic liquids.	79
Figure 34	Characterization of un-milled (UM) and differentially pre-treated crude $\alpha$ -chitin substrate by FTIR (A and B), pXRD (C) and BET analysis (D).	80
Figure 35	Average fraction of acetylation ( $\bar{x}$ $F_A$ ) in the unmilled (UM) and different pre-treated $\alpha$ -chitin samples (UM+BMIA, CM and CM+BMIA).	81
Figure 36	Time-course of GlcNAc and (GlcNAc) <sub>2</sub> production from unmilled (UM), BMIA pretreated UM (UM+BMIA), cryo-milled (CM) and BMIA pre-treated CM (CM+BMIA) crude $\alpha$ -chitin substrates using 1 $\mu$ M Chi5 from <i>Paenibacillus</i> sp. LS1, in presence or absence of 1 $\mu$ M <i>Ec</i> LPMO from <i>E. cloacae</i> MCC 2072.	83
Figure 37	Time-course of GlcNAc production from unmilled (UM), BMIA pre-treated UM (UM+BMIA), cryo-milled (CM) and BMIA pre-treated CM (CM+BMIA) crude α-chitin substrates using 1 μM Chi3 from <i>Paenibacillus</i> sp. LS1, in presence or absence of 1 μM <i>Ec</i> LPMO from <i>E. cloacae</i> MCC 2072.	84
Figure 38	Time-course of GlcNAc and (GlcNAc) <sub>2</sub> production from unmilled (UM), BMIA pretreated UM (UM+BMIA), cryo-milled (CM) and BMIA pre-treated CM (CM+BMIA) crude α-chitin substrates using 1 μM <i>Str</i> ChiA from <i>Streptomyces</i> sp. UH6, in presence or absence of 1 μM <i>Ec</i> LPMO from <i>E. cloacae</i> MCC 2072.	85
Figure 39	Time-course of (GlcNAc) <sub>2</sub> , (GlcNAc) <sub>3</sub> and (GlcNAc) <sub>4</sub> production from unmilled (UM), BMIA pre-treated UM (UM+BMIA), cryo-milled (CM) and BMIA pre-treated CM (CM+BMIA) crude α-chitin substrates using 1 μM <i>Ca</i> GH18 from <i>Chitinispirillum alkaliphilum</i> DSM 24539, in presence or absence of 1 μM <i>Ec</i> LPMO from <i>E. cloacae</i> MCC 2072.	86
Figure 40	Proposed pathway for chitin degradation and metabolism in <i>Paenibacillus</i> sp. LS1.	90

Chapter-5

Figure 41 Schematic representation of the proposed 92 bioprocess for efficient production of chitooligosaccharides from crude  $\alpha$ -chitin.

# **List of Tables**

Chapter Number	Table Number	Table Description	Page Number
Chapter 1	Table 1	OrthoANIu and <i>in silico</i> DDH values for <i>Paenibacillus</i> sp. LS1 compared against its phylogenetic neighbours	30
Chapter 3	Table 2	List of primers used for the cloning of chitinases from <i>Paenibacillus</i> sp. LS1.	41
	Table 3	Optimised over-expression conditions for Chi3 and Chi5.	50
	Table 4	Kinetic parameters of purified Chi5 (0.5 $\mu$ M) from <i>Paenibacillus</i> sp. LS1 obtained over CC and $\beta$ -chitin under similar assay conditions.	55
Chapter 4	Table 5	Crystallinity Index ( $I_{CR}$ ) of the un-milled and pre-treated $\alpha$ -chitin substrates determined by pXRD.	76
	Table 6	$S_{BET}$ analysis of the un-milled and pretreated $\alpha$ -chitin substrates.	77
	Table 7	Yields of different CHOS products (represented as mg/g of chitin) and chitin conversion efficiency (in %) obtained after 48 h of reaction, over unmilled and different pretreated crude α-chitin substrates upon hydrolysis with different chitinases in absence or presence of <i>Ec</i> LPMO.	87

# **Chapter-1**Introduction

### 1.1 From waste-to-value: shellfish waste as a rich source of chitin

To address the escalating food demands of our expanding population, there has been a corresponding surge in the demand for seafood, leading to a rapid expansion of the seafood industry. This growth, however, has resulted in the generation of substantial quantities of shell waste, with approximately 60-70% of the total weight of crustaceans being discarded as such waste (Yan & Chen, 2015; Hamed *et al.*, 2016; Duhsaki *et al.*, 2022). Globally, an estimated 6-8 million tonnes of shell waste are produced annually, with 1.5 million tonnes originating from Southeast Asia alone, often ending up being incinerated or dumped into the environment, thereby contributing to pollution (Yan & Chen, 2015). Notably, these shell wastes are rich in chitin, with varying content among different crustacean species, ranging from 60-75% in lobsters to 18% in prawns, presenting an opportunity for their conversion into value-added products (Hamed *et al.*, 2016). Chitin, a natural homopolymer consisting of *N*-acetyl-D-glucosamine (GlcNAc) monomers linked by  $\beta$ -1,4-glycosidic bonds, ranks as the second most abundant biopolymer in nature, surpassed only by cellulose. It serves as the primary structural component in the exoskeletons of arthropods and crustaceans, as well as in the cell walls of fungi (Aam *et al.*, 2010; Duhsaki *et al.*, 2023).

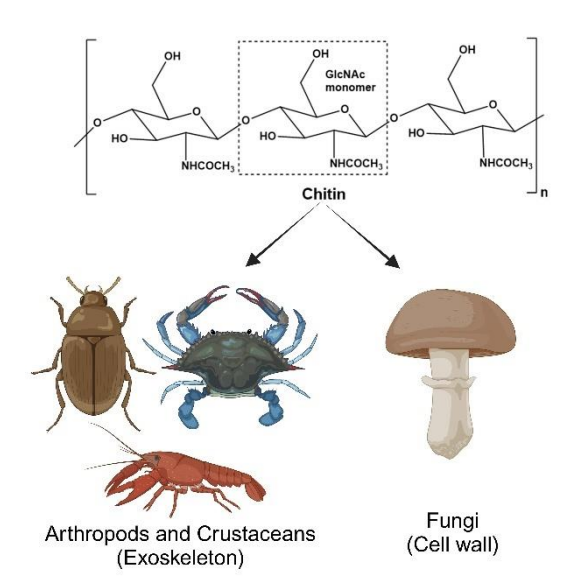


**Figure 1:** Chitin structure and its sources. Chitin is a homopolymer of GlcNAc residues (marked in the structure) derived from exoskeleton of arthropods and crustaceans and from cell walls of fungi. Chemical structure of chitin has been taken from Schmitz *et al.* (2019). This figure was prepared using BioRender (BioRender.com).

### 1.2 Chitooligosaccharides and their applications

Chitin can be valorized into low molecular weight products such as GlcNAc, *N*,*N*-diacetylchitobiose [(GlcNAc)<sub>2</sub>] and *N*-acetyl chitooligosaccharides (NA-CHOS or CHOS) of

varying degree of polymerization (DP). These chitin products exhibit significant commercial value due to their biodegradability, biocompatibility, and non-toxic properties (Cao et al., 2022; Duhsaki et al., 2023; Mukherjee et al., 2020; Rani et al., 2020). Among the major products derived from chitin valorization are GlcNAc and [(GlcNAc)2], which hold significant commercial importance in the realms of food and medicine. GlcNAc serves as a food additive known to enhance synovial fluid synthesis and skin hyaluronic acid content (Cao et al., 2022). Additionally, as a food supplement, GlcNAc has been shown to alleviate symptoms associated with hepatitis and diabetes (Cao et al., 2022). On the other hand, (GlcNAc)<sub>2</sub> can be utilized as an antimicrobial coating for food materials, prolonging their shelf life by inhibiting the growth of foodborne pathogens during storage (Abidin et al., 2023). Moreover, (GlcNAc)<sub>2</sub> exhibits anti-inflammatory properties, capable of reducing the levels of various pro-inflammatory mediators such as IL-6, TNF-α, NO, and ROS, and has been proposed as a potential functional food ingredient to ameliorate metabolic disorders associated with type-2 diabetes (Liu et al., 2023; Wu et al., 2017). Additionally, CHOS (a mixture of (GlcNAc)<sub>1-6</sub>) has been identified as a potential anti-tumor functional food, demonstrating the ability to suppress tumor growth, induce apoptosis in tumor tissues, and enhance innate immunity upon oral administration (Masuda et al., 2014). Further, chitin oligosaccharides (\ge DP4) have been reported for their elicitor activities in different plant defence mechanisms. Barber et al. (1989) reported elicitor activity of (GlcNAc)<sub>4-6</sub> resulting in lignification in wounded wheat leaves. While, in a different study, application of very low concentration (10 pM) of (GlcNAc)<sub>4-6</sub> was reported to elicit extracellular alkalinization and protein phosphorylation in tomato cell suspension culture (Felix et al., 1993). Collectively, these findings underscore the significance of GlcNAc and (GlcNAc)<sub>2</sub> and also CHOS, in the realm of nutraceuticals and agriculture, respectively, highlighting the need for optimized production methods through efficient and sustainable approaches for chitin valorization.

### 1.3 Chitin types: $\alpha$ - and $\beta$ -chitin

In nature, chitin mainly exists as two allomorphs namely,  $\alpha$ - and  $\beta$ -chitin. The  $\beta$ -chitin is a rarer form of chitin mostly derived from squid pens (Rinaudo, 2006). It is also found in the tubes synthesized by pogonophoran and vestimetiferan worms, aphrodite chaetae, in the lorica formed by few seaweeds or protozoa and in the monocrystalline spines excreted by *Thalassiosira fluviatilis* (Rinaudo, 2006). In  $\beta$ -chitin, the sugar chains are arranged in parallel orientation in the same direction (Figure 2A), comprising of only intra-sheet and no intersheet hydrogen bonds (Cao *et al.*, 2022). Contrary to  $\beta$ -chitin,  $\alpha$ -chitin is the most prevalent

and crystalline form, found in the exoskeleton of arthropods such as crustacean shells and insect epidermis, as well as in the fungal cell walls (Rinaudo, 2006; Cao *et al.*, 2022). The high degree of crystallinity in  $\alpha$ -chitin is conferred by the tightly packed anti-parallel chains (Figure 2B) due to the presence of both inter- and intra-sheet hydrogen bonds (Figure 2C) (Cao *et al.* 2022; Duhsaki *et al.*, 2023). These characteristics make  $\alpha$ -chitin resistant to degradation, thereby hindering efficient valorization for CHOS production.

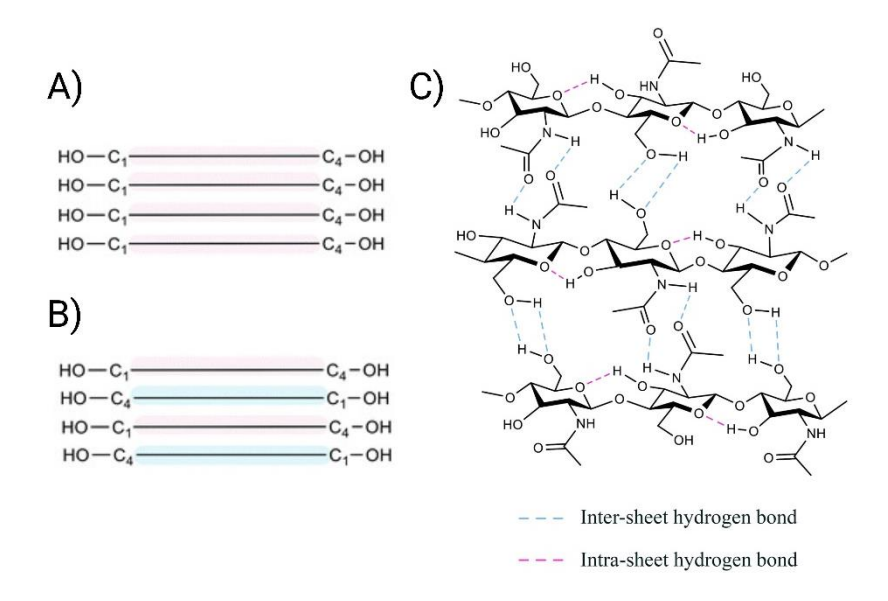


**Figure 2:** Chain orientation in polymorphs of chitin and hydrogen bond structure in α-chitin. A and B represents parallel and anti-parallel chain orientation in β- and α-chitin. C represents the inter- and intra-sheet hydrogen bonding in α-chitin. The individual figures have been taken from Cao *et al.* (2022) and arranged together using BioRender (BioRender.com).

### 1.4 Methods of CHOS production: preference towards enzymatic method

Since α-chitin is the most abundant allomorph in nature, it is the most sought-after raw material for production of CHOS. CHOS production directly from chitin can be mediated by either chemical (concentrated acid/alkali-mediated hydrolysis) or biological methods (microbial chitin-active enzymes). While there was a major dependence on chemical methods in the past, they are least preferred in the current times due to the major drawbacks associated with them. Not only are they harmful to the environment, but they also require anti-corrosion equipment and/or complex acidic waste discard strategies, leading to low economic competitiveness (Cao *et al.*, 2022). In addition to this, chemical methods are also difficult to control and results in production of a mixture of CHOS along with unwanted by-products (might be toxic), which may complicate the CHOS purification procedures (Kaczmarek *et al.*, 2019; Kumar *et al.*, 2020). In order to avoid the hassles and drawbacks associated with chemical methods, the preference has shifted towards biological (enzymatic) approaches.

This approach is mild, environment friendly and promotes selectivity towards the generation of desired products – GlcNAc, (GlcNAc)<sub>2</sub> or CHOS of desired DP, by use of specific enzyme(s).

### 1.5 Pre-treatment of chitin is necessary for efficient valorization

While enzymatic chitin valorization is effective and eco-friendly, it demands a substantial enzyme load to enable the efficient hydrolysis of such highly crystalline substances, resulting in elevated process costs (Cao et al., 2022). Pre-treatment of a biopolymer (such as chitin) prior to enzymatic hydrolysis, is an effective approach that induces alterations within the polymer structure which in turn, reduces crystallinity. Pre-treatment mainly disrupts the intrinsic hydrogen bonding within the chitin polymer, which reduces the overall compactness and rigidity of the polymeric structure. This makes the GlcNAc chains in the polymer, more accessible and susceptible to enzymatic hydrolysis, therefore, enhancing CHOS yields (Duhsaki et al., 2023; Zhang, A. et al., 2021). Consequently, integrated strategies like mechano-enzymatic (Duhsaki et al., 2023; Liu, Y. et al., 2020; Nakagawa et al., 2013), chemo-enzymatic (Zhang, A. et al., 2021; Berton et al., 2018; Xu et al., 2018; Husson et al., 2017) or a combination of these approaches are in high demand. These approaches mainly involve mild pre-treatment of crystalline chitin using mechanical (milling) or chemical (alkali or ionic liquids) methods, followed by enzymatic hydrolysis to improve overall CHOS yields, particularly GlcNAc and (GlcNAc)<sub>2</sub> (Duhsaki et al., 2023).

#### 1.5.1 Chemical pre-treatment methods

Among the chemical pre-treatment methods, use of alkali/alkali-urea solvent systems are well known for chitin amorphization/dissolution without affecting degree of acetylation (DA). In a study reported by Sivaramakrishna *et al.* (2020), pre-treatment of commercial α-chitin with different combinations of KOH/KOH-urea, led to alteration in chitin structure and reduction in crystallinity. Also, the pre-treatment resulted in significant increase in total CHOS production up to 10-25 -folds as compared to their untreated counterpart, upon hydrolysis with the uni-modular chitinase, *Ec*Chi1 (Sivaramakrishna *et al.*, 2020). In a different study, NaOH/KOH-mediated dissolution of commercial chitin via freeze-thaw method, resulted in reduction in crystallinity by 1.4-2.0 -folds and increase in surface area by 2.2-2.6 -folds, without affecting the chemical groups and DA (Zhang, A. *et al.*, 2021). The pre-treatment subsequently resulted in enhanced GlcNAc yield up to 14-16.5 -folds upon hydrolysis with the chitinase cocktail from *C. meiyuanensis* SYBC-H1 (Zhang, A. *et al.*, 2021). While, alkalibased pre-treatment of chitin is efficient, this method is time-consuming and might lead to

generation of unwanted by-products. Further, usage of strong bases such NaOH and KOH might pose problems of corrosion, tedious discard procedures and/or complex wastewater treatment (when applied at an industrial scale). These issues render this method, hazardous to the environment and lowers its overall economic competitiveness (Cao *et al.*, 2022).

As an alternative to hazardous solvents, use of green solvents such as ionic liquids for chitin dissolution/amorphization have become an attractive and eco-friendly option in the present times. Ionic liquids (ILs) are organic salts with melting temperature below 373K/100°C (Shamshina and Berton, 2020). They are defined as a large category of salts, that stay liquid at room temperature or at temperatures below 100°C, due to differences in their cation and anion sizes (Hessel et al., 2022). ILs are considered green solvents as per the 12 principles of Green Chemistry and possess significant properties such as thermal and chemical stability, negligible vapor pressure, low flammability and recyclability (Hessel et al., 2022). Cations such as ammonium, imidazolium, phosphonium and pyrrolidinium, with anions such as, acetate, amide, bis(trifluoromethane sulfonyl), halides and tetrafluoroborate are the most common choices for ILs in recent times (Hessel et al., 2022). ILs are highly tunable as their physicochemical properties can be altered as per requirement, by simply changing the type of cation and anion (Hessel et al., 2022). Further, IL utilizing reactions are carried out under less harsh conditions and have shorter reaction times (Shamshina and Berton, 2020). While extensive research has been done in line of IL-based chemo-enzymatic conversion of cellulose and lignocellulosic biomass, the same in case of chitin is still in its infancy (Shamshina and Berton, 2020). Use of ionic liquids as a pre-treatment agent for chitin was first demonstrated by Husson et al. (2017). In this study, they developed a chemoenzymatic bioprocess comprising of IL-based pretreatment of commercial chitin, followed by enzymatic hydrolysis for obtaining improved yields of GlcNAc and (GlcNAc)<sub>2</sub> (Husson et al. 2017). Over the years, few more studies substantiating the impact of different ILs on chitin amorphization and subsequent enzymatic valorization have been reported by different research groups (Berton et al., 2018; Xu et al., 2019; Kumar et al., 2020). Apart from utility, ILs also have their own disadvantages. Major disadvantages being their high cost and the difficulty in complete removal of IL remnants from the pre-treated chitin substrate, which may compromise enzymatic activity (Dong et al., 2024). However, considering the tremendous impact of ILs on chitin amorphization and improving enzymatic hydrolysis, there might be a possibility of combining it with another pre-treatment method (for example, mechanical) which may help in reducing the amount of IL required. This in turn, may minimize the problems of cost and tedious IL-removal procedures.

### 1.5.2 Mechanical pre-treatment methods

Among the mechanical methods of chitin pre-treatment, ball-milling has gained the most extensive usage, involving high-energy rotation of the substrate and hard material balls (mixed in a specific ratio) within a sealed chamber (Duhsaki *et al.*, 2023; Pohling *et al.*, 2022). Ball-milling not only alters the chitin structure and reduces crystallinity, but also significantly enhances enzymatic hydrolysis (Duhsaki *et al.*, 2023; Liu, Y. *et al.*, 2020; Nakagawa *et al.*, 2013). However, it is not without its drawbacks. Ball-milling is an energy-intensive process, often referred to as 'high-energy milling' (Shamshina *et al.*, 2021). The autogenous heat generated during milling can be detrimental to the polysaccharide, causing charring and loss of essential functional properties. Additionally, this heat can lead to a considerable loss of CHOS during the process (Mukherjee *et al.*, 2024).

Cryo-milling has gained prominence in recent years for mechanical amorphization of polysaccharide substrates (Shamshina et al., 2021; Dhital et al., 2010 and 2011; Crofton et al., 2016). It involves grinding a material at low temperatures (<123 K), achieved by cooling with liquid nitrogen, either by mixing it with the material or externally cooling the milling chamber (Shamshina et al., 2021). Operating at these low temperatures effectively suppresses several side processes that could impact the retention of the material's functional properties during milling. Furthermore, the reduced temperature helps prevent charring of the polysaccharide and minimizes the loss of oligosaccharides during the milling process. These factors render cryo-milling significant advantage over the extensively used ball-milling process. The application of cryo-milling to polysaccharides was initially demonstrated with various starch substrates (Dhital et al., 2010 and 2011). In a separate study, cryo-milling was employed to overcome the soft and ductile nature of chitosan, producing chitosan powder suitable for pharmaceutical purposes (Crofton et al., 2016). Shamshina et al. (2021) for the first time, showed that cryo-milling could reduce the crystallinity of commercial chitin powder to a level comparable to ball-milling, without inducing significant structural changes or defibrillation of the chitin substrate. In a more recent study, for the first time, cryo-milling was shown to have positive impact on the surface area and enzymatic hydrolysis of a crude (unprocessed) α-chitin substrate, while not exhibiting any significant impact on crystallinity and DA (Mukherjee et al., 2024). These recent studies portray cryo-milling as a potential pretreatment method for amorphizing crystalline chitin substrates. However, as reported by Mukherjee et al. (2024), the impact of cryo-milling might vary depending on the nature of the

substrate. Considering the studies by Shamshina *et al.* (2021) and Mukherjee *et al.* (2024), it is quite possible that cryo-milling might have greater impact on processed chitin substrates in comparison to crude, close-to-natural substrates. Hence, cryo-milling operated under considerably mild conditions, may not be sufficient for efficient pre-treatment of crude chitin substrates. This provides an avenue for the inclusion of a second pre-treatment method (for example, ionic liquids), along with cryo-milling to achieve significant amorphization and improve enzymatic hydrolysis of such crude chitin substrates.

While mechanochemical approaches have been reported for direct synthesis of GlcNAc, (GlcNAc)<sub>2</sub> and CHOS from chitin substrates (Kobayashi *et al.*, 2023; Margoutidis *et al.*, 2018), only one report exists, where a mechanochemical approach (chitin treated with super-critical water at 400°C, followed by ball-milling) has been used as pre-treatment method to improve enzymatic hydrolysis of chitin to (GlcNAc)<sub>2</sub> (Osada *et al.*, 2013). Therefore, the possible combination of cryo-milling with IL-treatment as a pre-treatment procedure for crude  $\alpha$ -chitin substrates, could be an innovative approach towards significant reduction of crystallinity for efficient valorization to GlcNAc, (GlcNAc)<sub>2</sub> and CHOS.

### 1.6 Enzymatic valorization of chitin: emphasis on chitinases

When considering the sustainability and environment-friendly methods, biological, specifically enzyme-catalysed chitin degradation is the most preferred approach. In nature, microorganisms, particularly bacteria, degrade chitin using chitinolytic enzymes for nutrition. Enzymatic chitin degradation involves a synergistic interplay between different chitinolytic enzymes, such as lytic polysaccharide monooxygenases (LPMOs), chitinases, and  $\beta$ -*N*-acetylhexosaminidases (also known as  $\beta$ -*N*-acetylglucosaminidases) (Duhsaki *et al.*, 2023). During this interplay, LPMOs (copper-containing CAZymes) mediate oxidative cleavage of glycosidic bonds in the chitin polymer, which generates nicks on the chitin surface, thereby disrupting the surface topology. This disruption in the chitin surface enables the chitinases (hydrolytic enzymes) to mediate efficient hydrolysis of chitin to CHOS, which in turn, gets further broken down to monomeric GlcNAc by the action of  $\beta$ -*N*-acetylhexosaminidases (Vaaje-Kolstad *et al.*, 2013).

Chitinases (EC 3.2.1.14) are glycoside hydrolases (GHs) capable of breaking down the  $\beta$ -1,4-glycosidic bonds between GlcNAc moieties in chitin polymer and CHOS. These carbohydrate-active enzymes (CAZymes) mainly occur in families, GH18 and GH19, while chitinase activity has also been observed in few members of GH23 and GH48 (Chen *et al.*, 2020). The GH18 chitinases, among all chitinase families, are widely distributed across the

tree of life - found in bacteria, archaea, fungi, viruses, nematodes, insects, plants and mammals (Figure 3). They are involved in diverse functions such as tissue degradation and remodelling, pathogenicity, immune defence, nodulation and quorum sensing, apart from regular chitin hydrolysis (for cell-wall remodelling in chitin-containing organisms and for nutrition in case of several microorganisms such as bacteria) (Figure 3). Apart from this, involvement of GH18 chitinases have also reported during the events of cross-talk between chitin-containing and non-chitin-containing organisms (Chen *et al.*, 2020).

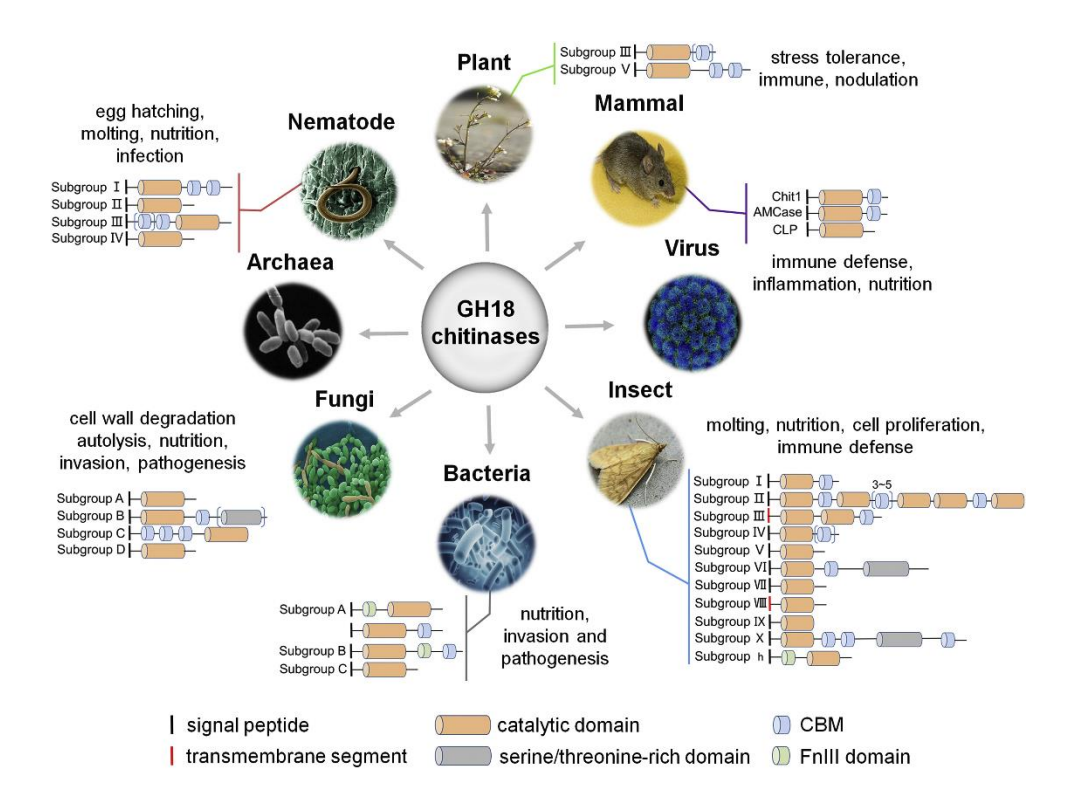


**Figure 3:** Diversity and functionalities of GH18 chitinases across the tree of life. The figure has been taken from Chen *et al.*, 2020.

Chitinases are mainly classified into two major categories: exo- and endo-chitinases. Exo-chitinases are those, which cleaves from either end (reducing or non-reducing) of the chitin chain. These are further divided into chitobiosidases (also known as chitobiases), which cleaves (GlcNAc)<sub>2</sub> into two GlcNAc units and  $\beta$ -*N*-acetylglucosaminidases (also called NAGases), which cleaves CHOS to generate GlcNAc (Li and Greene, 2010). Endochitinases, on the other hand, hydrolyses glycosidic linkages randomly at internal sites along the chitin chain (Li and Greene, 2010). Chitin hydrolysis by exo-chitinases leads to generation of mainly GlcNAc and/or (GlcNAc)<sub>2</sub>, while endo-chitinases generate a variety of products, which could be of shorter or longer chain lengths. Both of these mechanisms may

occur in combination with a processive mode of action. The processivity of a chitinase is influenced by the aromatic residues lining its substrate-binding cleft and in this event, the substrate is not released after successful cleavage but slides through the active site for the next cleavage event to occur. (Li and Greene, 2010).

The structure of the GH18 catalytic domain comprises of a signature  $(\beta/\alpha)_8$  TIMbarrel fold containing eight  $\beta$ -strands tethered by eight  $\alpha$ -helices. There are two signature motifs present along the amino acid sequence of GH18 catalytic domains: the SxGG motif and the DxDxE motif (crucial for chitinase catalysis) (Chen *et al.*, 2020). Some GH18 chitinases (of subfamily A) also possess an  $(\alpha+\beta)$  insertion domain sandwiched between the 7<sup>th</sup> and 8<sup>th</sup>  $\beta$ -strands of the TIM barrel fold in the catalytic domain. This extra domain defines the topology and depth of the active site and is often responsible for tunnel-like deep clefts and processivity in chitin degradation (Oyeleye and Normi, 2018).

GH18 chitinases are known to follow the retaining mechanism of catalysis by maintaining the configuration of  $\beta$ -anomeric carbon of substrates in products. This mechanism is influenced by the DxDxE catalytic motif (where, D – aspartic acid; E – glutamic acid; x – any amino acid) and it is attained by a substrate-assisted type of double displacement hydrolytic mechanism (Oyeleye and Normi, 2018). The catalysis by a GH18 chitinase comprises of three steps (Vaaje-Kolstad *et al.*, 2013; Chen *et al.*, 2020), which are:

- 1) Binding of the substrate (can be several GlcNAc units) to the substrate-binding cleft. Previous studies discussing chitinase crystal structures have shown that the middle aspartate (Asp) residue of the DxDxE motif (Asp142 in SmChiB) is especially important (among several other amino acids) for the binding of the -1 sugar (Synstad et al., 2004). In the substrate-free state, Asp142 interacts with an adjacent Asp (i.e., Asp140 in SmChiB) and keeps away from Glu144, which is a proton donor. However, upon substrate binding to the -1 subsite, the side chain of Asp142 rotates toward Glu144, thus forming hydrogen bonds between the hydrogen of the acetamido group of the -1 sugar, and the amino acid residues, Asp142 and Glu144. It is to be noted that during this process, the conformations of Asp140 and Glu144 remain unchanged.
- The distorted -1 sugar promotes interaction between the oxygen of the glycosidic bond and Glu144. Since Glu144 is a proton donor, it transfers a proton to the oxygen

2) Formation of intermediate and breaking of glycoside bond.

bond and Glu144. Since Glu144 is a proton donor, it transfers a proton to the oxygen moiety, therefore, facilitating leaving group departure. Subsequently, the 2-acetamido group of the -1 sugar is polarized by an enzymic carboxyl group, thus turning it as a nucleophile. Attack on the anomeric centre by the 2-acetamido carbonyl oxygen

forms a covalent bicyclic oxazolinium-ion intermediate and breaks the glycoside bond. The positive charge on the anomeric carbon is rearranged and mainly held by the oxazolinium group, which is stabilized by Asp142.

3) Departure of product and ring opening via attack from a water molecule.

After the glycosidic bond breakage, the product at the reducing end leaves the active site of the enzyme and a water molecule enters the active pocket. The intermediate is broken open by general base-catalysed attack of the water molecule on the anomeric center. Both the cyclization and ring opening steps occur with inversion of stereochemistry at the anomeric center, such that the overall reaction proceeds with net retention of stereochemistry.

**Figure 4:** The general catalytic mechanism of a GH18 chitinase (*Sm*ChiB in this case). The figure has been taken from Vaaje-Kolstad *et al.*, 2013.

Chitinases may contain one or more accessory domains, which could be carbohydrate binding modules (CBM) or other domains such as the fibronectin type-III (fnIII) domain

(Oyeleye and Normi, 2018). The presence of these domains in a chitinase, makes it multimodular. These domains assist in improving chitinase hydrolysis in several ways such as by mediating strong adherence to the chitin surface, improving substrate accessibility and/or ensuring correct positioning of the substrate to the active site of the GH18 domain (Oyeleye and Normi, 2018). CBMs in particular, are highly target-specific and are known to recognise and bind to only specific polymorphs of a certain polysaccharide (i.e.,  $\alpha$ - or  $\beta$ -chitin specific CBMs). In the current scenario, CBMs are more than just binding domains, and are known to facilitating enzyme movement along the polymeric chain, disintegrate the polymeric structure (local decrystallization) or find new sites for hydrolysis (Poshina *et al.*, 2018). Among the CBM families, members such as CBM2, CBM5, CBM12, CBM73 are known to be chitin-specific (Bai et al., 2016; Forsberg et al., 2016).

### 1.7 Paenibacillus: a ubiquitous genus of polysaccharide degrading bacteria

The name *Paenibacillus*, has been derived from the latin adverb *paene*, which means almost; hence the name means "almost a Bacillus" (Ash et al., 1993; Grady et al., 2016). Paenibacillus, a genus under the phylum Bacillota, comprises of bacterial species that are gram-positive, gram-negative or gram-variable (Grady et al., 2016). These bacteria are rodshaped, motile (by means of a peritrichous flagella), aerobic or facultatively anaerobic and endospore-forming (Ash et al., 1993; Grady et al., 2016). They are ubiquitous in nature and have been isolated from a wide range of environments and/or sources (Grady et al., 2016). Originally, species of this genus were included under Bacillus, however, they were later reclassified into a new genus, Paenibacillus, based on phylogenetic differences (Ash et al., 1993). Till date, there are 320 validly published species under the genus *Paenibacillus* (https://lpsn.dsmz.de/). Among the beneficial functions, *Paenibacillus* are known to promote plant growth by producing phytohormones and siderophores, and by phosphate solubilization and nitrogen fixation (Grady et al., 2016). They are also known to produce anti-microbial compounds that provide plant protection from pathogens as well as find importance in the field of medicine (Grady et al., 2016). On the other hand, they are also known to secrete a multitude of CAZymes that can valorize different recalcitrant and industrially-relevant polysaccharides, including chitin (Grady et al., 2016).

Deciphering the chitinolytic potential of some *Paenibacillus* species has been limited to biochemical studies comprising of bacterial growth and degradation of chitin substrates and/or production and optimisation of the crude-enzyme cocktail from the bacteria (Juarez-Jimenez *et al.*, 2008; Song *et al.*, 2012 and 2015; Kumar *et al.*, 2018). Whereas, investigation

of chitinolytic potential for a few *Paenibacillus* species has been restricted to genome-based analysis, as in case of P. xylanilyticus W4 (Liao et al., 2019) and P. elgii YSY-1.2 (Tran et al., 2024). A large number of studies has been conducted on the structural-functional characterization of chitinases isolated from different Paenibacillus species. Three multimodular GH18 chitinases (PbChi74, PbChi70 and PbChi67) and a uni-modular GH18 β-Nacetylglucosaminidase (PbNag39) have been characterized from P. barengoltzii CAU904 (Fu et al., 2014; Yang et al., 2016; Fu et al., 2016; Liu, Y. et al., 2020). Two multi-modular GH18 chitinases, Chip1 and Chip2 were isolated and characterized from P. pasadenensis CS0611 (Xu et al., 2019), whereas, another multi-modular chitinase, CHI was isolated and characterized from *P. chitinolyticus* UMBR 0002 (Liu, C. et al., 2020). Additionally, *Px*Chi52 from P. xylanexedens Z2-4 was reported to show antifungal activity against some of the wellknown phytopathogenic fungi, along with regular chitin hydrolysis (Zhang, W. et al., 2021) Further, PpChi from P. pabuli was biochemically characterized and reported to produce partially-acetylated CHOS of DP3 and DP4, carrying a single N-acetylation at their reducing end (Li, J. et al., 2021). Recently, a bifunctional chitinase, PsChi82 from P. shirakamiensis was biochemically characterized and reported to exhibit both chitinase and chitosanase activities producing diverse NA-CHOS (Liu et al., 2024). Paenibacillus sp. FPU-7 is the only isolate whose chitinolytic potential has been fairly investigated in-depth, combining biochemical and genomic approaches (Itoh et al., 2013). Furthermore, in the same and as well as subsequent studies, in-depth characterization along with crystal structure of a cell-surface expressed, dual GH18 domain-containing chitinase, ChiW was reported (Itoh et al., 2013, 2014 and 2016). Interestingly, among the *Paenibacillus* chitinases characterized till date, crystal structure is available for only ChiW (Itoh et al., 2016) and PbNag39 (Liu, Y. et al., 2020). On the other hand, proteomic investigation of any *Paenibacillus* species during growth on highly crystalline chitin substrates was found conspicuously lacking.

Paenibacillus sp. LS1 was isolated from a decaying wood sample collected from Lachung village, North Sikkim district (27°40′13″N, 88°43′37″E), Sikkim, India (Mukherjee *et al.*, 2020). The isolate was rod-shaped (Figure 5A) and produced relatively large and prominent zone of clearance on M9-colloidal chitin agar plate within just 3 days of incubation at 28°C (Figure 5B) (Mukherjee *et al.*, 2020), indicating untapped chitinolytic potential.

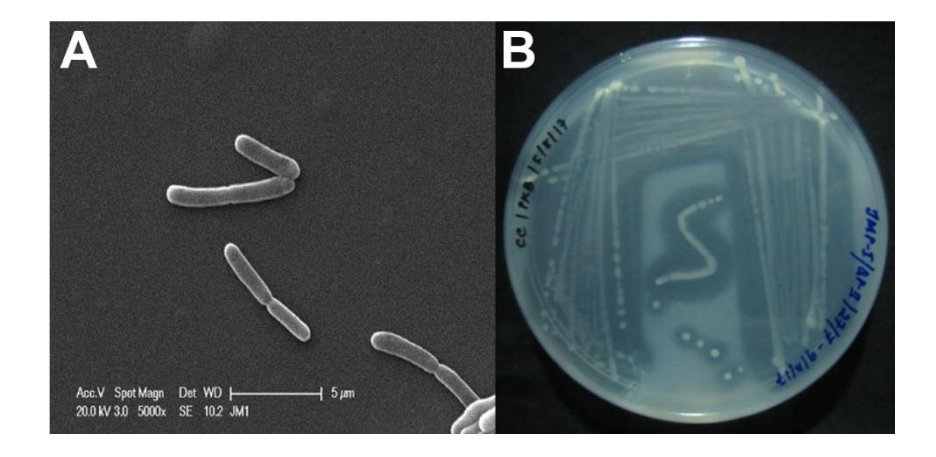


**Figure 5:** Morphology of and chitin degradation by *Paenibacillus* sp. LS1. A – Rod-shaped morphology of *Paenibacillus* sp. LS1 examined under SEM. B - Hydrolysis of colloidal chitin (CC) by *Paenibacillus* sp. LS1 can be observed by the formation of zone of clearance around the bacteria in the CC-agar plate.

16S rRNA-based identification and phylogenetic analysis revealed ~99% sequence identity with *P. amylolyticus* NBRC 15957<sup>T</sup> (99.34%), *P. tundrae* A10b<sup>T</sup> (99.27%), and *P. tylopili* MK2<sup>T</sup> (99.18%), with the former being the closest phylogenetic neighbour (Figure 6). Among these nearest phylogenetic neighbours of *Paenibacillus* sp. LS1, the whole genome sequence is only available for *P. amylolyticus* NBRC 15957<sup>T</sup>, which contain four putative chitinases as per CAZyme annotation of the genome on the dbCAN3 server (Zheng *et al.*, 2023). On the other hand, *P. tylopili* MK2<sup>T</sup> was reported to be a chitinolytic strain (Kuisiene *et al.*, 2008). But, none of these strains were analysed in detail for their ability to degrade different polymeric forms of chitin (Mukherjee *et al.*, 2020), till date.

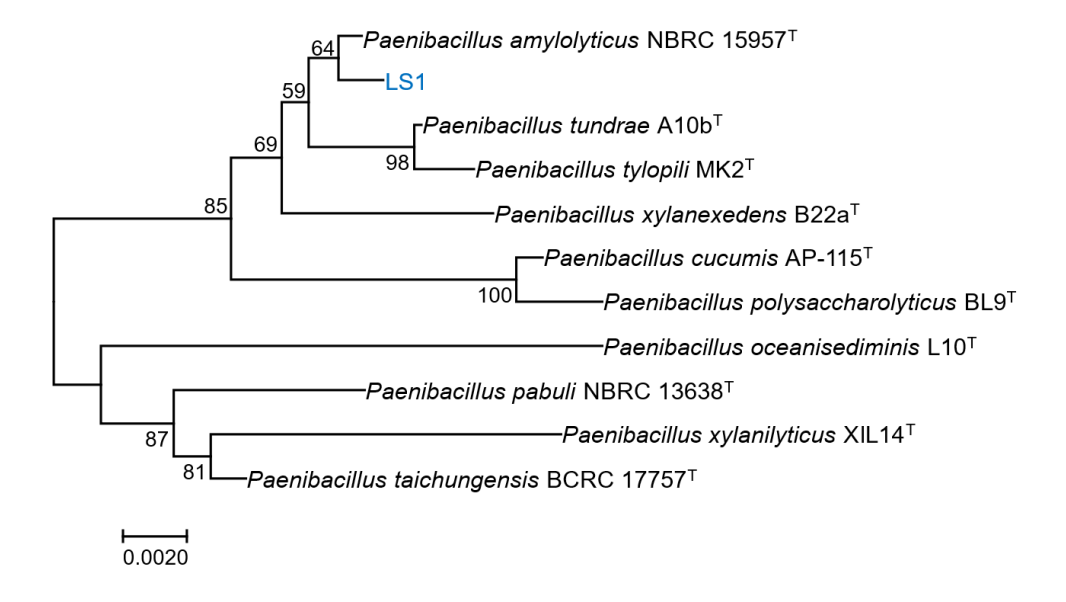


**Figure 6:** Phylogenetic analysis of *Paenibacillus* sp. LS1. Phylogenetic tree was constructed based on 16S rRNA gene sequences using MEGA 7.0 by employing neighbour joining method and Kimura 2-parameter model. The numerical values displayed at each node is the bootstrap percentage (based on 1000 replicates) and the scale bar indicates 0.002 substitutions per nucleotide position.

Based on the existing literature and preliminary data on a seemingly new/novel isolate in hand, there were presumably two directions for the current project:

- Exploring the untapped chitinolytic potential of Paenibacillus sp. LS1: Two key questions were raised under this direction, which were:
- 1) How efficient is the *Paenibacillus* sp. LS1 chitinolytic system for valorization of crystalline chitin substrates?
- 2) What are the potential chitinase targets within the chitinolytic system of *Paenibacillus* sp. LS1?
- ➤ Developing a process for the efficient valorization of natural, highly crystalline chitin: What could be the best approach to improve the overall chitin bioconversion to GlcNAc and (GlcNAc)<sub>2</sub>?

The current project revolves around addressing these questions, and hence, the following objectives were framed accordingly:

- 1) Deciphering the genomic and proteomic insights into chitin degradation by *Paenibacillus* sp. LS1.
- 2) Molecular characterization of selected chitinases from *Paenibacillus* sp. LS1.
- 3) Development of a bioprocess for efficient and selective production of GlcNAc and (GlcNAc)<sub>2</sub> directly from chitin.

# **Chapter-2**

Deciphering the genomic and proteomic insights of chitin degradation by *Paenibacillus* sp. LS1

# 2.1 Materials & Methods

#### 2.1.1 Chemicals and reagents

Both α-chitin and β-chitin were procured from Stellar Bio-Sol (formerly, Mahtani Chitosan Pvt. Ltd.), Gujarat, India. Glycol chitosan, Calcoflour white M2R dye and Bradford reagent were procured from Sigma Aldrich, USA. NucleoSpin Microbial DNA kit was procured from Macherey-Nagel, Germany. Pierce<sup>TM</sup> BCA protein assay kit was procured from ThermoFisher Scientific, USA. All chemicals and reagents were obtained from either HiMedia or Sisco Research Laboratories Pvt. Ltd., India unless specified otherwise.

#### 2.1.2 Colloidal and glycol chitin preparation

Colloidal chitin (CC) was prepared as described previously by Duhsaki *et al.* (2022). The α-chitin flakes (30 g; Stellar Bio-Sol, Gujarat, India) were crushed and dissolved in 400 mL concentrated HCl under mild stirring and incubated for 2 h at room temperature. After incubation, 3 L of chilled MilliQ water was slowly added and the setup was incubated at 4°C for overnight. The colloidal mixture was then centrifuged at 8000 rpm for 20 min at 4°C and the precipitate obtained was thoroughly washed with double distilled water for several times until the pH reaches 7.0. The final precipitate was dissolved in 200 mL of autoclaved MilliQ water.

Glycol chitin was prepared as described previously by Trudel & Asselin (1989). Glycol chitosan (5g; Sigma Aldrich, USA) was dissolved by grinding in 100 mL of 10% acetic acid and was incubated at 22°C overnight. Methanol (450 mL) was slowly added to the viscous solution and the solution was vacuum filtered through a Whatman No. 4 filter paper. Acetic anhydride (7.5 mL) was added to the filtrate and mixed thoroughly on a magnetic stirrer. The resulting gel was allowed to stand for 30 min at room temperature and cut into small pieces. The solid gel pieces were then homogenized in methanol for 4 min at high-speed using a Waring Blendor. The resulting suspension was centrifuged at 10000 rpm for 30 min at 4°C. The resulting gel-like pellet was homogenized in 1 vol Methanol and centrifuged as in the previous step. The final pellet was further homogenized in 500 mL autoclaved MilliQ water containing 0.2% (w/v) sodium azide, and stored as 1% (w/v) stock solution of glycol chitin at 4°C until further use.

#### 2.1.3 Utilization of different chitin substrates

Growth of *Paenibacillus* sp. LS1 was monitored in M9 medium containing 47.7 mM Na<sub>2</sub>HPO<sub>4</sub>, 22 mM KH<sub>2</sub>PO<sub>4</sub>, 8.5 mM NaCl, 9.4 mM NH<sub>4</sub>Cl, 1 mM MgSO<sub>4</sub> and 0.3 mM CaCl<sub>2</sub>. The media was enriched with 1X trace elements and vitamins (1 mM each of biotin and thiamine) and supplemented with 0.5% of the different chitin substrates (α-, β- or colloidal chitin) as sole carbon source. While, M9 medium and M9 supplemented with 0.5% glucose were used as negative and positive controls, respectively. The preculture was prepared by growing *Paenibacillus* sp. LS1 in Luria Bertani (LB) broth for 24 h at 28°C. The fully grown culture was harvested and the cell pellet was washed with sterile MilliQ water and resuspended in 1X M9 medium to measure the optical density (OD) at 600 nm. The OD was adjusted to 0.1 and 1% inoculum was added to the conical flasks containing minimal media with different chitin substrates. The culture flasks were incubated at 28°C and 180 rpm. One mL culture from each flask at different time intervals was collected and centrifuged at 10000 rpm for 15 min to collect the secretome (culture supernatant). Both the pellet and secretome were stored separately at -20°C until further analysis. All the experiments were performed in biological triplicates.

#### Estimation of total cellular protein

Growth of the bacteria on various chitin substrates was analysed by estimating the total cellular protein in the culture pellet collected at different time points as described previously (Mukherjee *et al.*, 2020). The pellets were treated with 0.2 N NaOH and boiled at 120°C for 10 min for cell lysis, followed by centrifugation at 11000 rpm for 15 min at 4°C. Total cellular protein was estimated using the standard Bradford's method, essentially as described in the manufacturer's protocol (Sigma Aldrich, USA).

# Estimation of extracellular chitinase activity

Reducing end assay (Schales' assay) was performed to measure the chitinase activity as described earlier (Mukherjee *et al.*, 2020). A 200 μL of reaction mixture consisting of 50 mM sodium acetate buffer (pH 5.5), 0.5% CC and 50 μL of secretome, was incubated at 37°C for 1 h at 800 rpm shaking in an Eppendorf Thermomixer C (Eppendorf, Germany). The samples were centrifuged at 11000 rpm for 10 min at 4°C and 100 μL of the supernatant was boiled for 15 min with 300 μL Schales' reagent (0.5 M sodium carbonate and 0.5 g/L potassium ferricyanide). The amount of reducing sugar generated was calculated using a GlcNAc standard curve. One unit was defined as the amount of enzyme that liberated 1 μmol of reducing sugar per hour.

#### 2.1.4 Detection of extracellular chitinases by semi-native PAGE

For detection of chitinase isozymes expressing in presence of different chitin substrates, the secretome samples collected at their respective optimal activity time points were analysed by 12% SDS-PAGE containing 2.5% of glycol chitin (Mukherjee *et al.*, 2020). Samples were prepared by boiling 10 μL of secretome with 4 μL of SDS-loading dye (1M Tris-HCl pH 6.8, 10% SDS, 50% Glycerol, 0.05% bromophenol blue and 14.3 M β-mercaptoethanol) at 80°C for 10 min. After electrophoresis, the gels were thoroughly washed with double distilled water, followed by washing thrice with 50 mM Tris-HCl (pH 8.0) containing 0.1% Triton X-100, twice with 50 mM Tris-HCl (pH 8.0) and followed by incubation in the same buffer at 37°C for overnight. After incubation, the gels were stained with Calcofluor-white M2R dye for 20 min and washed thoroughly with double distilled water before examination for the presence of bands under UV transilluminator.

#### 2.1.5 Field emission-scanning electron microscopy

Direct visualization of crystalline chitin degradation by *Paenibacillus* sp. LS1 was performed using field emission-scanning electron microscopy (FE-SEM) (Mukherjee et al., 2020). Five different experimental setups were prepared, of which three were control setups consisting of the isolate alone and untreated  $\alpha$ - and  $\beta$ -chitin separately. The other two were test setups consisting of Paenibacillus sp. LS1 grown in M9 media supplemented with the crystalline chitin substrates independently as sole carbon source. The isolate was grown in both the test setups and samples for analysis were collected at 48 h and 96 h. Whereas, the control containing the bacteria alone was cultivated in LB broth for 24 h (optimum growth time). The control and test samples were harvested by centrifugation at 10000 rpm for 5 min at 4°C. The harvested pellet was resuspended in 2.5% glutaraldehyde and incubated at 4°C overnight (pre-fixation). Glutaraldehyde was removed and the prefixed specimen was dehydrated in graded ethanol (10, 30, 50, 70, 90 and 100% [v/v]) through progressive washing. One microliter of the bacterial specimen and a single chitin flake in case of the treated/untreated chitin were placed on a clean coverslip attached to a dual-sided magnetic tape on a stub. The specimens were gold-coated for 90 s prior to analysis using the Hitachi E-1010 ion sputter. FE-SEM analysis was performed on the Ultra 55 model of Carl Zeiss, Germany. The parameters for high resolution imaging were set at 10-50 µm of working distance at 5 kV accelerating voltage. The magnification range was varied from 1500-12000x.

#### 2.1.6 Genome sequencing, assembly and annotation

Whole genome sequencing of *Paenibacillus* sp. LS1 was performed as described by Mukherjee *et al.* (2023). *Paenibacillus* sp. LS1 was grown in LB broth for 24 h and the harvested culture pellet was used for genomic DNA isolation using the standard procedure, essentially described in the manufacturer's protocol of the NucleoSpin Microbial DNA kit. The quality and quantity of the isolated DNA was measured on a 0.8% agarose gel and using Qubit<sup>TM</sup> dsDNA HS assay kit (Thermo Fisher Scientific, USA), respectively. The DNA fragmentation and library construction was done using a Nextera DNA Flex Library preparation kit (Illumina), following manufacturers' protocol. After library construction, dual index adapters were ligated at the blunt end of the DNA fragments. The quality and quantity of the fragment library was estimated and checked using the Qubit<sup>TM</sup> dsDNA HS assay kit and Agilent 2200 Tapestation, respectively. The good quality library was normalized, pooled and subsequently sequenced using 2 x 250 bp chemistry on a MiSeq platform (Illumina Inc., San Diego, CA, USA). The quality of the raw sequence was checked using FastQC (Brown *et al.*, 2017). Adapter removal and trimming was done by using Cutadapt (Martin, 2011).

Genome assembly and annotation were performed as previously reported (Mukherjee et al., 2023). Assembly of trimmed good quality reads was performed using the unicycler assembler v.0.4.8 (Wick et al., 2017) in PATRIC (currently known as the Bacterial and Viral Bioinformatics Resource Center - BV-BRC) (Wattam et al., 2014). The quality of genome assembly was checked as per the QUAST (v.5.0.2) report (Gurevich et al., 2013). The assembled contig file was annotated using PATRIC and RAST server (Overbeek et al., 2014). The annotation in PATRIC was performed using the default parameters, while that in RAST, the RASTtk pipeline (Brettin et al., 2015) was used with few customizations. The quality of the annotated genome was assessed using the genome report file generated, based on which, further analyses were performed using PATRIC (or) RAST and other bioinformatic tools as per the requirements. The genome upon submission to NCBI (GenBank/RefSeq) was annotated by the NCBI Prokaryotic Genome Annotation Pipeline (PGAP) v.6.6 (Li, W. et al., 2021). The annotation method used were "best-placed reference protein set" and "GeneMarkS-2+". Quality of the annotated genome was assessed using CheckM analysis v.1.2.2 (Parks et al., 2015).

#### 2.1.7 Estimation of ANI and in silico DDH values

Genome-based relatedness between *Paenibacillus* sp. LS1 and its phylogenetic neighbours (Mukherjee *et al.*, 2020) was estimated by comparing the OrthoANIu and *in silico* DDH values

as described by Mukherjee *et al.* (2023). The ANI calculator of the EzBioCloud database (Yoon *et al.*, 2017) and Genome-to-Genome Distance Calculator (GGDC) of DSMZ (Meier-Kolthoff *et al.*, 2013) were used for calculating OrthoANIu and DDH values, respectively. The genomes of the phylogenetic neighbours used for estimating OrthoANIu and DDH values were restricted to the type strains only.

#### 2.1.8 Genome mining for CAZymes involved in chitin degradation/modification

The CAZymes of *Paenibacillus* sp. LS1 were annotated using the dbCAN3 server (Zheng *et al.*, 2023). An integrated approach using all three designated tools/databases of the dbCAN3 server i.e., HMMER:dbCAN, Diamond:CAZy and HMMER:dbCAN-sub, was employed for CAZyme prediction and annotation. Only those proteins or domains annotated by at least two tools were considered for further analysis (Zheng *et al.*, 2023). Additionally, substrate prediction and CAZyme gene clusters (CGCs) prediction for the annotated CAZymes were performed using both the dbCAN-PUL and dbCAN-sub modules of dbCAN3 (Zheng *et al.*, 2023).

CAZymes involved in chitin degradation (the chitinases, in particular) were identified based on the dbCAN3 output and the protein sequences were retrieved from the annotated genome. Domain architecture was predicted considering the results from both InterPro (https://www.ebi.ac.uk/interpro/) and NCBI Conserved Domain Database (https://www.ncbi.nlm.nih.gov/Structure/cdd/cdd.shtml). SignalP 6.0 (https://services.healthtech.dtu.dk/services/SignalP-6.0/) was used to predict the presence and nature of signal peptide. Protein parameters such as molecular weight and isoelectric point (pI) were computed using ProtParam - Expasy (<a href="https://web.expasy.org/protparam/">https://web.expasy.org/protparam/</a>). The retrieved chitinase sequences were screened against the PDB database using blastp to understand the extent of their uniqueness compared to the already existing well-characterized counterparts. Additionally, arrangement of the chitinase genes in the genome was visualized using the RAST server.

# 2.1.9 Proteome analysis of chitin-active secretome from Paenibacillus sp. LS1

#### 2.1.9.1 Sample preparation for proteome analysis

Paenibacillus sp. LS1 was grown in M9 minimal medium supplemented with 0.5% of the different crystalline chitin substrates ( $\alpha$ - and  $\beta$ -chitin). While, M9 supplemented with 0.5% glucose and GlcNAc were used as control. The primary culture was prepared by growing the isolate in LB broth for 36 h at 28°C. The fully grown culture was harvested at 8000 rpm and

 $4^{\circ}$ C for 10 min. The cell pellet was washed with sterile 1X M9 medium and resuspended again in 1X M9 medium to measure the OD at 600 nm. The OD was adjusted to 0.1 and 1% of the primary culture was inoculated into conical flasks containing M9 medium supplemented with α- or β-chitin, glucose or GlcNAc. The culture flasks were incubated at 28°C and 180 rpm shaking up to the desired time intervals (48 h, 96 h or 216 h). A total of four biological replicates per time-point per substrate were kept.

At the desired time points, the cultures were harvested at 5000 rpm for 20 min at 4°C and the culture supernatants were collected for secretome analysis. The supernatants were lyophilized and dissolved in 2 mL of 5 mM Tris HCl, pH 8.0. Freshly prepared ice cold 100% trichloroacetic acid (TCA) was added to the protein sample(s) in 1:4 ratio (0.5 mL:2 mL). The mixture was incubated at -80°C for 30 min for precipitation, followed by centrifugation at 14000 rpm for 5 min. The supernatant was discarded and the pellet was washed with 200 μL cold acetone (0.01 M HCl in 90% acetone) by centrifugation at 14000 rpm for 5 min. The acetone wash was repeated 2-3 times to completely remove TCA from the protein precipitates. The protein precipitates were air-dried at room temperature until entire acetone was evaporated. The precipitates were then dissolved in 5 mM Tris HCl, pH 8.0 containing 8M urea. Proper care was taken to avoid frothing during mixing. The protein was estimated using Pierce<sup>TM</sup> BCA protein assay kit.

Protein samples (100-150 μg) mixed with freshly prepared 10 μL of SDS-PAGE loading dye (4% β-mercaptoethanol, 0.02% bromophenol blue, 30% glycerol, 10% SDS, 250 mM Tris HCl, pH 6.8) were run on 12% SDS-PAGE until they just entered the resolving gel. The electrophoresis was then stopped and the protein bands were excised using sterile scalpel. Further, the gel pieces were lyophilized for in-gel digestion. The SDS-PAGE slices were homogenized with a Retsh mill and destained with 50% (v/v) acetonitrile in 50 mM ammonium bicarbonate. Samples were reduced with 10 mM DTT, alkylated with 30 mM indole acetic acid, and digested overnight with trypsin (Promega, USA). Desalting of the samples was done using the C18 solid phase extraction (SPE) cartridge (Phenomenex, USA).

# 2.1.9.2 Nano LC-MS/MS analysis of the tryptic peptides and bioinformatics for proteome analysis

The methodology described by Berková *et al.* (2024) was used with slight modifications. Peptides were analysed by nanoflow reverse-phase liquid chromatography-mass spectrometry using a 15 cm C18 Zorbax column (Agilent, USA), a Dionex Ultimate 3000 RSLCnano-UPLC system, and the Orbitrap Fusion Lumos Tribrid Mass Spectrometer equipped with a FAIMS Pro Interface (ThermoFisher Scientific, USA). All samples were analysed using FAIMS

compensation voltages of -40, -50, and -75 V. The measured spectra were recalibrated and searched against the *Paenibacillus* protein database (Proteome ID: UP000216732, UniProt) and common contaminants databases using Proteome Discoverer 2.5 (ThermoFisher Scientific, USA) with algorithms SEQUEST and MS Amanda (Dorfer *et al.*, 2014). The protein relative abundance was estimated by Minora, employing precursor ion quantification followed by normalization (total area). As an important criterion, proteins were considered present only if detected in three of the four replicates for atleast one substrate. ANOVA and post hoc analyses were done with MetaboAnalyst v.5.0 (Pang *et al.*, 2021). PCA analysis was done in ClustVis v.2.0 (Metsalu and Vilo, 2015). Significant differences between control vs. test samples refer to p-value ≤ 0.5.

Different bioinformatic servers were used during the proteome analysis, which included SignalP v.6.0 (https://services.healthtech.dtu.dk/services/SignalP-6.0/), SecretomeP v.2.0 (https://services.healthtech.dtu.dk/services/SecretomeP-2.0/) and DeepTMHMM v.1.0.39 (https://dtu.biolib.com/DeepTMHMM) and dbCAN3 server (https://bcb.unl.edu/dbCAN2/) (Zheng et al., 2023). The presence of signal peptide (and their respective cleavage sites) was determined using SignalP, while SecretomeP was used for prediction of non-classical protein secretion, and DeepTMHMM was used for prediction of transmembrane helices in proteins. A protein was considered secreted if it was predicted by atleast two of these algorithms. Annotation of Carbohydrate Active-enZymes (CAZymes) was performed using dbCAN3 (Zheng et al., 2023) as described in section 2.1.8. The label free quantification (LFQ) intensities (abundances) were log10 transformed prior to analysis. Heatmap generation and hierarchical clustering (by Euclidian distance measure and average linkage) was done using Morpheus (https://software.broadinstitute.org/morpheus/).

# 2.2 Results & Discussion

Chitin is a compact biopolymer due to presence of intrinsic hydrogen bonding between the polymeric chains that restricts efficient hydrolysis by a single enzyme. In nature, chitinolytic bacteria are known to devour chitin as a source of nutrition by breaking it down to CHOS with the help of chitinolytic enzymes. *Paenibacillus sp.* LS1 is a rod-shaped chitinolytic bacteria, isolated from a decaying wood sample collected from Lachung village, North Sikkim district (27°40′13″N, 88°43′37″E), Sikkim, India (Mukherjee *et al.*, 2020). It produced significant zone of clearance on M9-CC agar plate, confirming untapped chitinolytic potential (Figure 5B). Moreover, none of the three nearest phylogenetic neighbours of the isolate, i.e., *P. amylolyticus*, *P. tundrae* and *P. tylopili* (Figure 6), have been studied for their ability to degrade different polymeric forms of chitin till date. In this chapter, the chitin degradation by *Paenibacillus* sp. LS1 has been explored using biochemical, genomic and proteomic approaches.

#### 2.2.1 Paenibacillus sp. LS1 prefers β- and colloidal chitin substrates

Growth of the isolate, *Paenibacillus* sp. LS1 was analyzed using M9 medium supplemented with different chitin substrates ( $\alpha$ -,  $\beta$ - and colloidal chitin) up to 10 days. The growth studies revealed that the isolate least preferred the  $\alpha$ -chitin substrate and displayed very slow degradation over the course of 10 days (Figure 7 – 1<sup>st</sup> panel). However, visible bacterial growth and subsequent disappearance of the substrates,  $\beta$ -chitin and CC was observed from the onset of 3<sup>rd</sup> and 2<sup>nd</sup> day of culturing, respectively and the entire substrate was utilized by the end of 10 days (Figure 7 – 2<sup>nd</sup> and 3<sup>rd</sup> panels).

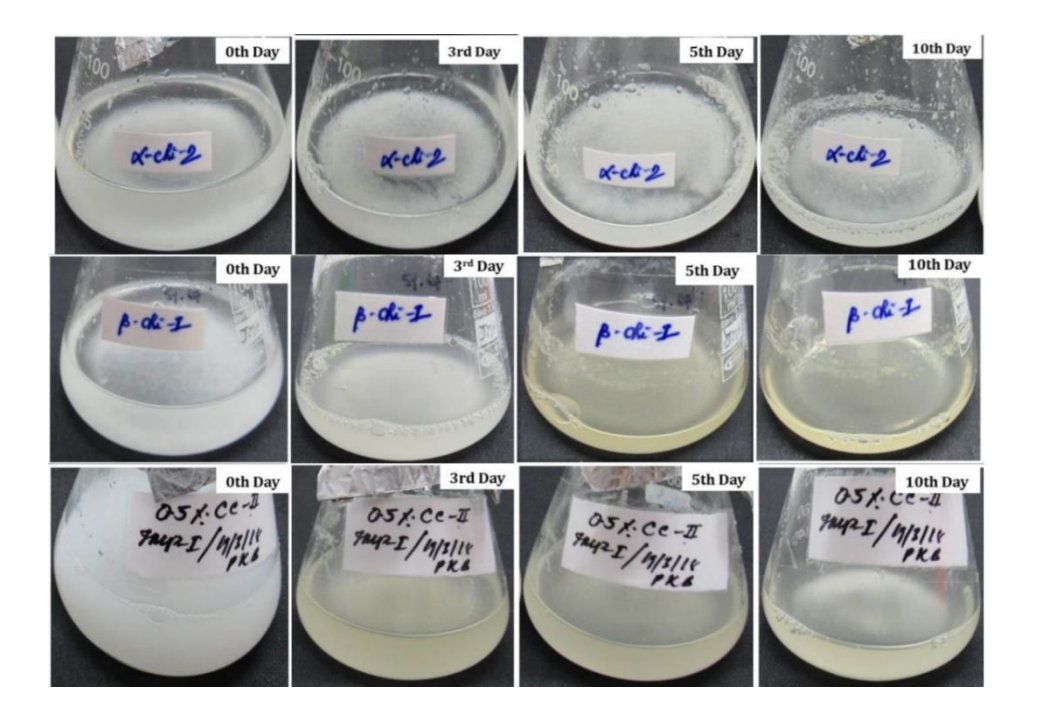
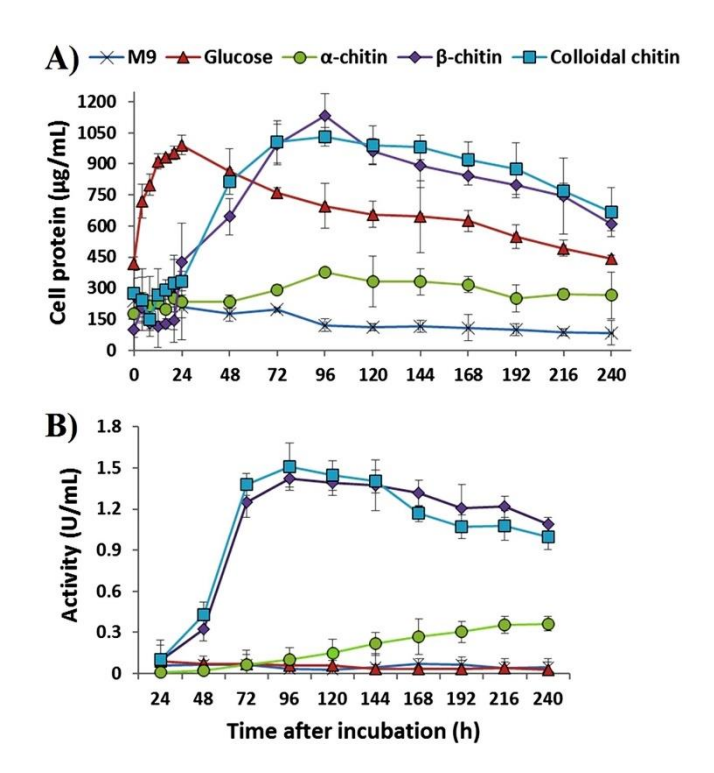


Figure 7: Growth of *Paenibacillus* sp. LS1 on various chitin substrates. *Paenibacillus* sp. LS1 was grown in M9 minimal medium supplemented with 0.5% of α-chitin (top panel),  $\beta$ -chitin (middle panel) and colloidal chitin (lower panel), respectively. Complete utilization of  $\beta$ -chitin and CC was observed within 10 days; however, a significant degradation of α-chitin was not observed during the time-span. This indicates that the isolate prefers  $\beta$ -chitin and colloidal chitin over α-chitin when provided as sole source of carbon.

Samples were collected at regular time intervals to analyse the total cellular protein (indication of growth) and chitinase activity. A gradual increase in the cell growth (protein concentration) was observed on both  $\beta$ -chitin and CC up to 96 h (point of highest protein concentration), followed by a typical stationary phase and further the growth was decreased (Figure 8A). A similar trend was observed in case of extracellular chitinase activity, which also reached maximum at 96 h in case of  $\beta$ -chitin and CC (Figure 8B). In line with the observations from the flask-based culture systems, total cellular protein and chitinase activity were highest on  $\beta$ -chitin and CC, compared to  $\alpha$ -chitin (Figure 8). This further indicated the substrate preference of *Paenibacillus* sp. LS1 when grown on different chitin substrates. Probable reason for less growth on and utilization of  $\alpha$ -chitin could be its high crystalline nature that may hinder access of the chitinolytic enzymes to the polysaccharide and in turn, reducing the efficiency of saccharification.



**Figure 8:** Cell growth and chitinase activity analysis. Growth of *Paenibacillus* sp. LS1 on different crystalline chitin substrates was followed up to 10 days by measuring the total cellular protein (A). In parallel, the same set of samples were used for obtaining the clear supernatant (secretome) through centrifugation. The secretome rich in chitin-active enzymes was used to measure the chitinase activity at the respective time points (B). The highest total cellular protein concentration and extracellular chitinase activity was observed for *Paenibacillus* sp. LS1 grown on β-chitin and colloidal chitin, indicating the substrate preference of the bacteria. All experiments were performed in biological triplicate and error bars represent standard deviations.

#### 2.2.2 Chitinase isozymes were detected in secretome collected over different chitin substrates

Secretome fractions collected over  $\alpha$ -,  $\beta$ - and colloidal chitin were resolved using semi-native PAGE, containing 2.5% glycol chitin to investigate the expression pattern of different chitinase isozymes. Six isozymes were observed in the secretome fractions collected over  $\alpha$ -chitin, and CC with molecular weights ranging from 40-90 kDa (Figure 9). Whereas, only five very prominent bands were observed in the secretome fraction collected over  $\beta$ -chitin with the same range of molecular weights (Figure 9). The intensity of the bands detected was very low for the fraction collected over  $\alpha$ -chitin, which further confirms the substrate preference of the isolate *Paenibacillus* sp. LS1 (Figure 9). Previously, Song *et al.* (2015) reported differential expression pattern of chitinase isozymes for *P. chitinolyticus* MP-306 grown on various chitin substrates at 30°C for 3 days. A very low expression of chitinases was observed for *P. chitinolyticus* grown on crab shell powder chitin (crab shell  $\alpha$ -chitin). In contrast, the isolate *Paenibacillus* sp. LS1

has expressed six chitinase isozymes when grown on  $\alpha$ -chitin flakes, indicating its potential to utilize highly recalcitrant form of chitin.

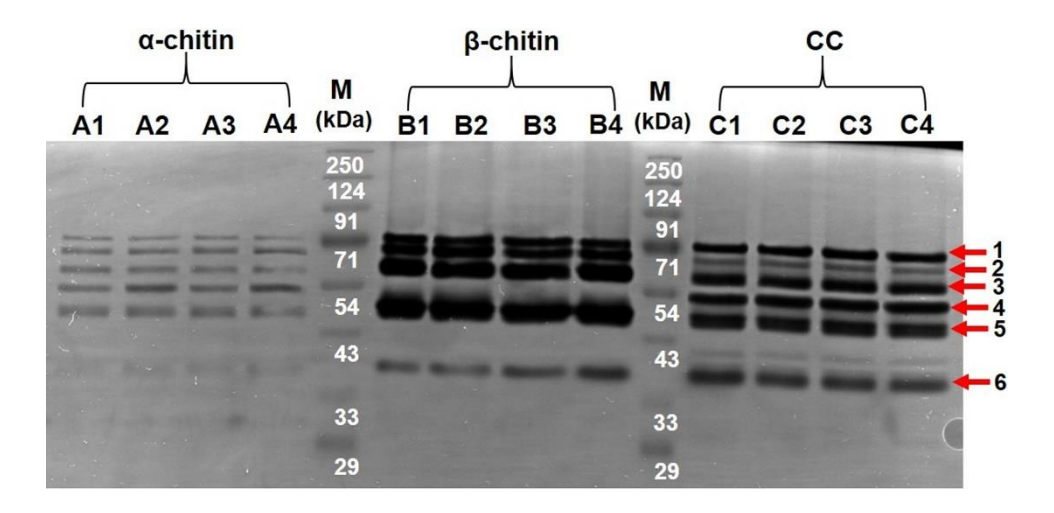


**Figure 9:** Detection of chitinase isozymes by semi-native PAGE. The isolate *Paenibacillus* sp. LS1 was grown in minimal media supplemented with different crystalline chitin substrates at 28°C for 10 days. Chitinase isozymes expressed at different time points in presence of α-chitin (216 h), β-chitin (96 h) and CC (96 h) were resolved on SDS-polyacrylamide gel containing glycol chitin substrate. Bands were visualized by staining with calcofluor white M2R after electrophoresis. A1-4; B1-4 and C1-4 represent the samples resolved from biological replicates. M – Molecular weight marker.

#### 2.2.3 FE-SEM analysis of chitin particles

Figure 10 represents the field emission-scanning electron micrographs of  $\alpha$ -chitin treated with *Paenibacillus* sp. LS1. The untreated  $\alpha$ -chitin have distinct shape and smooth surface (Figure 10A). However, after 48 h of incubation the  $\alpha$ -chitin particles were colonized by the isolate and visible perforations were formed on the crystalline surface, possibly due to the chitinolytic enzymes secreted by *Paenibacillus* sp. LS1 (Figure 10B). At 96 h, the  $\alpha$ -chitin particle looked much more amorphous and the perforations were much more intensified (Figure 10C). On the other hand, the degradation of  $\beta$ -chitin by the isolate was much faster compared to  $\alpha$ -chitin. As compared to the smooth surface of the untreated  $\beta$ -chitin (Figure 11A), the surface of the treated  $\beta$ -chitin was found to be densely covered by the isolate within 48 h, with areas showing crumbled fibrils and distorted surface (Figure 11B). An almost complete degradation of  $\beta$ -chitin was observed at 96 h and no trace of  $\beta$ -chitin flakes could be observed under FE-SEM (data not shown). The observations were in good agreement with the growth studies performed on different substrates. Also, these results clearly indicate that the isolate *Paenibacillus* sp. LS1 mediates degradation of crystalline chitin through direct surface attachment and colonization.

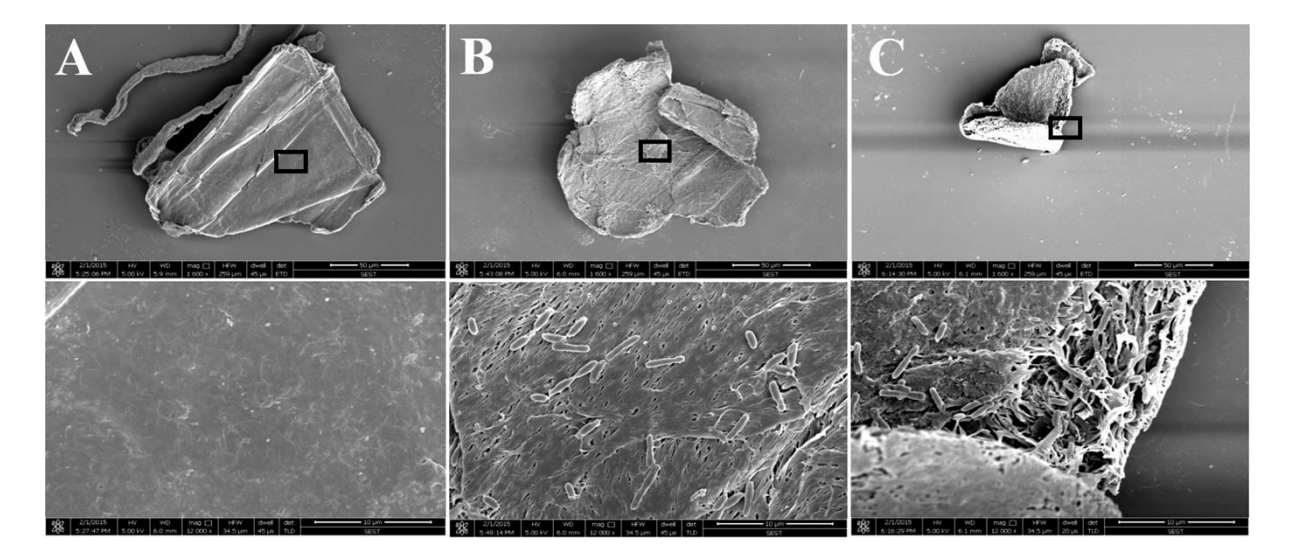


**Figure 10:** FE-SEM analysis of α-chitin treated with *Paenibacillus* sp. LS1. The figure show structures of α-chitin particle alone (A) and incubated with *Paenibacillus* sp. LS1 after 48 h (B) and 96 h (C). The upper panel represents the untreated and treated individual α-chitin particles while the lower panel represents the close-up images of the target area (shown in black frame) of the respective particle. The scale bar of the images in the upper panel is 50 μm and those in the lower panel is 10 μm.

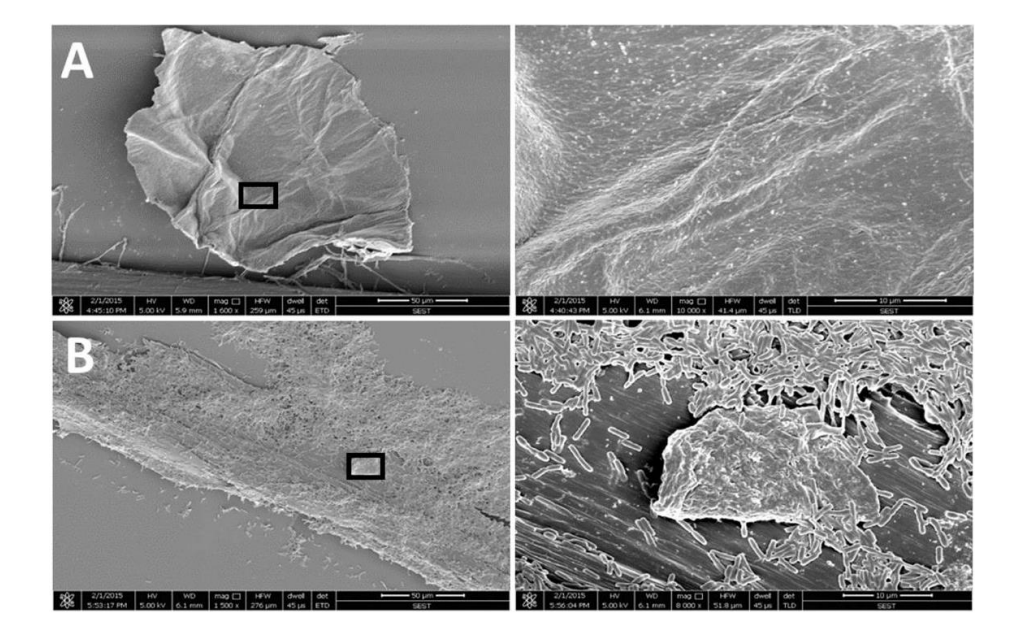


**Figure 11:** FE-SEM analysis of β-chitin treated with *Paenibacillus* sp. LS1. The figure show structures of β-chitin particle alone (A) and incubated with *Paenibacillus* sp. LS1 after 48 h (B). The left panel represents the untreated and treated individual β-chitin particles and the right panel represents the close-up images of the target area (shown in black frame) of respective particle. The scale bar of the images in the left panel is 50 μm and those in the right panel is  $10 \, \mu m$ .

#### 2.2.4 General features of the Paenibacillus sp. LS1 genome

The genome of Paenibacillus sp. LS1 has been deposited at DDBJ/ENA/GenBank under accession no. JAPDOE000000000. The current version of the accession is version JAPDOE010000000. The NCBI GenBank and RefSeq assembly accessions for the genome are GCA 026013365.1 and GCF 026013365.1, respectively. Since the NCBI RefSeq comprises of non-redundant and well-annotated set of sequences, the RefSeq annotations were considered for the genome analysis. The assembled genome of *Paenibacillus* sp. LS1 comprised a total of 40 contigs, with an N<sub>50</sub> contig size of 0.43 Mb. The genome size was estimated to be 7.2 Mb, and the GC content was 45.5%. The genome comprised of 6,350 genes, of which 6,265 were coding sequences (CDS) and 85 were RNA coding genes. Three copies of 23S and two copies each of the 16S and 5S rRNA genes, 4 ncRNA and 74 tRNA genes coding all 20 amino acids were identified. Among the CDS, the genome annotation revealed a total of 6,225 protein coding genes, 5,225 (83.9%) of which were functionally assigned. The function of the remaining 1,000 genes could not be predicted, and hence they were designated hypothetical. Also, 40 CDS were annotated as pseudo genes. Quality analysis of the genome revealed 99.7% completeness, indicating high quality of the genome sequenced. The genome of *Paenibacillus* sp. LS1 included all 107 known housekeeping (marker) genes (McLean et al., 2013), further emphasizing the completeness of the genome. RAST annotation further classified the identified protein-coding genes into 26 categories of 316 subsystems (Figure 12).

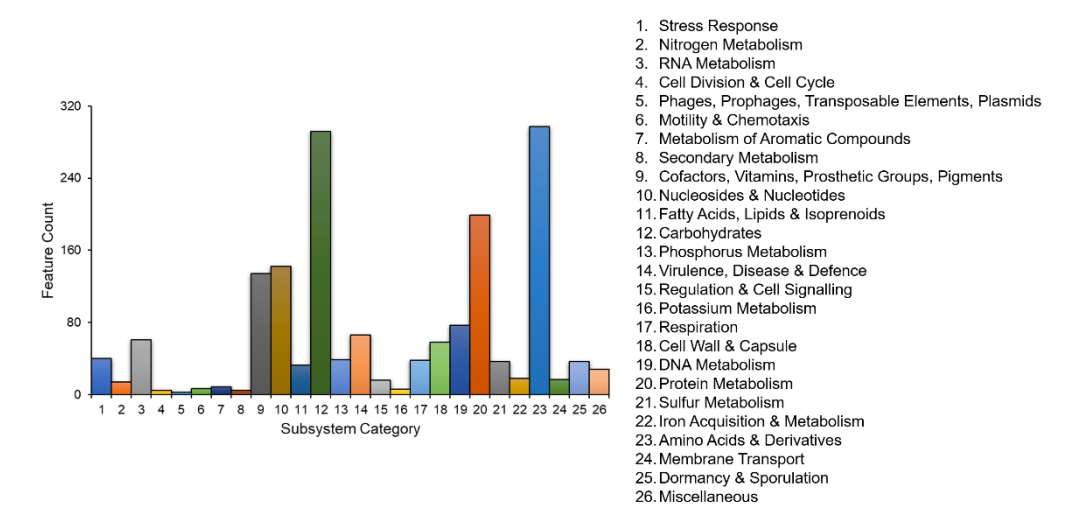


**Figure 12:** Distribution of features among 26 subsystem categories in the annotated of genome of *Paenibacillus* sp. LS1 by the Rapid Annotation using Subsystem Technology (RAST) server.

#### 2.2.5 Paenibacillus sp. LS1 is a novel species

Genome-based relatedness was estimated in terms of OrthoANIu and *in silico* DDH. Among the phylogenetic neighbours (Figure 6), genomes for the *Paenibacillus* strains, *P. tundrae* A10b<sup>T</sup>, *P. tylopili* MK2<sup>T</sup>, *P. cucumis* AP-115<sup>T</sup>, and *P. oceanisediminis* L10<sup>T</sup> were not available in the NCBI genome database, and hence these were not considered for calculating OrthoANIu and DDH values. On the other hand, in a comparison against the closest phylogenetic neighbours, *P. amylolyticus* NBRC 15957<sup>T</sup> and *P. xylanexedens* DSM 21292<sup>T</sup>, OrthoANIu values of 92.17% and 92.28% and DDH values of 46.9% and 47.1%, respectively were obtained (Table 1). Furthermore, the OrthoANIu and DDH values obtained for the other phylogenetic neighbours, *P. polysaccharolyticus* BL9<sup>T</sup>, *P. pabuli* NBRC 13638<sup>T</sup>, *P. xylanilyticus* LMG 21957<sup>T</sup>, and *P. taichungensis* DSM 19942<sup>T</sup> were in the range of 78 to 82% and 22 to 25.5%, respectively (Table 1). Clearly, the genome relatedness values were below the assigned cutoffs for ANI (<95%) and DDH (<70%), therefore indicating *Paenibacillus* sp. LS1 as a novel species in the *Paenibacillus* genus.

**Table 1:** OrthoANIu and *in silico* DDH values for *Paenibacillus* sp. LS1 compared against its phylogenetic neighbours

Phylogenetic neighbours	OrthoANIu	DDH
Paenibacillus amylolyticus NBRC 15957	92.17%	46.90%
Paenibacillus xylanexedens DSM 21292	92.28%	47.10%
Paenibacillus polysaccharolyticusBL9	78.53%	22.50%
Paenibacillus pabuli NBRC 13638	81.87%	25.20%
Paenibacillus xylanilyticus LMG 21957	80.60%	23.90%
Paenibacillus taichungensis DSM 19942	82.07%	25.50%

#### 2.2.6 Exploring the chitin-active enzyme repertoire of Paenibacillus sp. LS1

The CAZyme repertoire of *Paenibacillus* sp. LS1 consisted of 299 unique proteins comprising of 315 CAZyme domains. The genome of *Paenibacillus* sp. LS1 was dominated by 181 glycoside hydrolases (GH), followed by 61 carbohydrate-binding modules (CBM), 27 glycosyl transferases (GT), 30 carbohydrate esterases (CE), 15 polysaccharide lyases (PL) (Figure 13),

and 1 auxiliary activity (AA) family 7 protein. No putative AA10 lytic polysaccharide monooxygenases (LPMOs) were identified.

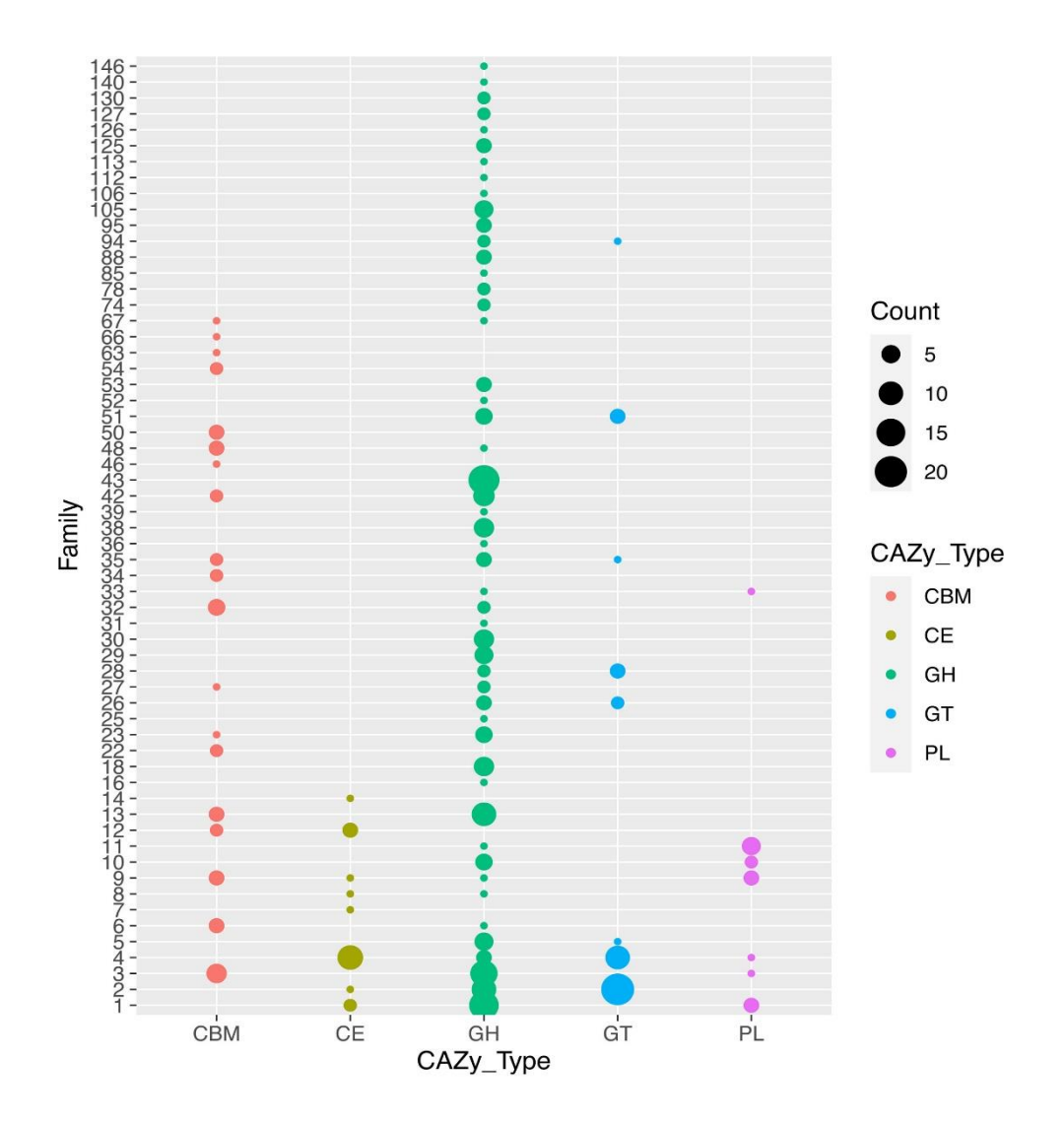


**Figure 13:** Family-wise distribution of different CAZyme classes in the genome of *Paenibacillus* sp. LS1. The different CAZyme classes shown are CBM, carbohydrate binding modules; CE, carbohydrate esterases; GH, glycoside hydrolases; GT, glycosyl transferases; PL, polysaccharide lyases.

The genome of *Paenibacillus* sp. LS1 was dominated by CAZymes that primarily targets hemicellulose, particularly xylan (Mukherjee *et al.*, 2023). Interestingly, the genome of *Paenibacillus* sp. LS1 comprised of at least one representative member from each xylan-active CAZyme family, which is a unique feature shared by only five other *Paenibacillus* species (Mukherjee *et al.*, 2023). Furthermore, in the study conducted by Mukherjee *et al.* (2023), comparative genome analysis involving 238 *Paenibacillus* genomes comprehensively

confirmed that the members of the *Paenibacillus* genus are predominantly xylan degraders, irrespective of the habitat in which they thrive.

The genome of *Paenibacillus* sp. LS1 was investigated to understand the chitinolytic machinery encoded. The genome encoded six CAZymes belonging to the GH18 family, which were named as Chi1 (WP\_264925983.1), Chi2 (WP\_264929137.1), Chi3 (WP\_264931687.1), Chi4 (WP\_264932899.1), Chi5 (WP\_264930993.1) and Chi6 (WP\_264931502.1). Among these, Chi5 and Chi6 were found to be present in the same genetic locus, forming a CAZyme gene cluster (CGC) along with two non-chitin-active enzymes, CE8 (WP\_264930994.1) and GH105 (WP\_264930995.1), a transcription factor (WP\_264930996.1 - LacI family DNA-binding transcriptional regulator) and components of an ABC transport system (WP\_264930997.1 - sugar/solute binding protein; WP\_264930998.1 and WP\_076332232.1 - permeases) (Figure 14). The other GH18 family proteins of *Paenibacillus* sp. LS1, i.e., Chi1-Chi4 were located in distinct genetic loci and were not a part of any CGC (Figure 14). Interestingly, chitin was predicted as the substrate for only Chi5 and Chi6 by the substrate prediction modules of dbCAN3. This indicates that Chi5 and Chi6 could be chitinases. No substrate was detected for the other GH18 family proteins of *Paenibacillus* sp. LS1.

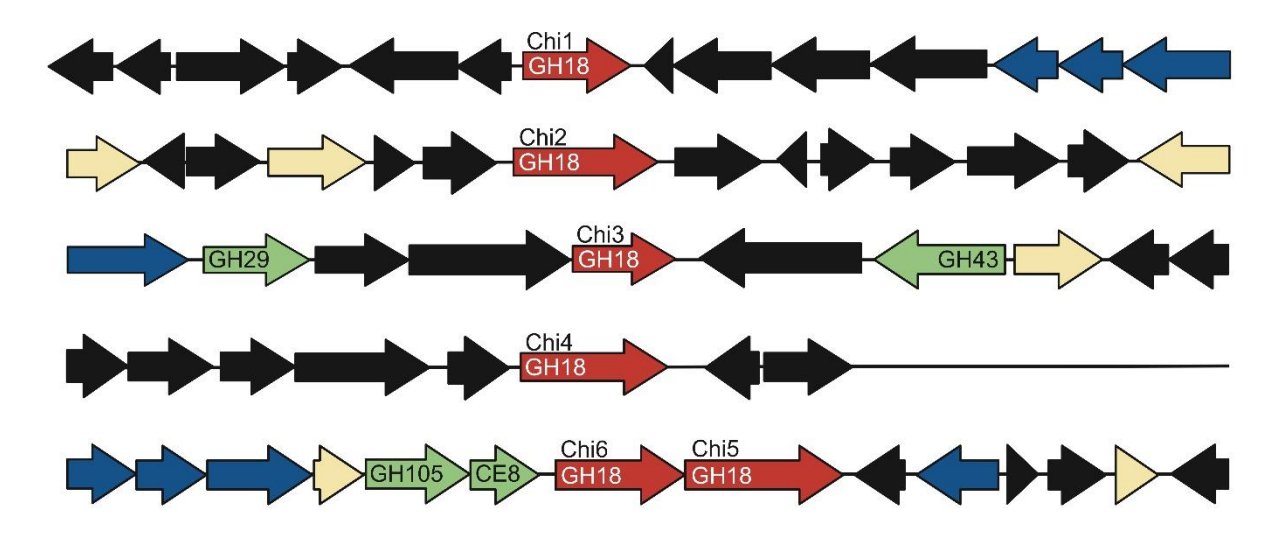


**Figure 14**: Arrangement of the chitinase genes in the genome of *Paenibacillus* sp. LS1. The direction of the arrows indicates the strand in which they are located. Arrows in red: represent the genes coding for the chitinases; green: genes coding for other CAZymes; blue: genes of transporter components; yellow: transcription factors/regulators; black: unrelated genes or genes coding for hypothetical proteins. Only the chitinases are labelled with their respective names at the top of the arrows.

Distinct domain architecture was observed for the six GH18 family proteins from *Paenibacillus* sp. LS1 (Figure 15). Among them, Chi1, Chi2, Chi5 and Chi6 had a N-terminal

signal peptide (Sec/SPI type signal peptide - transported by the Sec translocon and cleaved by Signal Peptidase I), indicating translocation of these chitinases to the bacterial cell membrane and/or secretion outside the cell (Figure 15). Whereas, signal peptide was absent in Chi3 and Chi4, suggesting their cytosolic localization and putative role inside the cell. Chi1 (45.6 kDa; pI 8.7) and Chi4 (64.3 kDa; pI 5.2) are bi-modular enzymes, having a copper amine oxidase-like N-terminal domain (CuAO), along with a GH18 catalytic domain (Figure 15). Till date, presence of a CuAO was not reported for any GH18 family protein. BLAST analysis against the PDB database did not provide any hits for Chi1. Chi4 on the other hand, shared 24.5% sequence identity with SleL from *Bacillus megaterium* QM B1551 (PDB ID: 4S3K), which is a *N*-acetylglucosaminidase with catalytic activity against fragments of cortical peptidoglycan surrounding the bacterial spore protoplast (Üstok *et al.*, 2015). Interestingly, the GH18 and the CuAO domains of Chi1 and Chi4 shared very low sequence identity (20-21%) among each other.

Chi2 (60.2 kDa; pI 5.3) comprised of three tandemly arranged S-layer homology domains (SLH) at the N-terminal and a GH18 catalytic domain at the C-terminal (Figure 15). The SLH domains are highly conserved in bacterial surface layer enzymes/proteins that binds non-covalently to the bacterial cell surface or peptidoglycan (Itoh *et al.*, 2014). Therefore, the presence of SLH domains in Chi2 suggest that it might be a cell surface-expressed GH18 enzyme with potential activity towards peptidoglycan. Further, Chi2 shared only 25.4% identity with an uncharacterized GH18 family protein from *Pseudomonas protegens* Pf-5 (PDB ID: 4Q6T), indicating its enigmatic nature. Further, the genome of *Paenibacillus* sp. LS1 encoded only one uni-modular chitinase, Chi3 (38.9 kDa; pI 5.0), which shared 71.7% identity with the GH18 *N*-acetylglucosaminidase from *P. barengoltzii* CAU904 (PDB ID: 6INX). Lack of signal peptide combined with putative β-*N*-acetylglucosaminidase activity, suggests that Chi3 is an intracellular GH18 protein, that may have implication towards hydrolysis of (GlcNAc)<sub>2</sub> or CHOS into GlcNAc inside the cell.

The genome of *Paenibacillus* sp. LS1 encoded only two multi-modular chitinases, that comprised of accessory/binding domains known for attachment to the chitin substrate for efficient hydrolysis. Chi5 consisted of two tandemly arranged fnIII domains, followed by a putative CBM12 domain at the C-terminal (Figure 15). On the other hand, Chi6 had the putative CBM12 domain at the N-terminal, followed by an fnIII domain and a C-terminal GH18 domain. Considering the position of the binding domains, Chi5 and Chi6 can be predicted to mediate hydrolysis from non-reducing and reducing end of a chitin chain, respectively Horn et al., 2006a). Chi5 (73.5 kDa; pI 5.9) shared 97.6% sequence identity with Chitinase A1 of *B*.

circulans WL-12 (PDB ID: 1ITX) (Matsumoto et al., 1999), one of the well-characterized chitinase known till date. On the other hand, Chi6 (55.5 kDa; pI 6.4) shared 52.7% identity with a chitinase from B. anthracis (PDB ID: 5KZ6). Additionally, the putative CBM12 modules in Chi5 and Chi6 shared 84.4% and 61.9% identity, respectively, with the CBM12 module appended to Chitinase A1 of B. circulans WL-12 (PDB: ID: 1ED7) (Ikegami et al., 2000). Interestingly, the CBM12 modules of the two chitinases, shared only 55.3% identity between each other, suggesting uniqueness at the sequence-level and possibly in the binding properties as well. Furthermore, there was sequence-level variation among the fnIII domains of the chitinases. The two fnIII domains of Chi5 shared sequence identity of 75.6% among each other, while the fnIII domain of Chi6 shared ~57% identity with those of Chi5.

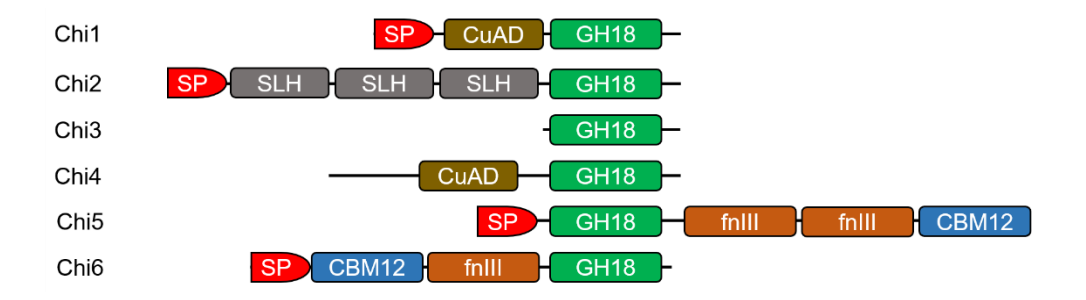


**Figure 15:** Schematic representation of the domain organization of the predicted GH18 family proteins in *Paenibacillus* sp. LS1. SP, signal peptide; GH, glycoside hydrolase; CBM, carbohydrate-binding module; CuAD, copper amine oxidase-like N-terminal domain; SLH, S-layer homology domain; fnIII, fibronectin type-III domain.

Furthermore, the chitinolytic machinery of *Paenibacillus* sp. LS1 also comprised of three β-*N*-acetylglucosaminidases of the GH3 family (WP\_264926219.1, WP\_264927774.1 and WP\_264933369.1) and a FAD-binding oxidoreductase of the AA7 family (WP\_264929783.1). These proteins were predicted to have a preference towards chitin as per the dbCAN3-substrate prediction module.

# 2.2.7 Chi5 and Chi6 are responsible for extracellular chitin degradation by Paenibacillus sp. LS1

The secretome fractions produced by *Paenibacillus* sp. LS1 over the substrates,  $\alpha$ -chitin,  $\beta$ -chitin and glucose were collected at three different time intervals (48 h, 96 h and 216 h) in quadruplicates (i.e., four culture flasks per condition per time point) for proteomic investigation. While the isolate was also inoculated into M9 media supplemented with 0.5% GlcNAc, it showed no growth in GlcNAc, indicating a lack of required transporters for the

uptake of GlcNAc into the cell for metabolism. The secretome analysis revealed detection of a total of 1133 proteins, of which, only 161 proteins (14.2%) were identified as secreted, based on the combined analysis using SignalP v.6.0, SecretomeP v.2.0 and DeepTMHMM v.1.0.39. Previously, proteomic investigation of the chitin-active secretome produced by *Cellvibrio japonicus* Ueda107 revealed the secreted protein content to be 29% and 75%, obtained from shaking flask culture method and agar-plate method, respectively (Tuveng *et al.*, 2016). In a different study reporting secretome analysis of *Andreprevotia ripae* IGB-42, only 18% of the total detected proteins were identified as secreted (Lorentzen *et al.*, 2021). The detection of cytosolic proteins in the bacterial secretomes is a common phenomenon and is mainly attributed to several factors such as: i) cell lysis during culturing process; ii) secretion of cytosolic proteins via known or unknown non-classical mechanisms; iii) some proteins may be "moonlighting" by having functions both in and out of the cell (Tuveng *et al.*, 2016).

A total of 23 CAZymes were identified among the secreted proteins (Figure 16). A heat map depicting hierarchical clustering of these CAZymes based on their abundance on the three substrates tested (α-chitin, β-chitin and glucose) revealed four distinct clusters. Of the four clusters, I and III were the stand out. Cluster I comprised of proteins showing high abundance on all three substrates, but distinctively high on  $\alpha$ - and  $\beta$ -chitin than glucose (Figure 16). On the other hand, cluster III include proteins showing moderately high abundance in all three substrates (Figure 16). Cluster I comprised of the two multi-modular chitinases encoded in the genome of *Paenibacillus* sp. LS1, i.e., Chi5 (WP 264930993.1) and Chi6 (WP 264931502.1), which showed the highest abundance among all the secreted CAZymes in both  $\alpha$ - and  $\beta$ -chitin as compared to glucose (Figure 16). This indicates the significance of these multi-modular chitinases in the extracellular chitin degradation by Paenibacillus sp. LS1. As compared to Chi6 (WP 264931502.1), Chi5 (WP 264930993.1) showed ~2-folds higher abundance on αchitin in all the time points and 2-, 7.5- and 3-folds higher abundance on β-chitin at 48, 96 and 216 h, respectively. This in turn, suggests that Chi5 is more efficient in crystalline chitin degradation than Chi6. Additionally, a weak abundance was observed for the CuAO-domain containing Chi4 (WP 264932899.1) in the secretome fractions collected over all the three substrates (Figure 16), indicating no significant contribution to the extracellular chitin degradation process. Notably, Chi4 is a part of cluster IV in the heatmap, which comprised of proteins that showed low abundance or were not detected in atleast one time point of atleast one substrate (Figure 16). None of the other GH18 family proteins encoded in the genome of Paenibacillus sp. LS1 (i.e., Chi1, Chi2 and Chi3) were detected in the secretome fractions. This

suggests that these proteins may not have any possible role in crystalline chitin degradation at the extracellular level.

Most of the CAZymes detected in the secretome fractions are not canonically known for chitin degradation. Of these, the most relevant ones were WP\_264929146.1 (GH5\_8), WP\_264929559.1 (GH30\_8+CBM35) and WP\_319951928.1 (PL11) from cluster I and WP\_264935300.1 (GH53) from cluster III (Figure 16). These CAZymes showed high abundance on both chitin substrates as compared to glucose, therefore indicating promiscuous chitinase activity towards highly crystalline chitin substrates. A similar observation was made during the secretome analysis of *C. japonicus* Ueda107 grown over different chitin substrates (Tuveng *et al.*, 2016).

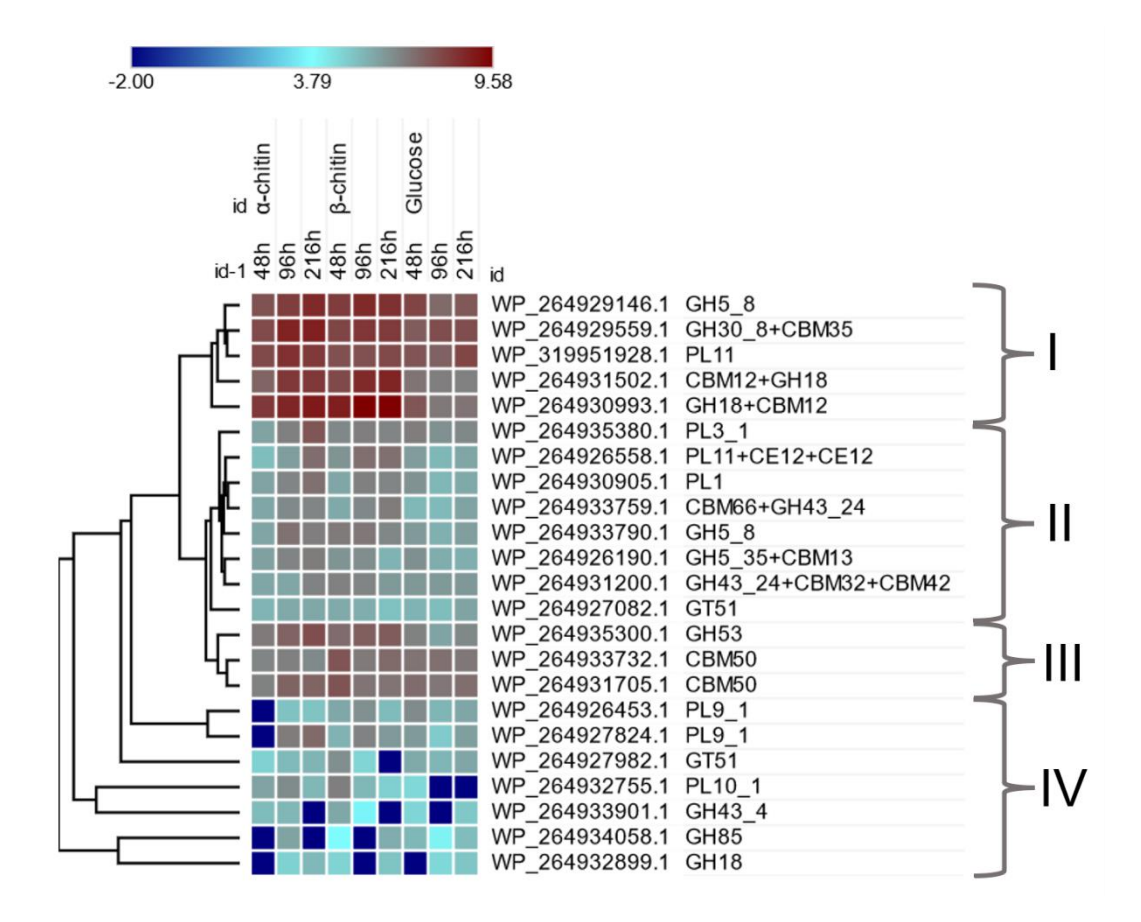


**Figure 16:** Heatmap of secreted CAZymes from *Paenibacillus* sp. LS1. The figure shows a heat map of 23 detected CAZymes that were secreted during growth of *Paenibacillus* sp. LS1 on α-chitin, β-chitin and glucose at different time-points (48 h, 96 h and 216 h). The color indicates protein abundance, log<sub>10</sub> label free quantitation (LFQ) and represents the average of three biological replicates. The LFQ scale is shown on top of the heatmap. Protein accession numbers (RefSeq) and the CAZy annotations are shown in the columns. Abbreviations: GH – Glycoside Hydrolase; CBM – Carbohydrate Binding Module; PL – Polysaccharide Lyase; GT – Glycosyl Transferase. The proteins were hierarchically clustered based on protein abundance patterns which segregated dividing into four clusters (I-IV): I – high abundance in all three

substrates, but distinctively high on the chitin substrates; II – moderate or moderately low abundance in all substrates; III – moderately high abundance in all substrates; IV – low abundance in all substrates. The proteins were hierarchically clustered based on protein abundance patterns.

Apart from CAZymes, a total of 63 substrate-binding proteins of different transporter complexes were detected among the secreted proteins (Figure 17). Interestingly, only WP 264927784.1 (annotated as an extracellular solute-binding protein) showed significantly high abundance on both  $\alpha$ - and  $\beta$ -chitin as compared to glucose, indicating its specificity towards the transport of chitin-derived products, possibly (GlcNAc)<sub>2</sub> (not GlcNAc, since the bacteria is unable to utilize the substrate). The protein showed nearly 34-, 276- and 96-folds high abundance on α-chitin at 48 h, 96 h and 216 h, respectively, as compared to glucose (Figure 17). Similarly, the protein showed nearly 102-, 122- and 2-folds high abundance on βchitin at 48 h, 96 h and 216 h, respectively, as compared to glucose (Figure 17). The geneencoding this protein, was found to be part of a transporter complex, comprising of two permeases (WP 264927782.1 and WP 264927780.1) and a sensor histidine kinase (WP 264927778.1) present downstream of WP 264927784.1. This putative CHOS-specific transporter might be a part of a CAZyme gene cluster (CGC) since the same genetic locus also harbours the GH3 β-N-acetylglucosaminidase (WP 264927774.1) located downstream of the transporter complex. Additionally, the accession numbers, WP 264931395.1 (annotated as oligopeptide ABC transporter substrate-binding protein), WP 062833423.1 (annotated as BMP family ABC transporter substrate-binding protein) and WP 264928076.1 (annotated as ABC transporter substrate-binding protein) showed nearly equal abundances in all three substrates (Figure 17), suggesting that they might also facilitate transport of (GlcNAc)2, but are not specific towards the substrate. Surprisingly, the sugar-binding protein (WP 264930997.1) of the transporter complex that is part of the Chi5-Chi6 CGC, was not detected in the secretome fractions, indicating that the transporter might have a distinct substrate preference. Apart from these, several other proteins (75 in number) were also detected in the chitin-active secretomes produced by Paenibacillus sp. LS1.

The results taken together provide a comprehensive insight into the chitinolytic potential of the novel isolate, *Paenibacillus* sp. LS1 through biochemical, genomic and proteomic approaches. The biochemical studies show the preference of the isolate towards crystalline chitin substrates, particular  $\beta$ -chitin. The genome analysis identified six GH18 family proteins, which could be putative chitinases. Whereas, the proteome analysis of the secretome fractions collected over  $\alpha$ - and  $\beta$ -chitin reveal the multi-modular chitinases, Chi5

and Chi6 as the key enzymes for extracellular chitin degradation by the bacteria. However, further investigation might be required to understand the possible reason(s) behind the expression of these two chitinases and the non-expression of the other encoded GH18 family proteins (particularly those with an N-terminal signal peptide) of *Paenibacillus* sp. LS1 during growth on chitin.

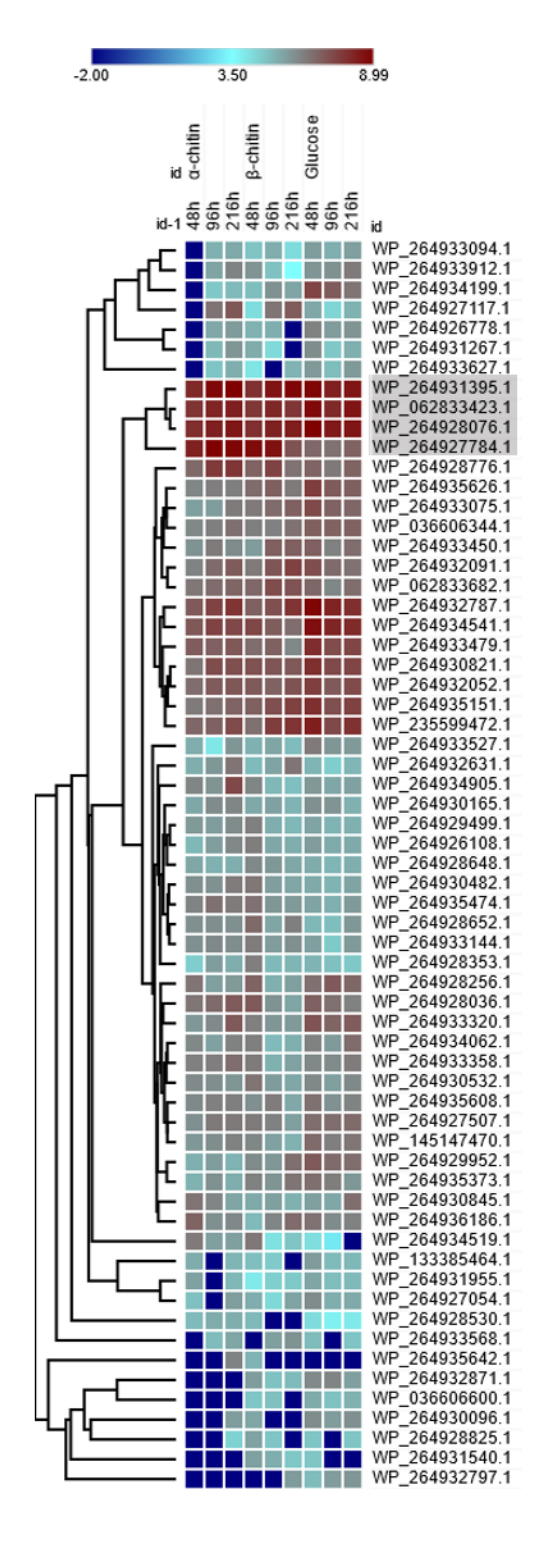


Figure 17: Heatmap of secreted substrate-binding proteins of the different transporter systems encoded by Paenibacillus sp. LS1. The figure shows a heat map of 63 detected substrate-binding proteins of different transporter systems that were secreted during growth of *Paenibacillus* sp. LS1 on α-chitin, β-chitin and glucose at different timepoints (48 h, 96 h and 216 h). The color indicates protein abundance, log<sub>10</sub> label free quantitation (LFO) and represents the average of three biological replicates. The LFQ scale is shown on top of the heatmap. Protein accession numbers (RefSeq) are shown in the columns. The proteins were hierarchically clustered based on protein abundance patterns. The four accessions highlighted in grey represent proteins that showed exceptionally high abundance on all three substrates, particularly  $\alpha$ - and  $\beta$ -chitin.

# **Chapter-3**

Molecular characterization of selected chitinases from *Paenibacillus* sp. LS1

# 3.1 Materials & Methods

#### 3.1.1 Chemicals and reagents

The different chitin substrates: α- and β-chitin and chitosans (75-85% DDA and 90% DDA) were procured from Stellar Bio-Sol, Gujarat, India. Colloidal chitin was prepared using chitin flakes (Stellar Bio-Sol, Gujarat, India) as described in section 2.1.2. CM-cellulose and Avicel were procured from Sigma Aldrich, USA. HPLC graded Acetonitrile was purchased from Merck (Merck KGaA, Germany). Q5<sup>®</sup> High-Fidelity DNA polymerase was procured from New England Biolabs, USA. Restriction enzymes (*EcoRI*, *NcoI*, *NdeI* and *XhoI*) and T4 DNA ligase were procured from ThermoFisher Scientific, USA. NucleoSpin Microbial DNA kit, Plasmid mini kit and Gel and PCR Clean-up mini kit were procured from Macherey-Nagel, Germany. GeneRuler 1 kb DNA Ladder and 3 colour Prestained Protein Ladder (10-250kDa) were procured from ThermoFisher Scientific, USA and Genetix Biotech Asia Pvt. Ltd., New Delhi, India, respectively. Ni-NTA agarose resin was procured from Qiagen, USA. Pierce<sup>TM</sup> BCA protein assay kit was procured from ThermoFisher Scientific, USA. All chemicals required for Schales' reagent, buffers and LB broth were obtained from HiMedia or Sisco Research Laboratories Pvt. Ltd., India unless specified otherwise.

#### 3.1.2 Structure-based sequence alignment

Structure-based sequence alignment of the GH18 family proteins from *Paenibacillus* sp. LS1 was performed against *Sm*ChiB from *Serratia marcescens* (PDB ID: 1E15) and *Bc*ChiA1 from *B. circulans* WL-12 (PDB: 1ITX) from the PDB database using T-Coffee web-server and the output was generated using ESPript 3.0. Amino acid sequences of only the catalytic (GH) domain were considered for alignment.

#### 3.1.3 Cloning and heterologous over-expression of the Paenibacillus sp. LS1 chitinases

Paenibacillus sp. LS1 was grown in LB broth for 24 h and the harvested culture pellet was used for DNA isolation using the standard procedure, essentially described in the manufacturer's protocol of the NucleoSpin Microbial DNA kit (Macherey-Nagel, Germany). The genes coding for the chitinases were amplified by PCR using the oligonucleotide genespecific forward and reverse primers listed under Table 2. The PCR products were analyzed by 1% agarose gel electrophoresis against the GeneRuler 1 kb DNA Ladder (ThermoFisher

Scientific, USA). The amplicons of desired size (Chi1- 1.3 kb; Chi2 – 1.6 kb; Chi3 – 1.1 kb; Chi4 – 1.7 kb; Chi5 - 2.1 kb; and Chi6 – 1.5 kb) were excised using a sterile scalpel under a UV transilluminator. Amplicon DNA extraction from the excised gel pieces was performed using Gel and PCR Clean-up mini kit (Macherey-Nagel, Germany). The amplicons (≥1 µg) were double digested for 8h at 37°C using the respective restriction enzymes indicated in Table 2 (underlined). The double digested amplicons were purified using Gel and PCR Clean-up mini kit (Macherey-Nagel, Germany) and ligated to the respective restriction sites (underlined in Table 2) of the pET-22b(+) or pET-28a(+) expression vector, with 6X-Histidine tag to its 3' end. Ligation was performed at 22°C for 60 min, using T4 DNA ligase (ThermoFisher Scientific, USA). The ligation mixture was then transformed into highly efficient competent cells of E. coli DH5a. Positive clones were screened on LB-agar plates containing ampicillin (100 μg/mL) or kanamycin (50 μg/mL) depending on the vector [pET-22b(+) or pET-28a(+), respectively] and further confirmed by colony PCR, double digestion and automated Sanger sequencing (availing services from Eurofins India Pvt. Ltd., Bengaluru, India). Note: high quality plasmids were isolated using Plasmid mini kit (Macherey-Nagel, Germany) for double digestion and sequencing.

**Table 2:** List of primers used for the cloning of chitinases from *Paenibacillus* sp. LS1. Underlined sequences indicate restriction sites: GAATTC – *Eco*RI; CCATGG – *Nco*I; CATATG – *Nde*I; CTCGAG – *Xho*I.

S.No.	Name of the gene	Template used for	Primer combination	Primer sequence (5'- 3')
		PCR	used	
1.	Chi1	Genomic	Chi1-Fp	AATAACCATGGCAATGTTCATTAAACGTGTA
		DNA	Chi1-Rp	AATAA <u>CTCGAG</u> TTCTTTGATCACAGAAGC
2.	Chi2	Genomic	Chi2-Fp	AATAA <u>CCATGG</u> TGAATAATAGATTAAAAG
		DNA	Chi2-Rp	AATAA <u>CTCGAG</u> GAAGTTATATGATTCAAA
3.	Chi3	Genomic	Chi3-Fp	AATAA <u>CCATGG</u> CAATGACGAAATATATTGCT
		DNA	Chi3-Rp	AATAA <u>CTCGAG</u> TCCTATTTTCCCAGCCGG
4.	Chi4	Genomic	Chi4-Fp	AATAA <u>GAATTC</u> AATGGGTAGAAAAAGCAGAT
		DNA	Chi4-Rp	AATAA <u>CTCGAG</u> TTTCTGGTAACCGGCCTG
5.	Chi5	Genomic	Chi5-Fp	AATAA <u>CCATGG</u> CAATGCCAAATGTAAATAAA
		DNA	Chi5-Rp	AATAA <u>CTCGAG</u> TTGGACCTGCCACAATGA
6.	Chi6	Genomic	Chi6-Fp	AATAA <u>CATATG</u> TTGAATAAAGCTGTTCAA
		DNA	Chi6-Rp	AATAA <u>CTCGAG</u> GTACACAACCTCCTTTGT

The sequence verified clones of the respective chitinases, were transformed into *E. coli* competent cells for over-expression of the proteins (BL21(DE3) or BL21(DE3)pLysS or Rosetta-gami 2(DE3)). A single colony was inoculated into LB broth containing 100 μg/mL ampicillin or 50 μg/mL kanamycin (along with 50 μg/mL chloramphenicol, only if the

respective clone was transformed into Rosetta-gami 2(DE3) cells) and incubated overnight at 37°C and 180 rpm shaking for overnight. This was treated as the primary inoculum. One percent primary inoculum was inoculated into fresh LB broth containing ampicillin (100 μg/mL) or kanamycin (50 μg/mL) (along with 50 μg/mL chloramphenicol, only if the respective clone was transformed into Rosetta-gami 2(DE3) cells) and incubated at 37°C and 180 rpm shaking. The cultures were grown until the OD<sub>600</sub> reaches between 0.4-0.6 and then IPTG was added to a final concentration of 0.3-0.7 mM. The cells were further grown at 37°C for 4 h or 18°C/28°C for 16 h, followed by harvesting at 8000 rpm for 10 min at 4°C. **Note:** The uninduced culture of the respective clones (control) were also maintained under similar experimental conditions.

The overexpressed protein was isolated by sonication using a Sonic-Ultrasonic Processor VCX-750 sonicator. The harvested cells were resuspended in the lysis buffer (50 mM NaH<sub>2</sub>PO<sub>4</sub>, 300 mM NaCl and 10 mM imidazole; pH 8.0) and 0.1 mM phenylmethylsulfonyl fluoride (PMSF) was added before cell disruption by sonication. The sonication was performed at 4°C and 30% amplitude for 5 min at 20 s on and 40 s off cycles. Frequent monitoring of the sample was done to avoid heating. The sonicated sample was then centrifuged at 10000 rpm for 60 min at 4°C to separate the pellet and supernatant. The sonicated pellet and supernatant along with the uninduced pellet were analyzed by 12% SDS-PAGE. Following electrophoresis, the gel was stained with Coomassie Blue G-250 for 10-12 h and destained using double distilled water.

#### 3.1.3 Purification, concentration and buffer-exchange of Chi3 and Chi5

The uni-modular chitinase, Chi3 and the multi-modular chitinase, Chi5 from *Paenibacillus* sp. LS1 were over-expressed following the method described in the section above, using 0.3 mM and 0.5 mM IPTG, respectively and growing the cells at 18°C for 16 h, post-induction. The over-expressed proteins were isolated by sonication as described in the section above. The sonicated cell lysate (supernatant) obtained was used for purification by Ni-NTA affinity chromatography as essentially described by Madhuprakash *et al.* (2015) with slight modifications.

Four mL ethanol suspension of Ni-NTA agarose (Qiagen, USA) was packed into a sterile 10 mL syringe. The column was equilibrated with 25 column volumes (CV) of lysis buffer, followed by application of the sonicated cell lysate onto the column. Flow through was collected and the column was washed with 13 column volumes of wash buffer (50 mM NaH<sub>2</sub>PO<sub>4</sub>, 300 mM NaCl and 20 mM imidazole; pH 8.0). Bound recombinant protein was

eluted in a gradient manner using elution buffers of varying imidazole concentrations (50 mM NaH<sub>2</sub>PO<sub>4</sub>, 300 mM NaCl and 50 mM (E1), 150 mM (E2) and 250 mM (E3) imidazole; pH 8.0). The purified fractions were analyzed on 12% SDS-PAGE and fractions with the highest purity were concentrated using Vivaspin Turbo 15 PES, MWCO 10 kDa centricon (Sartorius, Germany) and buffer exchanged with 50 mM Tris Cl pH 7.5. Both proteins were quantified using Pierce<sup>TM</sup> BCA protein assay kit (ThermoFisher Scientific, USA).

### 3.1.4 Determination of optimum pH, temperature and steady-state kinetics for Chi3 and Chi5

Purified Chi3 and Chi5 were used for all the characterization experiments. Both the chitinases at 1 μM final concentration was incubated with 5 mg/mL CC in 50 mM solution of various pH buffers and the reaction was performed at 37°C and 800 rpm for 1 h. The buffers used were glycine-HCl (pH 2.2 and 3), sodium citrate (pH 3, 4, 5 and 6), sodium acetate (pH 4, 5, and 5.5), sodium phosphate (pH 6, 7, and 8), Tris-HCl (pH 7.2, 8 and 9) and glycine-NaOH (pH 9 and 10). Optimum temperature for the chitinases was determined by screening the activity within a temperature range of 10-70°C, at their optimal pH estimated from the above experiment.

Further, the kinetic parameters of Chi3 were determined in 50 mM sodium citrate, pH 5.0 and at 40°C, by incubating 5 μM of the purified chitinase with different concentrations of CC (0–25 mg/mL) at 800 rpm for 1 h in an Eppendorf Thermomixer<sup>®</sup> C. Chitinase activity was determined by analysing the presence of reducing sugars using Schales' assay with slight modifications as described previously (Madhuprakash *et al.*, 2015). After 1 h of reaction, the samples were centrifuged at 11000 rpm for 10 min at 4°C and 40 μL of the supernatant was boiled with 300 μL Schales' reagent (0.5 M Na<sub>2</sub>CO<sub>3</sub> and 0.5 g L<sup>-1</sup> K<sub>3</sub>Fe(CN)<sub>6</sub>). The absorbance was measured at 420 nm and quantification of the reducing sugars was done using a GlcNAc standard curve. Kinetic parameters were determined by fitting the data from obtained from three independent experiments to the Michaelis-Menten equation using non-linear regression function available in GraphPad Prism software version 5.0 (GraphPad Software Inc., San Diego, CA). In case of Chi5, the kinetic parameters were determined in 50 mM sodium acetate, pH 5.0 and at 45°C, using 0.5 μM of the purified chitinase with different concentrations of CC (0-25 mg/mL) and β-chitin (0-50 mg/mL) using the same assay procedure as mentioned above.

### 3.1.5 Determination of substrate specificity of Chi3 and Chi5

Substrate specificity of Chi3 and Chi5 was determined using different chitin substrates like,  $\alpha$ -chitin (shrimp shell chitin),  $\beta$ -chitin (squid pen chitin), CC, chitosans (75–85% and 90% degree

of deacetylation (DDA)), and non-chitinous substrates such as avicel and carboxymethyl-cellulose (CM-cellulose). The substrates at 10 mg/mL final concentration were incubated with 1 μM of Chi3 or Chi5 in 50 mM sodium citrate, pH 5.0 at 40°C or in 50 mM sodium acetate, pH 5.0 at 45°C, respectively, under shaking at 1000 rpm for 1h in an Eppendorf Thermomixer<sup>®</sup> C. Following the reaction, the samples were centrifuged at 11000 rpm for 10 min and the clear supernatant was used for estimating the reducing sugars by Schales' assay as described in section 3.1.4.

#### 3.1.6 Activity of Chi3 and Chi5 towards CHOS

The activity of Chi3 and Chi5 on CHOS was determined by incubating 0.5 mM each of (GlcNAc)<sub>2-6</sub> under optimal reaction conditions (50 mM sodium citrate, pH 5.0 at 40°C or 50 mM sodium acetate, pH 5.0 at 45°C, respectively), with shaking at 1000 rpm in an Eppendorf Thermomixer® C. The reaction was monitored up to 6 h. The enzyme concentration was standardized for each oligomer to monitor the initial phase of reaction. The final Chi3 concentration used was as follows, 500 nM with (GlcNAc)<sub>2</sub> and 100 nM with (GlcNAc)<sub>3-6</sub>. Similarly, the final Chi5 concentration used was as follows, 500 nM with (GlcNAc)2, 50 nM with (GlcNAc)<sub>3-4</sub> and 25 nM with (GlcNAc)<sub>5-6</sub>. Fractions were collected at regular intervals and the enzyme was inactivated by adding equal volume of 70% acetonitrile. Products were analyzed by HPLC (Shimadzu, Japan) on Shodex Asahipak NH2P-50 4E (4.6 mm ID × 250 mm, Shodex, Japan) through isocratic elution using 70% acetonitrile at a flow rate of 0.7 mL/min and at 45°C column oven temperature. CHOS were detected by monitoring the absorbance at 210 nm and quantification was performed using the respective CHOS standards (Madhuprakash et al., 2012). CHOS quantification was done by comparing peak areas of the detected products in the test sample with peak areas obtained from known concentration of the CHOS. For preparing a CHOS standard curve, a mixture of CHOS (standard) ranging from (GlcNAc)<sub>1-6</sub> containing equal weight of the CHOS moieties was used. Standards of different concentrations were prepared (12.5, 25, 50, 125, 250 and 500 µM, in our case). A linear correlation between peak area and concentration of CHOS in the standard samples was established for quantification of products up to (GlcNAc)<sub>6</sub>. Standard curves were constructed separately for each CHOS moiety [i.e., (GlcNAc)<sub>1-6</sub>]. It was ensured that the obtained data points yielded a linear curve for each CHOS with a R<sup>2</sup> value ranging between 0.99-1.0, for determining molar concentration of that CHOS with confidence.

#### 3.1.7 Time-course degradation of crystalline chitin substrates

The ability of Chi3 and Chi5 to hydrolyse different crystalline chitin substrates was also analyzed in a time-dependent manner. All the reactions were performed in triplicates by incubating 1  $\mu$ M Chi3 or Chi5 with 10 mg/mL  $\alpha$ -chitin,  $\beta$ -chitin or CC in 50 mM sodium citrate pH 5.0 at 40°C or 50 mM sodium acetate, pH 5.0 at 45°C, respectively. The reactions were performed under shaking at 1000 rpm in an Eppendorf Thermomixer® C. Fractions were collected at different time points ranging from 1 to 24 h and filtered using a 96-well filter plate (0.45  $\mu$ m filters; Merck Millipore, USA) operated by a Millipore vacuum manifold. The filtered samples were then mixed with equal volume of 70% acetonitrile and analysed on HPLC essentially as described earlier in the section 3.1.6.

# 3.2 Results & Discussion

In Chapter-2, the chitinolytic potential of *Paenibacillus* sp. LS1 was determined through biochemical, genomic and proteomic approaches. While the genome of the isolate encoded six GH18 family proteins, only two i.e., Chi5 and Chi6 displayed significantly high abundance in secretome collected over both  $\alpha$ - and  $\beta$ -chitin. This indicates their pivotal role in extracellular chitin degradation by the isolate. In this chapter, a thorough structure-based sequence analysis of the GH18 family proteins of *Paenibacillus* sp. LS1 was done to understand the presence/absence of essential residues/motifs required for chitinase catalysis. Further, molecular cloning and over-expression, followed by in-depth biochemical characterization of two of the chitinases were also discussed.

#### 3.2.1 Structure-based sequence alignment revealed Chi3, Chi5 and Chi6 as true-chitinases

Structure-based sequence alignment of the six GH18 family proteins was performed on the T-Coffee web-server against the well-characterized chitinases, SmChiB (PDB ID: 1E15) and BcChiA1 (PDB ID: 1ITX) from the PDB database. The alignment was done using the amino acid sequences of the catalytic domain only. The structure-based sequence alignment revealed a conserved DxDxE catalytic motif in case of Chi3, Chi5 and Chi6 (Figure 18). The Asp-Asp-Glu triad of the DxDxE motif is absolutely essential for chitinase catalysis (Synstad et al., 2004) and these three residues were conserved in Chi3, Chi5 and Chi6 (Figure 18). On the other hand, conservation of this motif was not observed in case of Chi1, Chi2 and Chi4, where the first Asp residue of the motif was substituted with Val or Asn (Figure 18). This Asp residue, which is an analogue of Asp140 in SmChiB, respectively, was demonstrated to be crucial for chitinase activity by Synstad et al. (2004). Mutation of this Asp (acidic) residue to Ala (neutral) and Asn (basic) led to drastic reduction in chitinase activity of SmChiB, showing the significance of an acidic amino acid residue at that position (Synstad et al., 2004). Substitution of this Asp residue in Chi1, Chi2 and Chi4 might have led to drastic reduction or loss of chitinase activity of these GH18 family proteins as well. This might also explain the reason for not detecting Chi1 and Chi2 in the chitin-active secretome collected over  $\alpha$ - and  $\beta$ -chitin (despite having a signal peptide).

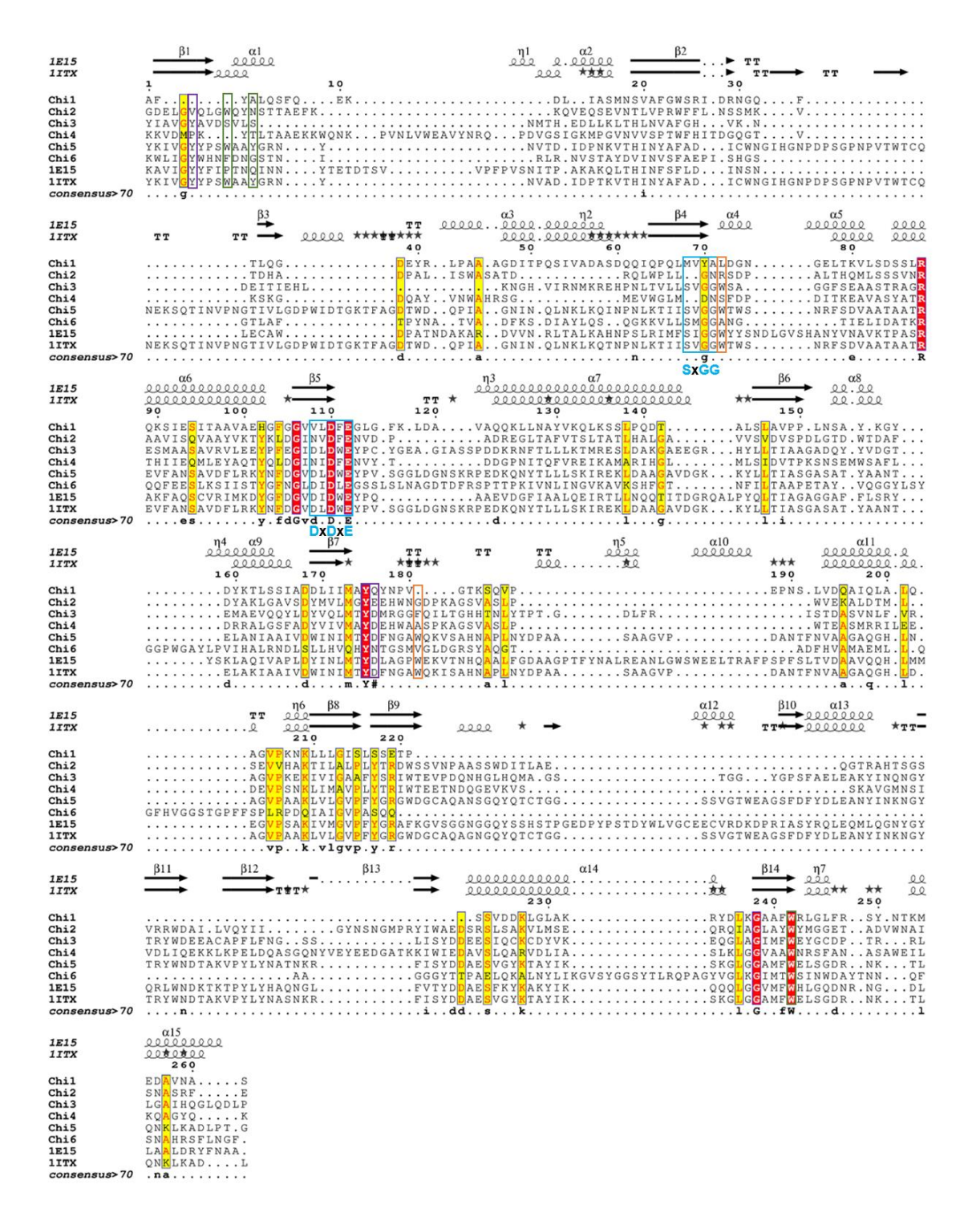


**Figure 18:** Structure-based sequence alignment of the GH18 family proteins from *Paenibacillus* sp. LS1. Catalytic (GH18) domains of Chi1 to Chi6 were aligned against the GH18 domains of *Sm*ChiB (PDB ID: 1E15) and *Bc*ChiA1 (PDB ID: 1ITX) from *S. marcescens* and *B. circulans*, respectively. The DxDxE and SxGG motifs are highlighted within blue marker. Amino acid residues (apart from those in the above-mentioned motifs) reported to be essential for catalysis in *Sm*ChiB (Synstad *et al.*, 2004) are highlighted within purple marker. Residues crucial for processivity in *Sm*ChiB (Horn *et al.*, 2006) are indicated within orange marker. Some residues reported to be crucial for chitinase activity of *Bc*ChiA1 (Watanabe *et al.*, 2003) are marked within green marker.

Similar to the catalytic motif, the SxGG motif was also conserved in case of Chi3, Chi5 and Chi6, while the other three proteins completely lacked it (Figure 18). The serine residue of the SxGG motif (Ser93 in SmChiB) along with a tyrosine residue (Tyr10 in SmChiB), were reported to play a major role in structural rearrangements for Asp functionality of the DxDxE motif (specifically, for Asp142 in SmChiB) during catalysis (Synstad et al., 2004). Moreover, mutation of these residues also caused drastic decrease in specific activity of SmChiB, further signifying the pivotal role of these residues in chitinase catalysis (Synstad et al., 2004). Interestingly, even the Tyr10 equivalent residue was only conserved in Chi3, Chi5 and Chi6 (Figure 18). Two other residues, i.e., Tyr214 and Asp215 in SmChiB are also crucial for catalysis as reported previously (Synstad et al., 2004). These residues along with Asp142 were crucial for binding the -1 sugar in a distorted boat conformation, where primary interaction with the N-acetyl group of the -1 sugar was mediated by Asp142 and Tyr214, while stabilization of the boat conformation was provided by Asp215 in SmChiB (Synstad et al., 2004). Furthermore, Asp215 was also found to increase pKa values in Asp142-Glu144 system (Synstad et al., 2004). The Asp residue equivalent to Asp215 (of SmChiB) was conserved in Chi3, Chi4 and Chi5, while it was substituted to a Gln, Glu and Asn residue in Chi1, Chi2 and Chi6, respectively (Figure 18). Previously, D215N mutation in SmChiB led to a substantial decrease in specific activity and  $K_{\text{cat}}$  value, along with considerable decrease in p $K_{\text{a}}$  value of the Asp142-Glu144 system (Synstad et al., 2004), therefore solidifying the importance of Asp215 in chitinase catalysis. This might also explain the reason for low abundance of Chi6 as compared to Chi5, in the chitin-active secretome collected over  $\alpha$ - and  $\beta$ -chitin (Section 2.2.7). Additionally, the Tyr residue equivalent to Tyr214 residue (of SmChiB) was conserved in all the GH18 family proteins of *Paenibacillus* sp. LS1 (Figure 18).

Furthermore, the amino acids Trp97 and Trp220 (of *Sm*ChiB) were shown to be crucial for processivity of a chitinase, with the former residue having the most profound effect (Horn *et al.*, 2006). The Trp residue equivalent to Trp97 (of *Sm*ChiB) was conserved in Chi3 and Chi5. Whereas, the Trp residue equivalent to Trp220 (of *Sm*ChiB) on the other hand, was only conserved in Chi5 (Figure 18). This indicated the processive nature of both Chi3 and Chi5, while also inferring that Chi6 and the other GH18 family proteins in *Paenibacillus* sp. LS1 were non-processive in nature due to absence of either of these Trp residues.

In addition to this, Watanabe *et al.* (2003) had reported drastic loss of activity of *Bc*ChiA1 exclusively on β-chitin substrate upon mutating the residues Trp53 and Tyr56. Interestingly, the Trp and Tyr residues equivalent to Trp53 and Tyr56 (of *Bc*ChiA1) were conserved only in Chi5 among the six GH18 family proteins (Chi2 showed conservation of

only the Trp53 equivalent residue) (Figure 18). This suggests possibility of remarkable activity of Chi5 on crystalline chitin substrates, particularly β-chitin, as compared to the other GH18 family proteins of *Paenibacillus* sp. LS1. Among the other amino acid residues studied by Watanabe et al. (2003), mutation of Trp433 was shown to be the most deleterious towards BcChiA1 activity, among all the single mutants. Notably, the Trp residue equivalent to Trp433 (of BcChiA1) was found to be conserved in all the GH18 family proteins of Paenibacillus sp. LS1 (Figure 18). The results taken together indicate that the conservation of a majority of the crucial amino acid residues responsible for catalysis and processivity of a chitinase were only present in the uni-modular Chi3 and the multi-modular Chi5 and Chi6. Hence, these three GH18 family proteins from *Paenibacillus* sp. LS1 could be inferred to as "true chitinases" and were selected for molecular cloning and in-depth biochemical characterization. However, considering the unique domain architecture and a high amino-acid level dissimilarity with canonical chitinases observed in case of Chi1, Chi2 and Chi4, they were also included for indepth biochemical characterization. This was done to understand the extent of their activity towards chitin and CHOS substrates, in comparison with the true chitinases of Paenibacillus sp. LS1.

#### 3.2.2 Chi3 and Chi5 were successfully obtained in the soluble fraction

The six GH18 family proteins of *Paenibacillus* sp. LS1 were successfully cloned into suitable expression vector [pET-28a(+) and/or pET-22b(+)] as confirmed by double digestion with suitable restriction enzymes (Figure 19A) and automated Sanger sequencing. However, even after several optimisations with protein over-expression, only two of the proteins could be obtained in the soluble fraction. Chi1 and Chi4 failed to over-express at all (Figure 19B), while no soluble protein could be obtained in case of Chi2 and Chi6 (found in the insoluble inclusion bodies) (Figure 19B and C). Previously, full-length protein of the SLH-domain containing ChiW from *Paenibacillus* sp. FPU-7 could not be obtained in the soluble fraction, while the truncation of the protein (removal of the SLH domains) led to the production of the soluble protein for further characterization (Itoh *et al.*, 2013). Considering this report, Chi2 was truncated (SLH domains were removed) and was successfully cloned in suitable expression vector. However, similar to the full-length protein, the truncated Chi2 also over-expressed but was found in the insoluble inclusion bodies (data not shown).

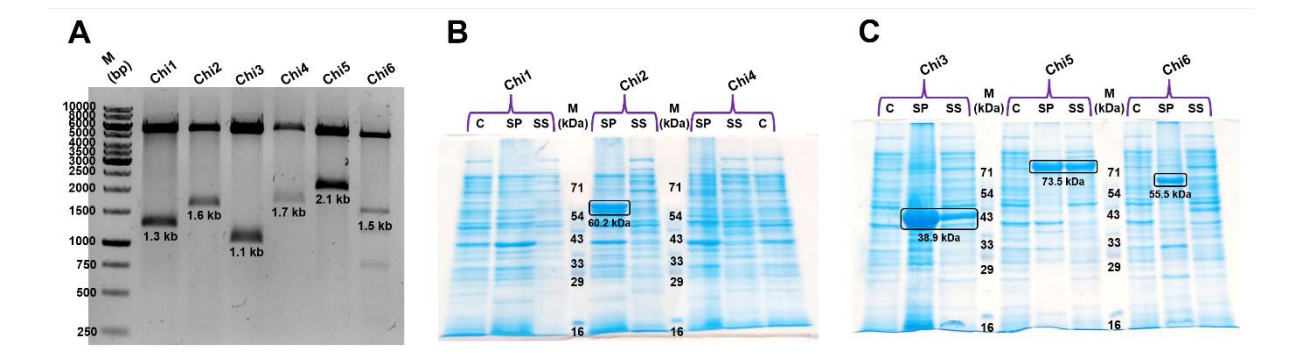


**Figure 19:** Cloning and over-expression of the six GH18 family proteins of *Paenibacillus* sp. LS1. A—represents double digestion confirmation of the six target genes, suggesting successful cloning. B and C—represents over-expression profile of the six recombinantly produced proteins. Over-expressed and/or respective soluble proteins are highlighted within black marker. Abbreviations: C—control/uninduced sample, SP—sonicated pellet, SS—sonicated supernatant, M—molecular weight marker/ladder (in bp or kDa).

After intensive standardisation, Chi3 and Chi5 were successfully over-expressed and most importantly, obtained in the soluble fraction (Figure 19B). The optimised over-expression conditions for Chi3 and Chi5 are listed in Table 3. Additionally, Chi3 and Chi5 could be successfully purified, concentrated and buffer-exchanged in suitable buffer (50 mM Tris-HCl, pH 7.5) and were produced in fairly good yields of ~71 mg/L and ~22 mg/L of culture, respectively. Both of these chitinases were taken forward for in-depth biochemical characterisation.

**Table 3:** Optimised over-expression conditions for Chi3 and Chi5. The yield of soluble protein obtained is indicated by '+', where "+++" indicate high yield and "+" demarcate low yield.

Name of the chitinase	Vector	Expression host	Expression type	Temperature and time	Remarks
Chi3	pET-28a(+)	BL21(DE3)pLysS	IPTG	37°C/18°C,	Over-expressed. Obtained in
			(0.35  mM)	16h	soluble fraction (+++).
Chi5	pET-28a(+)	BL21(DE3)	IPTG	37°C/18°C,	Over-expressed. Obtained
			(0.5  mM)	16h	in soluble fraction (++).

#### 3.2.3 Chi3 was optimally active at low pH and showed preference towards colloidal chitin

The enzyme Chi3 was optimally active in 50 mM sodium citrate, pH 5.0 on CC, and retained up to 92% activity at pH 6.0 of the same buffer (Figure 20A). It also showed 71% and 66% activity at 50 mM sodium acetate, pH 5.5 and Tris-HCl, pH 7.2, respectively, while showing no activity below pH 4.0 and above 8.0 (Figure 20A). This indicated that Chi3 functions at a narrow pH range of 5.0-6.0. Chi3 was optimally active at 40°C and retained up to 86-88%

activity between 30-45°C (Figure 20B). Chi3 shared that same pH and temperature optima with EcChi1 from E. cloacae subsp. cloacae (Mallakuntla et al., 2017) and SmChiD from S. marcescens GPS5 (Vaikuntapu et al., 2016). Chi3 also shared the same temperature optima with other uni-modular chitinases, such as SpChiD from S. proteamaculans 568 (Purushotham and Podile, 2012) and StmChiB from S. maltophilia \*434 (Suma and Podile, 2013), but not the pH optima, which was pH 6.0 and pH 7.0, respectively. Comparisons between Chi3 and its nearest homologue, PbNAG39 from P. barengoltzii CAU904 could not be made since the latter was inactive on CC (Liu, Y. et al., 2020). PbNAG39 was reported to show optimal activity at 50 mM sodium acetate, pH 5.5 and at 75°C on (GlcNAc)<sub>2</sub> as the substrate (Liu, Y. et al., 2020). The results collectively suggest that Chi3 is a mesophilic chitinase that shows preference towards acidic pH.

Michaelis-Menten kinetic parameters for Chi3 were derived with varied concentrations (0-25 mg/mL) of CC as substrate. The curve fitting with non-linear regression function revealed the kinetic parameters  $K_{\rm m}$  and  $V_{\rm max}$  to be  $28.8 \pm 6.7$  mg/mL and  $0.29 \pm 0.04$  nkat/mg of protein, respectively (Figure 20C). Previously,  $K_{\rm m}$  values of 83 mg/mL, 47.9 mg/mL, 15.2 mg/mL and 13.9 mg/mL were reported for the uni-modular chitinases, SpChiD, SmChiD, EcChi1 and CsChiL (Purushotham and Podile, 2012; Vaikuntapu et~al., 2016; Mallakuntla et~al., 2017; Bhuvanachandra and Podile, 2020) on CC as the substrate. Further, the  $K_{\rm cat}$  and overall catalytic efficiency ( $K_{\rm cat}/K_{\rm m}$ ) values obtained for Chi3 were 0.29 s<sup>-1</sup> and 0.01 s<sup>-1</sup> mg<sup>-1</sup> mL, respectively. The obtained values were similar to that of CsChiL ( $K_{\rm cat}$  of 0.20 s<sup>-1</sup>, and  $K_{\rm cat}/K_{\rm m}$  of 0.014 s<sup>-1</sup>mg<sup>-1</sup>mL) (Bhuvanachandra and Podile, 2020) obtained over CC using the similar assay procedure.

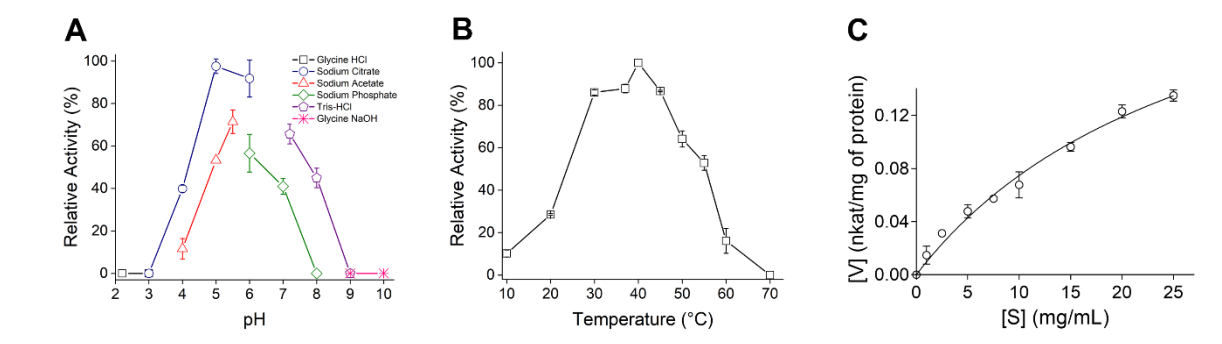


**Figure 20:** Optimal conditions for activity and steady-state kinetics of Chi3. A – represents pH optima for Chi3 activity measured in various buffers of 50 mM strength at different pH. B – represents temperature optima for Chi3 activity by incubating at different temperatures ranging from 10-70°C. C – represents Michaelis-Menten kinetics for Chi3. The kinetics experiment was performed under optimal reaction conditions using varied concentrations of CC as substrate. The kinetic parameters were derived by fitting the data from three independent experiments to the Michaelis-Menten equation using the non-linear regression function in GraphPad Prism v.5.0. All experiments were performed in triplicates and the standard deviations are represented in terms of error bars.

Furthermore, specificity of Chi3 towards different polysaccharides was investigated. In contrast with the reported uni-modular GH18 chitinases, Chi3 showed no activity on the highly crystalline chitin substrates, i.e.,  $\alpha$ - and  $\beta$ -chitin, as well as chitosan with 75-85% DDA (Figure 21). On the other hand, Chi3 showed maximum activity on CC, as well as chitosan with 90% DDA (Figure 21). Interestingly, Chi3 showing activity on CC was distinct from its homologue, *Pb*NAG39, which was inactive on CC (Liu, Y. *et al.*, 2020). Additionally, Chi3 did not exhibit any promiscuous activity on the cellulosic substrates, avicel and CM-cellulose (Figure 21), similar to *Sp*ChiD and *Sm*ChiD (Purushotham and Podile, 2012; Vaikuntapu *et al.*, 2016). Overall, the results indicate Chi3 shows higher preference towards amorphous chitin substrates instead of crystalline chitin.

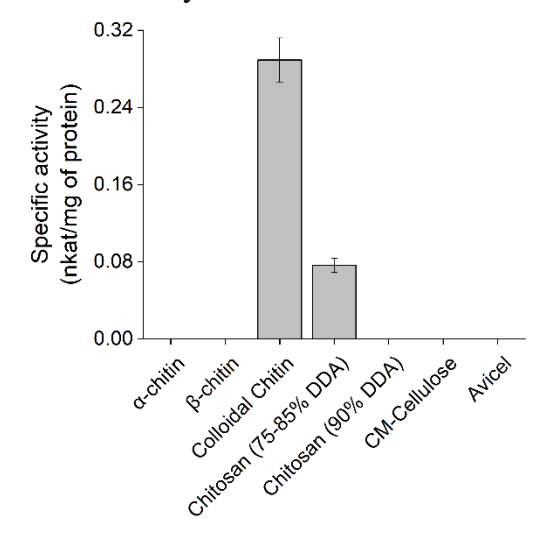
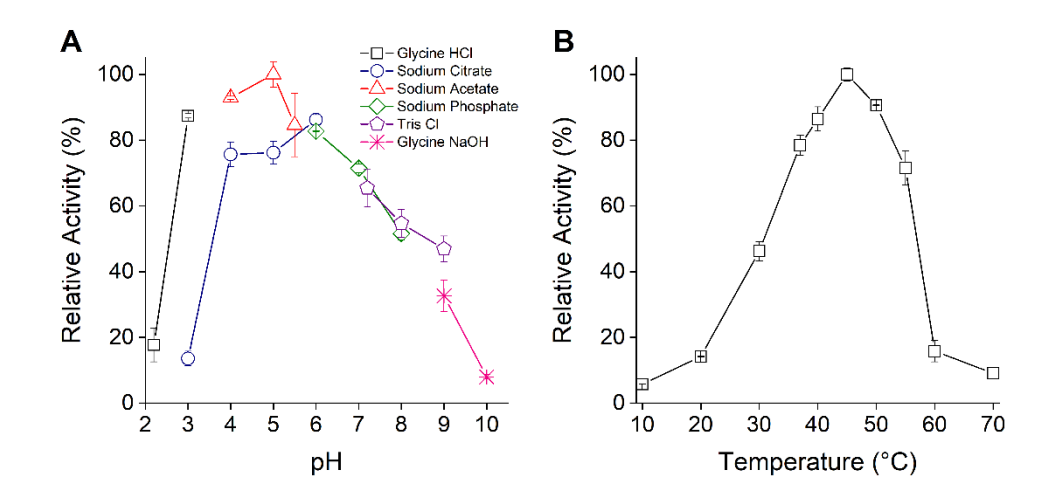


Figure 21: Substrate specificity of Chi3 on different chitin and non-chitin substrates. Reaction was performed under optimal conditions using 10 mg/mL of individual polysaccharide substrates. Activity was measured in terms of reducing sugars generated from 1h of reaction and determined using Schales' assay. Error bars represent standard deviation obtained from three individual experiments.

#### 3.2.4 Chi5 preferred acidic pH and displayed preference to \(\beta\)-chitin

The enzyme Chi5 was optimally active in 50 mM sodium acetate, pH 5.0 on CC and retained up to 93% activity at pH 4.0 of the same buffer (Figure 22A). Of note, the enzyme displayed 87% activity in the buffer glycine-HCl, pH 3.0. However, only 14% activity was observed at the same pH but in a different buffer system, i.e., 50 mM sodium citrate (Figure 22A). On the other hand, Chi5 displayed ~85% activity in both 50 mM sodium acetate, pH 5.5 and sodium citrate, pH 6.0 (Figure 22A). A substantial decrease in the Chi5 activity was observed beyond pH 6.0 (and also, below pH 3.0), confirming that the enzyme was active at low pH range of 3.0-6.0. Chi5 was optimally active at 45°C and retained up to 72-91% activity between 37-55°C (Figure 22B). The nearest homologue of Chi5, i.e., Chitinase A1 from B. circulans WL-12, showed optimal activity at pH 5.0 and 60°C on 4-methylumbelliferyl-(GlcNAc)<sub>2</sub> (Watanabe et al., 1990). Chi5 shared the same pH and temperature optima with the multi-modular chitinase, CHI from P. chitinolyticus UMBR 0002 (Liu, C. et al., 2020). On the other hand, Chi5 shared the same pH optima with the multi-modular chitinase, PsChi82 from P. shirakamiensis, but not the temperature optima, which was at 55°C, on CC as the substrate (Liu et al., 2024). Previously, the multi-modular chitinases, PbChi67, PbChi70 and PbChi74 from P. barengoltzii CAU904 exhibited optimal activity at pH 3.5 and 60°C, pH 5.5 and 55°C, and pH 4.5 and 65°C, respectively on CC (Fu et al., 2016; Yang et al., 2016; Fu et al., 2014). In a different study, the multi-modular chitinase PxChi52 from P. xylanexedens Z2-4, was reported to be active at pH 4.5 and 65°C, (Zhang, W. et al., 2021). The results collectively suggest the preference towards acidic pH for most *Paenibacillus* chitinases (also seen in section 3.2.3), while the temperature optima may differ.



**Figure 22:** Optimal conditions for the activity of Chi5. A – represents pH optima for Chi5 activity measured in various buffers of 50 mM strength at different pH. B – represents temperature optima for Chi5 activity by incubating at different temperatures ranging from 10-70°C.

Michaelis-Menten kinetic parameters for Chi5 were derived with varied concentrations (0-25 mg/mL) of CC as substrate. The curve fitting with non-linear regression function revealed the kinetic parameters  $K_{\rm m}$  and  $V_{\rm max}$  to be 10.32  $\pm$  1.69 mg/mL and 2.23  $\pm$  0.16 nkat/mg of protein, respectively (Figure 23A). Previously, the  $K_{\rm m}$  values for the multi-modular chitinases, PbChi67, PbChi70 and PbChi74 from P. barengoltzii CAU904 obtained over CC were reported to be 3.35 mg/mL, 7.91 mg/mL and 2.4 mg/mL, respectively (Fu et al., 2016; Yang et al., 2016; Fu et al., 2014). In a different study, PxChi52 from P. xylanexedens Z2-4 was reported to have a  $K_{\rm m}$  value of 3.06 mg/mL on CC (Zhang, W. et al., 2021). Further, the  $K_{\rm cat}$  and overall catalytic efficiency (K<sub>cat</sub>/K<sub>m</sub>) values obtained for Chi5 over CC were 2.23 x 10<sup>4</sup> s<sup>-1</sup> and 2.16 x 10<sup>3</sup> s<sup>-1</sup> mg<sup>-1</sup> <sup>1</sup> mL, respectively. Previously, PbChi67 and PxChi52 were reported to exhibit  $K_{\text{cat}}$  and  $K_{\text{cat}}/K_{\text{m}}$ values of 1.9 x  $10^{-2}$  s<sup>-1</sup> and 5.6 x  $10^{-3}$  s<sup>-1</sup> mg<sup>-1</sup> mL and 0.08 s<sup>-1</sup> and 2.6 x  $10^{-2}$  s<sup>-1</sup> mg<sup>-1</sup> mL, respectively on CC (Fu et al., 2016; Zhang, W. et al., 2021). Further, the Michaelis-Menten kinetic parameters for Chi5 were also derived with varied concentrations (0-50 mg/mL) of βchitin as substrate (Figure 23B). The curve fitting with non-linear regression function revealed the kinetic parameters  $K_{\rm m}$  and  $V_{\rm max}$  to be  $2.55 \pm 0.33$  mg/mL and  $2.03 \pm 0.05$  nkat/mg of protein, respectively (Figure 23B). Further, the  $K_{cat}$  and overall catalytic efficiency ( $K_{cat}/K_{m}$ ) values obtained for Chi5 on β-chitin were 2.03 x 10<sup>4</sup> s<sup>-1</sup> and 7.96 x 10<sup>3</sup> s<sup>-1</sup> mg<sup>-1</sup> mL, respectively. Comparison of the kinetic parameters for Chi5 obtained on CC and β-chitin (Table 4) revealed that Chi5 had high affinity and catalytic efficiency towards \beta-chitin over CC. Overall, the

kinetic parameters obtained suggest that the enzyme Chi5 is a potential chitinase target with possible implications in crystalline chitin bioconversion.

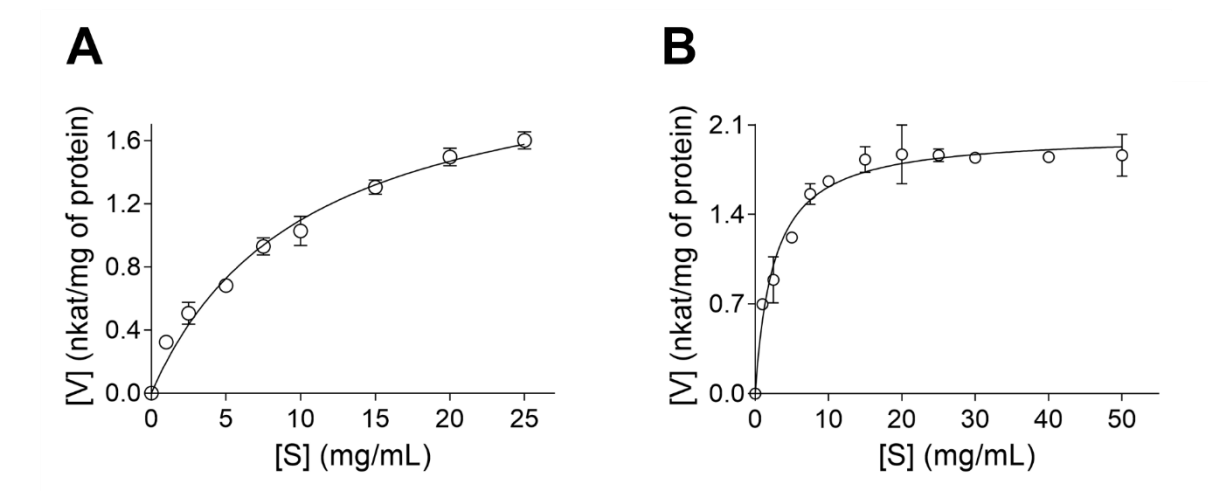


Figure 23: Michaelis-Menten kinetics for Chi5 on CC (A) and  $\beta$ -chitin (B). The kinetics experiment was performed under optimal reaction conditions using varied concentrations of CC or  $\beta$ -chitin as substrate. The kinetic parameters were derived by fitting the data from three independent experiments to the Michaelis-Menten equation using the non-linear regression function in GraphPad Prism v.5.0. All experiments were performed in triplicates and the standard deviations are represented in terms of error bars.

**Table 4:** Kinetic parameters of purified Chi5 (0.5  $\mu$ M) from *Paenibacillus* sp. LS1 obtained over CC and  $\beta$ -chitin under similar assay conditions.

Substrate	K <sub>m</sub> (mg/mL)	V <sub>max</sub> (nkat/mg of protein)	K <sub>cat</sub> (s <sup>-1</sup> )	$K_{\text{cat}}/K_{\text{m}}$ $(s^{-1} \text{ mg}^{-1} \text{ mL})$
Colloidal chitin	$10.32 \pm 1.69$	$2.23 \pm 0.16$	2.23 x 10 <sup>4</sup>	$2.16 \times 10^3$
β-chitin	$2.55 \pm 0.33$	$2.03 \pm 0.05$	2.03 x 10 <sup>4</sup>	$7.96 \times 10^3$

Furthermore, specificity of Chi5 towards different polysaccharides was investigated. Chi5 displayed highest specific activity towards β-chitin, followed by chitosan with 90% DDA and CC (Figure 24). The specificity towards β-chitin over CC correlates with the kinetics data (Table 4), confirming that Chi5 has higher affinity and catalytic efficiency towards β-chitin. This preference towards β-chitin was similar to that of the multi-modular chitinases, *Sp*ChiA, *Sp*ChiB and *Sp*ChiC from *S. proteamaculans* 568 (Purushotham *et al.*, 2012). The high specificity of Chi5 towards β-chitin could also be attributed to the presence of the amino acid residues equivalent to Trp53 and Tyr56 in *Bc*ChiA1, reported to be exclusively crucial for β-chitin degradation (Watanabe *et al.*, 2003) as mentioned in section 3.2.1. The enzyme also

showed a considerable activity on α-chitin, indicating its ability to hydrolyse highly crystalline chitin substrates (Figure 24). This could be due to the presence of accessory binding domains in Chi5 (Figure 15). Further, Chi5 also showed considerable activity on chitosan with 75-85% DDA (Figure 24). Additionally, Chi5 also displayed a promiscuous activity on the cellulosic substrates, avicel and CM-cellulose (Figure 24).

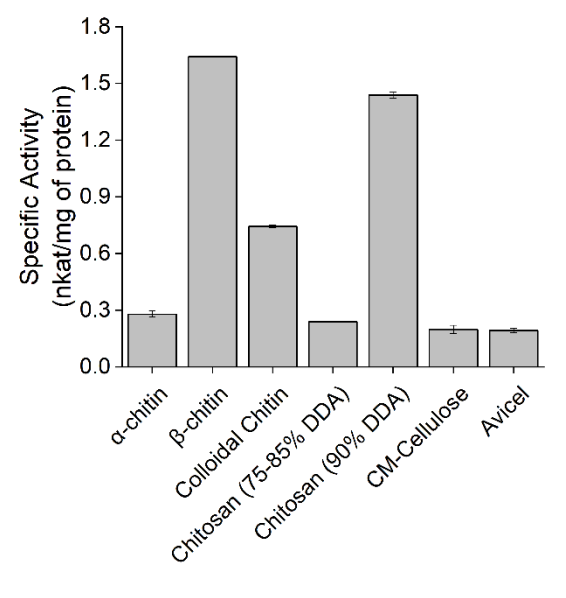


Figure 24: Substrate specificity of Chi5 on different chitin and non-chitin substrates. Reaction was performed under optimal conditions using 10 mg/mL of individual polysaccharide substrates. Activity was measured in terms of reducing sugars generated from 1h of reaction and determined using Schales' assay. Error bars represent standard deviation obtained from three individual experiments.

#### 3.2.5 Activity of Chi3 and Chi5 on CHOS

#### 3.2.5.1 Chi3 generates GlcNAc from CHOS via exo-acting mechanism

To gain deeper insights into the mode-of-action of Chi3, reactions were performed with CHOS of varying degree of polymerization and the product profiles generated were analysed by HPLC. Chi3 readily converted 59% of (GlcNAc)<sub>2</sub> to GlcNAc within 30 min of reaction (Figure 25A). The GlcNAc proportion further increased up to 93% by the end of 60 min, indicating nearly complete conversion of (GlcNAc)<sub>2</sub> (Figure 25A). Previously, *Ec*Chi1 was reported to completely hydrolyse (GlcNAc)<sub>2</sub> within 420 min of reaction (Mallakuntla *et al.*, 2017). In a separate study, *Sm*ChiD displayed very slow rate of hydrolysis, converting only 39% of (GlcNAc)<sub>2</sub> to GlcNAc by 720 min (Vaikuntapu *et al.*, 2016). A similar observation was made in case of *Cs*ChiL, where only 40% of (GlcNAc)<sub>2</sub> was converted to GlcNAc at the end of 96 h (Bhuvanachandra and Podile, 2020). The rapid and nearly complete conversion of (GlcNAc)<sub>2</sub> to GlcNAc by Chi3 highlights its β-*N*-acetylglucosaminidase activity, specifically chitobiase activity. Clearly, this suggests that (GlcNAc)<sub>2</sub> occupies the -1 to +1 subsites of Chi3 for the hydrolysis event.

Chi3 hydrolysed (GlcNAc)<sub>3</sub> into nearly equal proportions of GlcNAc and (GlcNAc)<sub>2</sub> throughout the course of reaction and their final proportion at the end of 360 min was 48% and 52%, respectively (Figure 25B). Chi3 hydrolysed 60% of (GlcNAc)<sub>3</sub> within 15 min and 71%

of the same within 30 min of reaction (Figure 25B). Following this, the rate of reaction slowed down and ~80% of (GlcNAc)<sub>3</sub> was hydrolysed to nearly equal proportions of GlcNAc and (GlcNAc)<sub>2</sub> by the end of the reaction, i.e., 360 min (Figure 25B). Previously, the uni-modular *Cs*ChiL showed poor hydrolytic efficiency on (GlcNAc)<sub>3</sub> even after 720 min of incubation (Bhuvanachandra and Podile, 2020). Whereas, *Sp*ChiD and *Ec*Chi1 showed complete hydrolysis of (GlcNAc)<sub>3</sub> within 120 and 240 min of reaction, respectively (Purushotham and Podile, 2012; Mallakuntla *et al.*, 2017). Considering the equal proportions of GlcNAc and (GlcNAc)<sub>2</sub> produced, it can be inferred that (GlcNAc)<sub>3</sub> occupies the subsites -1 to +2 of Chi3 for the hydrolysis event (Figure 26A).

In case of (GlcNAc)<sub>4</sub>, Chi3 rapidly hydrolysed 38% of (GlcNAc)<sub>4</sub> to GlcNAc (major product), (GlcNAc)<sub>2</sub> and (GlcNAc)<sub>3</sub> during the initial phase of reaction, i.e., 5 min (Figure 25C). Nearly 50% conversion of (GlcNAc)<sub>4</sub> was achieved within 10 min of reaction, which reached up to 82.5% by the end of 60 min (Figure 25C). The final proportions of the products achieved by the end of the reaction, i.e., 360 min, was 63.8%, 33.4% and 2.8% of GlcNAc, (GlcNAc)<sub>2</sub> and (GlcNAc)<sub>3</sub>, respectively (Figure 25C). A similar hydrolytic pattern was previously reported for *Stm*ChiB on (GlcNAc)<sub>4</sub>, leading to production of GlcNAc as the major product throughout the reaction (Suma and Podile, 2013). Also, in a separate study, hydrolysis of (GlcNAc)<sub>4</sub> by *Sm*ChiD resulted in the production of (GlcNAc)<sub>1-3</sub> in the relative proportions of 35.5%, 25.8% and 26.6%, respectively by the end of 720 min (Vaikuntapu *et al.*, 2016). The product profile for (GlcNAc)<sub>4</sub> hydrolysis by Chi3 suggests that the preferred (GlcNAc)<sub>4</sub> binding subsites might be -1 to +3 (Figure 26B).

Hydrolysis of (GlcNAc)<sub>5</sub> by Chi3 resulted in the production of (GlcNAc)<sub>1-4</sub> throughout the course of reaction where, GlcNAc was the major product (Figure 25D). Chi3 achieved 49% conversion of (GlcNAc)<sub>5</sub> within 30 min of reaction. After this, the rate of reaction slowed down, eventually reaching saturation by 90 min, resulting in a maximum substrate conversion of ~64% by the end of the reaction, i.e., 360 min (Figure 25D). The final proportions of (GlcNAc)<sub>1-4</sub> at the end of 360 min were 63.2%, 14.2%, 6.2% and 16.4%, respectively (Figure 25D). In a previous study, GlcNAc was the major end-product from (GlcNAc)<sub>5</sub> hydrolysis by *Sp*ChiD at the end of the reaction i.e., 720 min (Purushotham and Podile, 2012). Considering the product profile generated by Chi3 upon hydrolysing (GlcNAc)<sub>5</sub>, it can be inferred that the substrate occupies the subsites -1 to +4 of Chi3 for hydrolysis (Figure 26C).

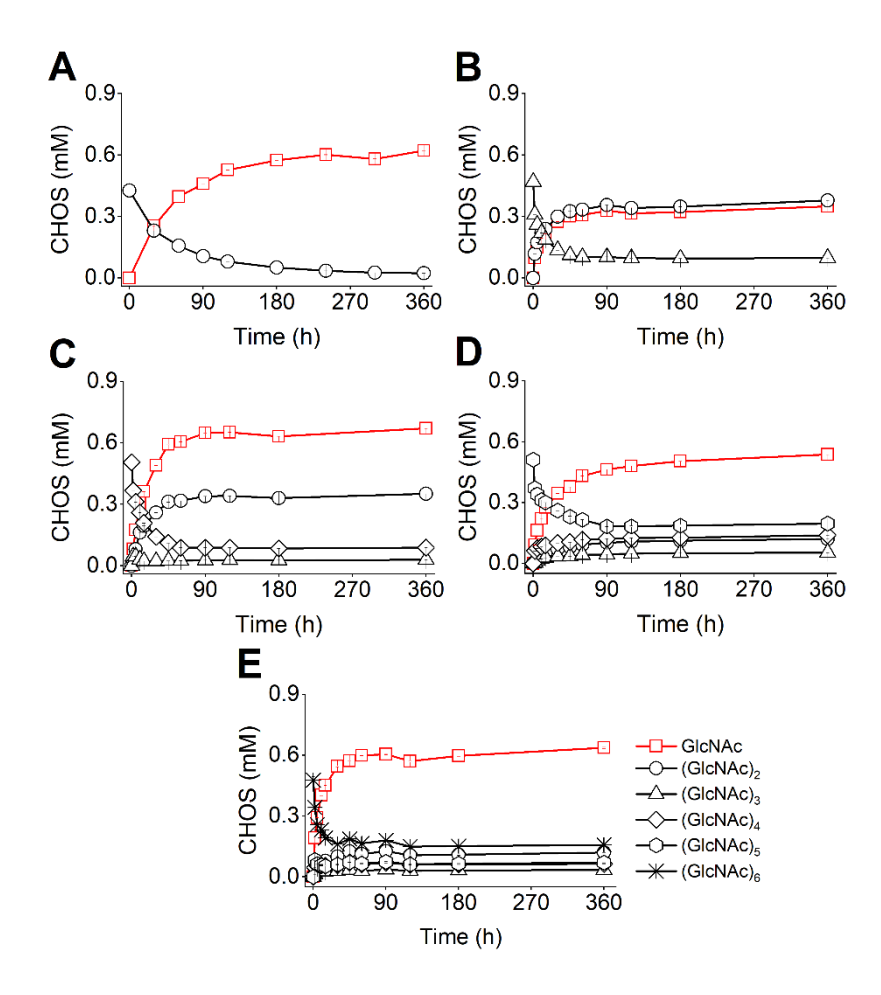


**Figure 25:** Hydrolytic activity of Chi3 on CHOS. Experiments were performed by incubating 0.5 mM each of (GlcNAc)<sub>2</sub> (A), (GlcNAc)<sub>3</sub> (B), (GlcNAc)<sub>4</sub> (C), (GlcNAc)<sub>5</sub> (D) and (GlcNAc)<sub>6</sub> (E) with 500 nM for (A), and 100 nM for (B) to (E) of Chi3 under optimal conditions. Product analysis was done using automated HPLC and quantification was done considering the respective peak areas and comparing against individual standard curves of (GlcNAc)<sub>1-6</sub>.

Chi3 hydrolysed (GlcNAc)<sub>6</sub> to generate a multitude of CHOS products, ranging from (GlcNAc)<sub>1-5</sub> (Figure 25E). GlcNAc was the major product reaching the proportion of 69% of the total amount of soluble sugars produced by the end of 360 min of reaction (Figure 25E). Chi3 also produced trace amounts of (GlcNAc)<sub>2</sub> in the proportion of 13% of the total amount of soluble sugars produced by the end of 360 min (Figure 25E). While, (GlcNAc)<sub>3-5</sub> were produced in feeble quantities (Figure 25E). Chi3 showed rapid hydrolysis of (GlcNAc)<sub>6</sub> initially as the substrate got reduced to 52% in proportion by the end of just 10 min. Subsequently, a rapid rise in GlcNAc concentration, up to 66% (in proportion with the total amount of soluble sugars produced) was achieved within 10 min of reaction. This concentration was maintained throughout the course of reaction, reaching up to a total of 68% proportion by the end of 360 min (Figure 25E). Previously, *Sp*ChiD was reported to generate GlcNAc as the

major product from (GlcNAc)<sub>6</sub>, by the end of the reaction i.e., 720 min (Purushotham and Podile, 2012). Interestingly, a trace concentration of (GlcNAc)<sub>5</sub> was also observed among the products upon (GlcNAc)<sub>6</sub> hydrolysis by Chi3, which could be an event of transglycosylation. Proportion of (GlcNAc)<sub>5</sub> among the total amount of soluble sugars produced was highest within 2 min of reaction, i.e., 24%, which gradually got reduced to 7.9% in proportion to the total amount of soluble sugars generated at the end of 15 min (Figure 25E). This proportion however, was maintained until the end of the reaction i.e., 360 min (Figure 25E). The product profile generated by Chi3 upon hydrolysing (GlcNAc)<sub>6</sub> inferred that the substrate most likely occupies the subsites -2 to +4 for hydrolysis (Figure 26D). Taken together, the results suggest that Chi3 shows high efficiency towards soluble CHOS substrates. A prevalence of GlcNAc as the major product was seen in the hydrolysis events of all the CHOS substrates tested, therefore suggesting exo-acting mechanism for Chi3.

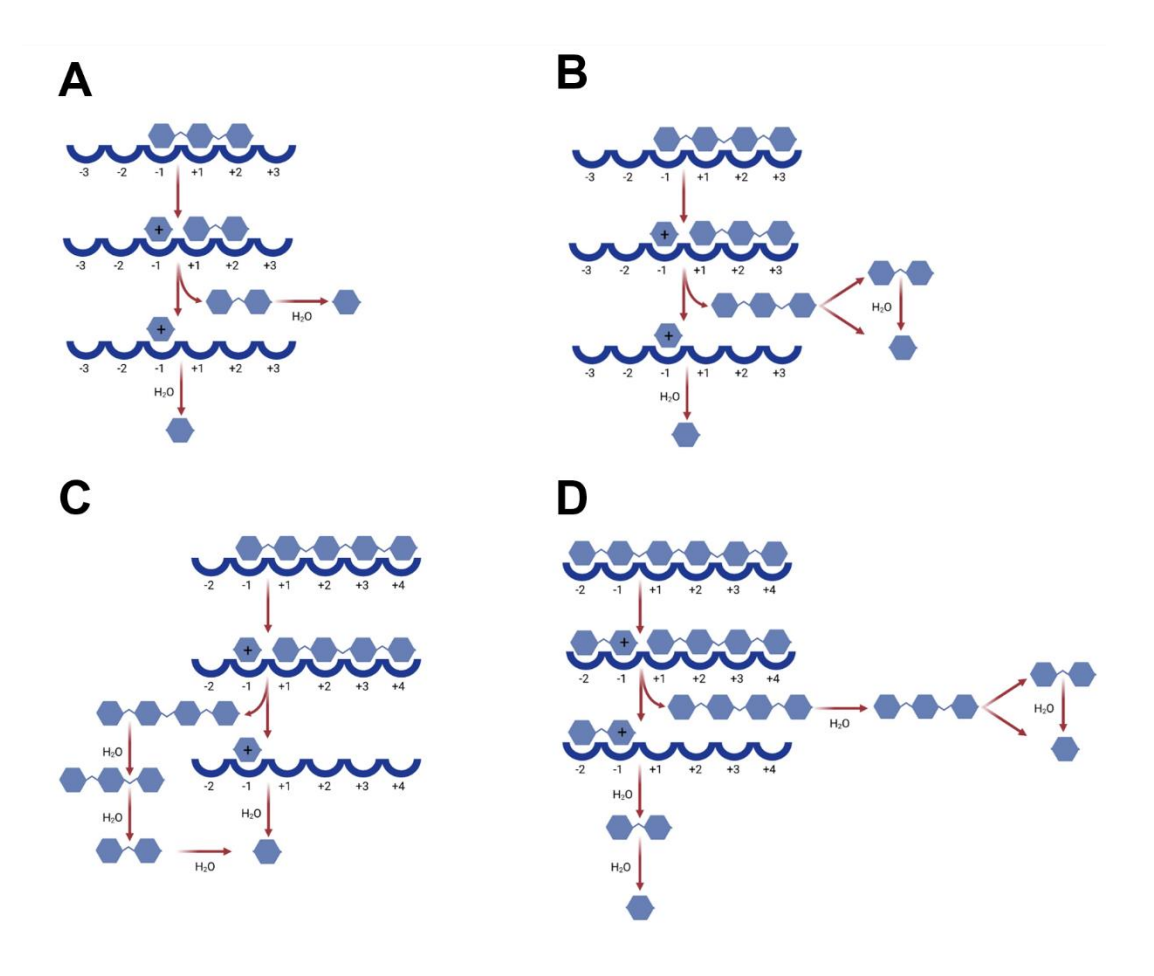
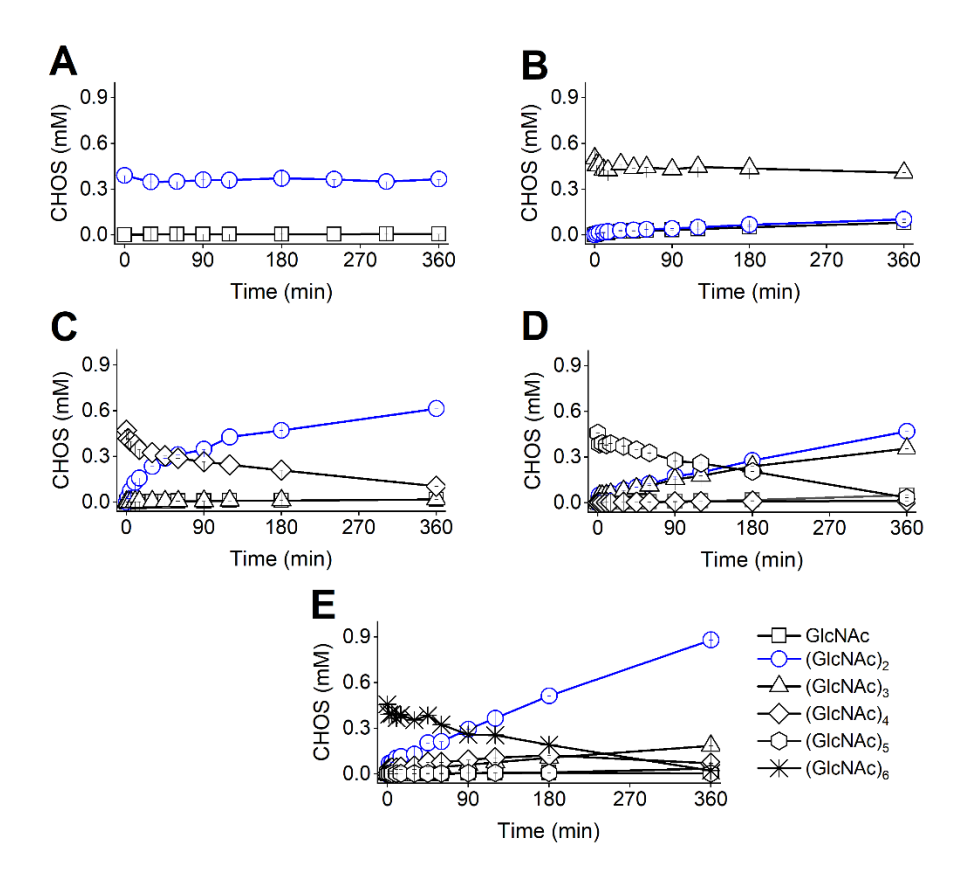


Figure 26: Schematic representation depicting the mode of action of Chi3 on (GlcNAc)<sub>3</sub> (A), (GlcNAc)<sub>4</sub> (B), (GlcNAc)<sub>5</sub> (C) and (GlcNAc)<sub>6</sub> (D) as the substrate. GlcNAc residues are shown as pale blue hexagons, and the binding subsites of the enzyme are numbered. For (GlcNAc)<sub>3</sub> (A), the substrate binds to the -1 to +2 subsites, and the glycosidic bond is cleaved to form a positively charged GlcNAc oxazolinium ion intermediate (marked with +) in the -1 subsite. A (GlcNAc)<sub>2</sub> product then exits and is replaced by an incoming water molecule. The leaving (GlcNAc)<sub>2</sub> molecule is further hydrolysed to two molecules of GlcNAc. In case of (GlcNAc)<sub>4</sub>, the substrate binds to the -1 to +3 subsites and the glycosidic bond is cleaved to form a positively charged GlcNAc oxazolinium ion intermediate (marked with +) in the -1 subsite. A (GlcNAc)<sub>3</sub> product then exits and is replaced by an incoming water molecule. The leaving (GlcNAc)<sub>3</sub> molecule is further hydrolysed to GlcNAc and (GlcNAc)<sub>2</sub>, which in turn is hydrolysed to two molecules of GlcNAc. In case of (GlcNAc)<sub>5</sub> (C) the binding possibly occurs at the -1 to +4 subsites. The glycosidic bond is cleaved to form a positively charged GlcNAc oxazolinium ion intermediate in the -1 subsite. A (GlcNAc)<sub>4</sub> product then exits and is replaced by a water molecule. The leaving (GlcNAc)<sub>4</sub> is hydrolysed further to finally produce GlcNAc. For (GlcNAc)<sub>6</sub> (D), the substrate binds to the -2 to +4 subsites, and the glycosidic bond is cleaved to form a positively charged (GlcNAc)<sub>2</sub> oxazolinium ion intermediate (marked with +) in the -1 and -2 subsites. A (GlcNAc)<sub>4</sub> product then exits and is replaced by an incoming water molecule. The released (GlcNAc)<sub>4</sub> then gets hydrolysed further into GlcNAc.

#### 3.2.5.2 Chi5 generates chitobiose as the major product from CHOS

To gain deeper insights into the mode-of-action of Chi5, reactions were performed with CHOS of varying DP and the product profiles generated were analysed by HPLC. The enzyme Chi5 displayed feeble activity on the substrates (GlcNAc)<sub>2</sub> and (GlcNAc)<sub>3</sub> (Figure 27A and B), indicating that the lower chain length CHOS are not suitable substrates. The substrate (GlcNAc)<sub>4</sub> was converted mostly to two molecules of (GlcNAc)<sub>2</sub>, while a very low fraction of it was converted to GlcNAc and (GlcNAc)<sub>3</sub> (Figure 27C). Chi5 converted only 16% of (GlcNAc)<sub>4</sub> to (GlcNAc)<sub>2</sub> during the initial phase of reaction i.e., 5 min. The proportion of (GlcNAc)<sub>2</sub> eventually increased to 50% by the end of 30 min, indicating conversion of nearly half of the substrate by Chi5. By the end of 6 h (360 min), up to 78% conversion of (GlcNAc)<sub>4</sub> was achieved (Figure 27C). Previously, the multi-modular chitinase, *Cs*ChiE was reported to achieve nearly complete hydrolysis of (GlcNAc)<sub>4</sub> (up to 96%) to (GlcNAc)<sub>2</sub> as the sole product by end of 360 min (Rani *et al.*, 2020). Considering the product profile, it seems that (GlcNAc)<sub>4</sub> primarily occupies the subsites -2 to +2 and thus produces (GlcNAc)<sub>2</sub> as the major end product (Figure 28A).



**Figure 27:** Hydrolytic activity of Chi5 on CHOS. Experiments were performed by incubating 0.5 mM each of (GlcNAc)<sub>2</sub> (A), (GlcNAc)<sub>3</sub> (B), (GlcNAc)<sub>4</sub> (C), (GlcNAc)<sub>5</sub> (D) and (GlcNAc)<sub>6</sub> (E) with 500 nM for (A), 50 nM for (B) and (C) and, 25 nM for (D) and (E) under optimal conditions. Product analysis was done using automated HPLC and quantification was done considering the respective peak areas and comparing against individual standard curves of (GlcNAc)<sub>1-6</sub>.

Similarly, in a different reaction, Chi5 converted (GlcNAc)<sub>5</sub> to molecules of (GlcNAc)<sub>2</sub> and (GlcNAc)<sub>3</sub> and their proportion was 51% and 39% by 360 min, respectively (Figure 27D). The proportion of (GlcNAc)<sub>2</sub> and (GlcNAc)<sub>3</sub> was maintained as 52% and 48% respectively, until 90 min (Figure 27D). After this, significant generation of GlcNAc was also observed which could be due to hydrolysis of (GlcNAc)<sub>3</sub> by Chi5. Proportion of GlcNAc increased up to 5.5% of the total soluble sugars generated by the end of 360 min. Feeble amount of (GlcNAc)<sub>4</sub> was also observed throughout the course of reaction, reaching up to 1% of the total soluble sugars produced at the end of 360 min. Previously, *Cs*ChiE was reported to generate nearly 15%, 58% and 24% of (GlcNAc)<sub>1-3</sub> upon (GlcNAc)<sub>5</sub> hydrolysis (Rani *et al.*, 2020). The highest proportion of (GlcNAc)<sub>2</sub> and (GlcNAc)<sub>3</sub> in the reaction suggests the (GlcNAc)<sub>5</sub> most likely binds to the subsites -2 to +3 or -1 to +4. The former situation leads to generation of (GlcNAc)<sub>2</sub> and (GlcNAc)<sub>3</sub> (which are hydrolysed further to GlcNAc and (GlcNAc)<sub>2</sub>, while the

later situation produces (GlcNAc)<sub>4</sub> as the product, which in turn, gets hydrolysed into two molecules of (GlcNAc)<sub>2</sub> (Figure 28B).

Further, Chi5 hydrolysed (GlcNAc)<sub>6</sub> to produce a multitude of CHOS ranging from (GlcNAc)<sub>1-5</sub>. (GlcNAc)<sub>2</sub> was the major product reaching the proportion of 73.2% of the total amount of soluble sugars produced by the end of 360 min of reaction (Figure 27E). Chi5 also generated trace amounts of (GlcNAc)<sub>3</sub> in the proportion of 15.4% of the total amount of soluble sugars produced by the end of 360 min (Figure 27E). While, GlcNAc, (GlcNAc)<sub>2</sub> and (GlcNAc)<sub>4</sub> were produced in feeble quantities from (GlcNAc)<sub>6</sub> hydrolysis by Chi5 (Figure 27E). (GlcNAc)<sub>6</sub> hydrolysis by Chi5 was slow initially as the substrate got reduced to only 55% in proportion by the end of 120 min. However, a consistent increase in the proportion of (GlcNAc)<sub>2</sub> was observed, reaching up to 46% by 60 min itself. This increase in the (GlcNAc)<sub>2</sub> proportion, despite of slow (GlcNAc)<sub>6</sub> hydrolysis could be due to the subsequent hydrolysis of the generated (GlcNAc)<sub>3-5</sub>, resulting from the (GlcNAc)<sub>6</sub> degradation. CsChiE also produced (GlcNAc)<sub>2</sub> as the major product from (GlcNAc)<sub>6</sub>, that reached up to a proportion of 76% of the total soluble sugars produced at the end of 360 min (Rani et al., 2020). The product profile inferred that (GlcNAc)<sub>6</sub> binds to -2 to +4 subsites of Chi5 as this would result in generation of (GlcNAc)<sub>2</sub> in highest proportions – first from (GlcNAc)<sub>6</sub> hydrolysis and then by hydrolyzing the resulting (GlcNAc)<sub>4</sub> into two molecules of (GlcNAc)<sub>2</sub> (Figure 28C). The results taken together suggests that Chi5 can efficiently hydrolyse CHOS substrates of longer chain length. Further, a prevalence of (GlcNAc)<sub>2</sub> as the major product was seen in the hydrolysis events with all CHOS substrates tested, which suggests an exo-acting mechanism for Chi5.

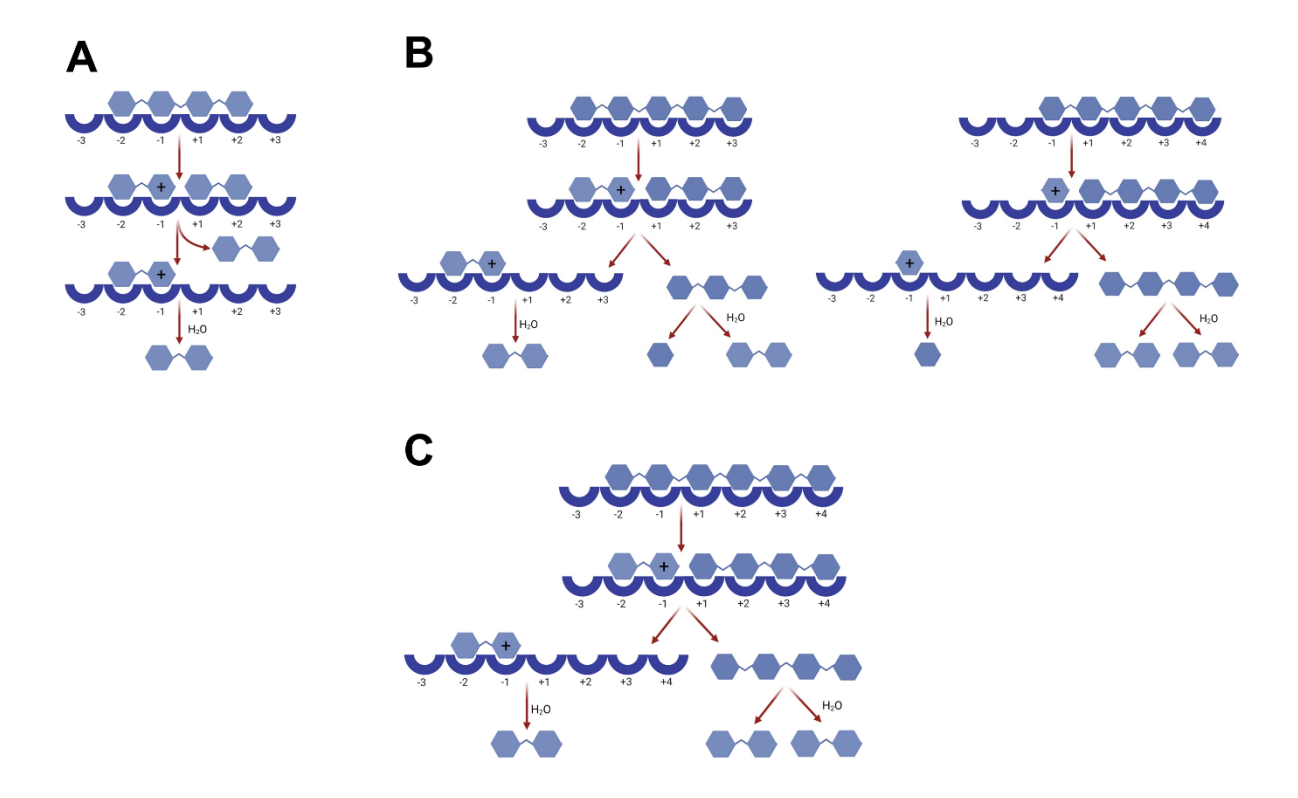


**Figure 28:** Schematic representation depicting the mode of action of Chi5 on (GlcNAc)<sub>4</sub> (A), (GlcNAc)<sub>5</sub> (B) and (GlcNAc)<sub>6</sub> (C) as the substrate. GlcNAc residues are shown as pale blue hexagons, and the binding subsites of the enzyme are numbered. For (GlcNAc)<sub>4</sub> (A), the substrate binds to the −2 to +2 subsites, and the glycosidic bond is cleaved to form a positively charged (GlcNAc)<sub>2</sub> oxazolinium ion intermediate (marked with +) in the −1 and −2 subsites. A (GlcNAc)<sub>2</sub> product then exits and is replaced by an incoming water molecule. The binding of (GlcNAc)<sub>5</sub> (B) can possibly occur at either at the -2 to +3 or -1 to +4 subsites. The glycosidic bond is cleaved to form a positively charged (GlcNAc)<sub>2</sub> or (GlcNAc) oxazolinium ion intermediate in the −1 and −2 subsites or −1 subsite, respectively. A (GlcNAc)<sub>3</sub> or (GlcNAc)<sub>4</sub> product then exits and is replaced by a water molecule. The exiting (GlcNAc)<sub>3</sub> or (GlcNAc)<sub>4</sub> then gets cleaved to GlcNAc and (GlcNAc)<sub>2</sub> or two molecules of (GlcNAc)<sub>2</sub>, respectively. For (GlcNAc)<sub>6</sub> (C), the substrate binds to the −2 to +4 subsites, and the glycosidic bond is cleaved to form a positively charged (GlcNAc)<sub>2</sub> oxazolinium ion intermediate (marked with +) in the −1 and −2 subsites. A (GlcNAc)<sub>4</sub> product then exits and is replaced by an incoming water molecule. The released (GlcNAc)<sub>4</sub> then gets hydrolysed into two molecules of (GlcNAc)<sub>2</sub>.

#### 3.2.6 Activity of Chi3 and Chi5 on crystalline chitin substrates

#### 3.2.6.1 Chi3 directly produced GlcNAc from $\beta$ - and colloidal chitin

The potential of Chi3 to hydrolyse crystalline chitin substrates was investigated in a time dependant manner using HPLC. Chi3 hydrolysed CC to produce GlcNAc as the sole product (Figure 29A). No other CHOS products were detected during the time-course degradation, making Chi3 as the first chitinase to generate GlcNAc as the only product, directly from a chitin substrate. Chi3 initiated CC hydrolysis by producing 0.18 mM GlcNAc after 1h of reaction, which reached up to 0.34 mM at 12h and ~0.4 mM at the end of 24h (Figure 29A).

Previously, 3 μM of *Sp*ChiD produced 0.01 mM GlcNAc as the major product in 12h from 25 mg/mL CC (Purushotham and Podile, 2012). Similarly, 0.8 μM *Ec*Chi1 was reported to produce ~0.06 mM of GlcNAc as the second major product at 10h from 30 mg/mL of CC (Mallakuntla *et al.*, 2017). In a different study, *Cs*ChiL (0.5 μM) upon incubation with 15 mg/mL of CC, produced slightly higher than 0.3 mM of GlcNAc as the major product at the end of 24h (Bhuvanachandra and Podile, 2020). In comparison with these studies, Chi3 (1 μM) was able to produce higher concentration of GlcNAc from a relatively low CC concentration (10 mg/mL), therefore, indicating its efficiency in valorizing CC to GlcNAc.

Chi3 showed feeble activity on  $\beta$ -chitin to produce GlcNAc as the sole product (Figure 29B), while not showing activity on  $\alpha$ -chitin at all throughout the time-course (data not shown). The trace amounts of GlcNAc detected upon  $\beta$ -chitin hydrolysis by Chi3 could be due to the high sensitivity of HPLC over Schales' assay which was used to determine the substrate specificity of Chi3 (section 3.2.3). Taken together, the results suggest that Chi3 shows fairly considerable efficiency towards an amorphous chitin substrate such as CC, while displaying feeble or no hydrolytic potential towards crystalline chitin substrates. Moreover, generation of GlcNAc as the sole product directly from chitin is a unique property that has not been reported till date for any GH18 chitinase.

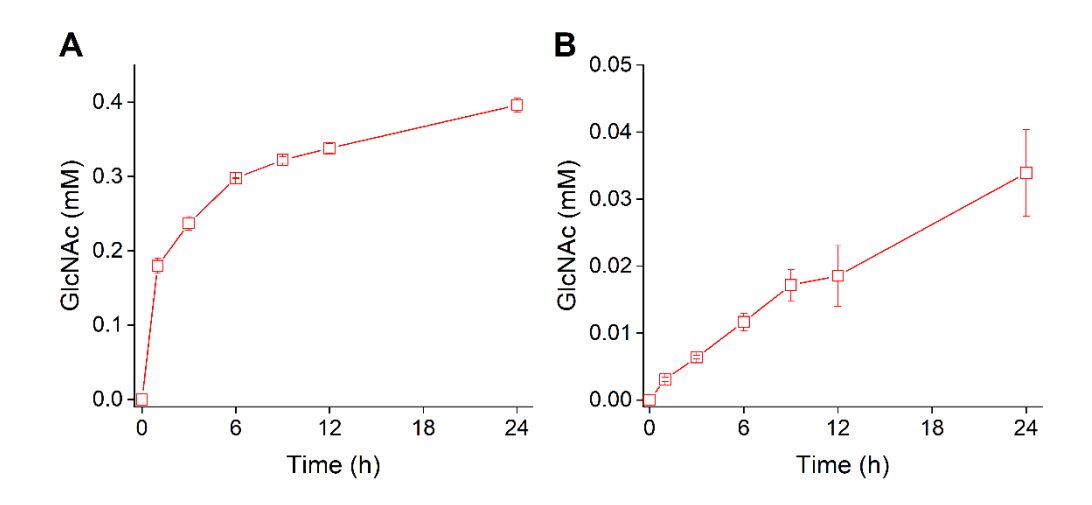


**Figure 29**: Hydrolytic activity of Chi3 on crystalline chitin substrates. Reactions were performed by incubating 1 μM of Chi3 with 10 mg/mL of colloidal chitin (A) and β-chitin (B), under optimal conditions. The products generated were analysed using HPLC and quantified considering the respective peak areas against individual CHOS standard curves of (GlcNAc)<sub>1-6</sub>. All experiments were performed in triplicates and the error bars represent standard deviation.

#### 3.2.6.2 Chi5 is capable of degrading crystalline chitin substrates to (GlcNAc)<sub>2</sub>

The potential of Chi5 to hydrolyse crystalline chitin substrates was investigated in a time dependant manner using HPLC. Chi5 produced (GlcNAc)<sub>2</sub> as the major product from all the substrates used, followed by GlcNAc (Figure 30). Trace amounts of (GlcNAc)<sub>3</sub> was also observed (Figure 30). Chi5 weakly hydrolysed α-chitin, producing 0.16 mM and 0.03 mM of (GlcNAc)<sub>2</sub> and GlcNAc, respectively after 1 h of reaction (Figure 30A). The total concentration of (GlcNAc)<sub>2</sub> and GlcNAc reached up to 0.29 mM and 0.08 mM, respectively at the end of 24 (Figure 30A). Therefore, the total amount of quantifiable soluble sugars [GlcNAc+(GlcNAc)<sub>2</sub>] obtained upon Chi5-mediated hydrolysis of α-chitin reached up to 0.37 mM at the end of 24 h. Chi5 displayed stronger degradation of β-chitin and CC as compared to α-chitin. Chi5 initially produced 1.72 mM and 0.16 mM of (GlcNAc)<sub>2</sub> and GlcNAc, respectively after 1 h of reaction on β-chitin (Figure 30B). On the other hand, degradation on CC was slow during the initial phase of reaction, producing 0.57 mM and 0.11 mM of (GlcNAc)<sub>2</sub> and GlcNAc, respectively after 1 h of reaction (Figure 30C). However, the total concentrations of (GlcNAc)<sub>2</sub> and GlcNAc reached up to 4.89 mM and 1.40 mM, respectively from β-chitin and 4.36 mM and 1.73 mM, respectively from CC at the end of 24 h (Figure 30B) C). Therefore, quantifiable and the total amount of soluble sugars [GlcNAc+(GlcNAc)<sub>2</sub>+(GlcNAc)<sub>3</sub>] obtained upon Chi5-mediated hydrolysis of β-chitin and CC reached up to 6.4 mM and 6.2 mM, respectively at the end of 24 h. The total amount of quantifiable soluble sugars obtained from β-chitin and CC were 17.3- and 16.8-times higher than of  $\alpha$ -chitin. This difference is due to the much higher crystallinity of  $\alpha$ -chitin, as compared to β-chitin and CC (acid-hydrolysed α-chitin), that restricts the access of Chi5 to the chitin chains for efficient hydrolysis.

Previously, the multi-modular chitinase, CsChiE (1  $\mu$ M) from Chitiniphilus shinanonensis SAY3 produced ~0.24 mM, ~1.4 mM and 11.3 mM of total quantifiable soluble sugars [GlcNAc+(GlcNAc)<sub>2</sub>+(GlcNAc)<sub>3</sub>] from  $\alpha$ - and  $\beta$ -chitin (both 5 mg/mL) and CC (15 mg/mL), respectively at the end of 12 h, under optimal reaction conditions (Rani et~al., 2020). In comparison, Chi5 produced 0.37 mM, 5.70 mM and 4.67 mM of total quantifiable soluble sugars from  $\alpha$ -,  $\beta$ - and colloidal chitin (10 mg/mL each), respectively under optimal reaction conditions. The comparison highlights the preference and potential of Chi5 towards highly crystalline chitin substrates, such as  $\alpha$ - and  $\beta$ -chitin. Overall, the results indicate the impressive potential of Chi5 towards the direct degradation of different crystalline chitin substrates, to generate bioactive chitooligosaccharides, particularly (GlcNAc)<sub>2</sub> and GlcNAc.

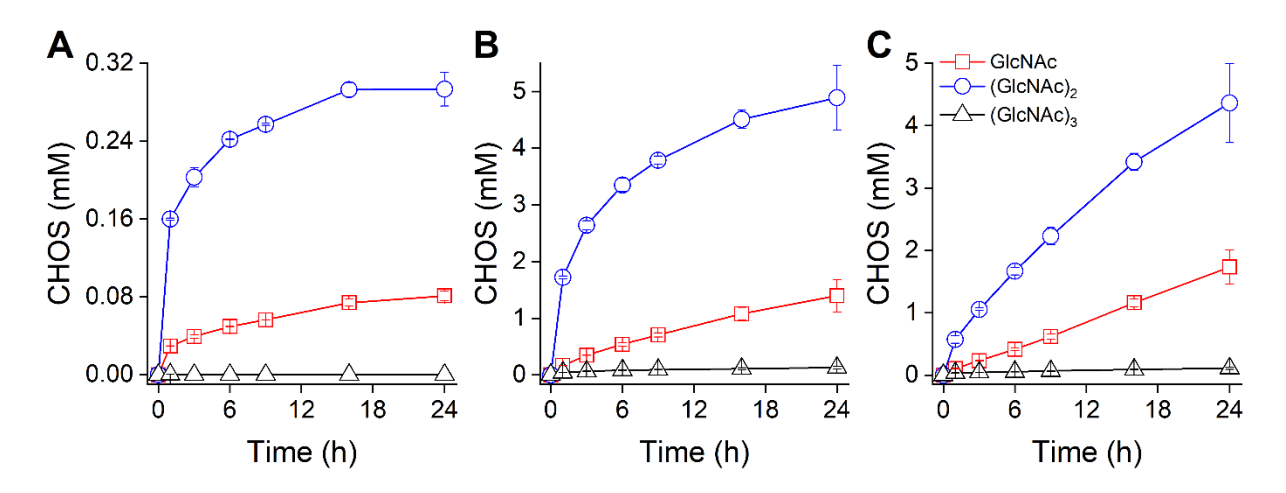


**Figure 30:** Hydrolytic activity of Chi5 on various crystalline chitin substrates. Reactions were performed by incubating 1  $\mu$ M of Chi5 with 10 mg/mL of α-chitin (A), β-chitin (B) and colloidal chitin (C), under optimal conditions. The products generated were analysed using HPLC and quantified considering the respective peak areas against individual CHOS standard curves of (GlcNAc)<sub>1-6</sub>. All experiments were performed in triplicates and the error bars represent standard deviation.

The results taken together provide deeper insights into two of the GH18 family proteins encoded in the genome of *Paenibacillus* sp. LS1. Among the six GH18 family proteins, Chi3, Chi5 and Chi6 were determined as true chitinases due to presence of amino acid residues and motifs that are crucial of chitinase activity. The unimodular chitinase, Chi3 and the multimodular chitinase, Chi5 were successfully cloned and produced as soluble proteins for in-depth biochemical characterization. Both chitinases preferred acidic pH for optimal activity, while the temperature optima differed between the two. Chi3 showed specificity towards amorphous chitin substrates, such as colloidal chitin, while Chi5 showed maximum activity on β-chitin, one of the highly crystalline chitin substrates known. Further, Chi3 showed remarkable activity towards soluble CHOS substrates of varying chain lengths, producing GlcNAc as the major product. On the other hand, Chi5 efficiently hydrolysed CHOS of higher chain length [(GlcNAc)<sub>4</sub> onwards] to (GlcNAc)<sub>2</sub>. Additionally, Chi<sub>3</sub> produced GlcNAc as the sole product from the amorphous chitin substrate, CC, while displaying feeble or no activity on crystalline chitin substrates. Preference towards soluble CHOS substrates and production of GlcNAc as major product from CHOS as well as CC confirms β-N-acetylglucosaminidase activity of Chi3. Furthermore, Chi5 efficiently hydrolysed different crystalline chitin substrates, particularly βchitin, to (GlcNAc)2 and GlcNAc as major products. Chi5 was previously detected in high abundance in the chitin-active secretome produced by *Paenibacillus* sp. LS1 over α- and βchitin. The biochemical insights strongly indicate that Chi5 is the key enzyme responsible for extracellular conversion of chitin to (GlcNAc)<sub>2</sub>, while Chi3 is an intracellular β-N-

acetylglucosaminidase of the GH18 family that further hydrolyses the (GlcNAc)<sub>2</sub> (internalized by the bacterial cell) into GlcNAc for metabolism. Additionally, Chi3 and Chi5 are also potential targets for development of a bioprocess for efficient saccharification of highly crystalline chitin substrates to GlcNAc and (GlcNAc)<sub>2</sub>.

### **Chapter-4**

Development of a bioprocess for efficient and selective production of GlcNAc and (GlcNAc)<sub>2</sub> directly from chitin

#### 4.1 Materials & Methods

#### 4.1.1 Chemicals and reagents

Crude α-chitin (powdered shrimp shell) was procured from Stellar Bio-Sol (formerly, Mahtani Chitosans), Gujarat, India. The ionic liquids, 1-ethyl-3-methylimidazolium acetate and 1-butyl 3-methyl imidazolium acetate were procured from Sigma Aldrich, USA, while 1-sulfobutyl 3-methyl imidazolium hydrosulfate was purchased from TCI chemicals, China. Pierce<sup>TM</sup> BCA protein assay kit was procured from ThermoFisher Scientific, USA. HPLC graded Acetonitrile was purchased from Merck (Merck KGaA, Germany). All chemicals and reagents were obtained from either HiMedia or Sisco Research Laboratories Pvt. Ltd., India unless specified otherwise.

#### 4.1.2 Pretreatment of crude α-chitin

#### Cryo-milling

The crude  $\alpha$ -chitin was subjected to milling using a Union Process (Model 1S-USA) cryo-mill equipped with stainless-steel balls, while maintaining a sample-to-ball ratio of 1:10. Prior to milling, the jar was pre-cooled using liquid  $N_2$  and the milling process was conducted at 86 K with a rotation speed ranging from 300 to 400 rpm for a duration of 3 to 4 h (Mukherjee *et al.*, 2024).

#### Ionic liquid treatment

The un-milled (UM) and cryo-milled (CM) α-chitin were treated with three different ionic liquids (ILs). The ILs were chosen based on the study by Xu *et al.* (2018) where these were reported to be most effective for pre-treatment of chitin: 1-ethyl 3-methyl imidazolium acetate (EMIA), 1-butyl 3-methyl imidazolium acetate (BMIA) and 1-sulfobutyl 3-methyl imidazolium hydrosulfate (SMIH). The treatment procedure was adapted and slightly modified from Husson *et al.* (2017). Chitin (2%) was incubated with 10 mL of IL at 110°C on an oil bath, under stirring for 40, 90 or 180 min. The resulting chitin suspension was cooled on ice bath and precipitated by adding 20 mL of sterile milliQ water. This suspension was then subjected to vigorous stirring for 30 min and centrifuged at 10733 g for 20 min at 4°C. The supernatant obtained (containing the used IL) was carefully stored at 4°C, while the pellet obtained was subjected to vacuum filtration, followed by wash with sterile milliQ water. The chitin solid was further sonicated in a water bath sonicator at 30% amplitude for 15 min and the pellet was collected by centrifugation. The sonication step was repeated for 3 times,

followed by freeze-drying using lyophilizer. The resulting substrates were stored at room temperature for further analyses.

#### 4.1.3 Characterization of pretreated chitin

#### 4.1.3.1 Fourier Transform Infrared Spectroscopy (FT-IR) analysis

The chitin samples were evenly compressed with KBr to form pellets/disks, which were then subjected to FT-IR analysis using a PerkinElmer Frontier FT-IR/FIR Spectrometer. The spectra were acquired using the attenuated total reflection method, covering a range from 4000 cm<sup>-1</sup> to 400 cm<sup>-1</sup>, as described by Duhsaki *et al.* (2023) and Mukherjee *et al.* (2024).

#### 4.1.3.2 Powder X-ray diffraction (pXRD)

Powder X-ray diffraction (pXRD) measurements were conducted using a PANalytical X'Pert<sup>3</sup> powder diffractometer equipped with Cu-K $\alpha$  radiation and a wavelength of 1.54 Å. The scans were performed within a 2 $\theta$  range of 5° to 40° with a step size of 0.0167°, following the methodology outlined by Duhsaki *et al.* (2023) and Mukherjee *et al.* (2024). Crystallinity index ( $I_{CR}$ ) of the samples were determined using the intensities of the (110) and ( $I_{am}$ ) peaks at 2 $\theta$  of ~20° (corresponding to the maximum intensity) and ~16° (corresponding to the amorphous halo contribution) according to the following equation:

$$I_{CR}$$
 (%) = [ $(I_{110} - I_{am})/I_{110}$ ] X 100

#### 4.1.3.3 Brunauer-Emmett-Teller (BET) analysis

The chitin samples were analyzed for their surface area using a surface area analyzer, the Quantachrome autosorb iQ, Germany. Prior to analysis, the samples underwent degassing at 60°C for 24 h under a N<sub>2</sub> atmosphere to eliminate any moisture adsorbed on the solid surface. The specific surface area was calculated using the BET surface area (S<sub>BET</sub>) method, as previously demonstrated by Duhsaki *et al.* (2023) and Mukherjee *et al.* (2024).

#### 4.1.3.4 Estimation of average fraction of acetylation ( $\bar{x} F_A$ )

Average fraction of acetylation ( $\bar{x}$   $F_A$ ) in the different treated and untreated crude  $\alpha$ -chitin samples was estimated based on a quantitative enzymatic-mass spectrometric analysis, reported previously (Urs *et al.*, 2023).

Sample preparation: The chitin samples were treated with 0.5 mL of 1M NaHCO<sub>3</sub>, followed by 50 μL of [<sup>2</sup>H<sub>6</sub>] acetic anhydride (Sigma Aldrich, USA), in order to *N*-acetylate the glucosamine (GlcN) units in the chitin samples. The reaction contents were mixed immediately to establish homogenous reaction conditions to impart higher selectivity towards *N*-acetylation, and in turn, avoid *O*-acetylation. The samples were first incubated at room temperature for 20 min, followed by 5 min at 100°C. The samples were then centrifuged at 16000 g for 15 min at 4°C and the resulting pellet were washed carefully with 0.5 mL of autoclaved milliQ water for

two times. The final chitin pellet was resuspended in 200 μL of 100 mM ammonium acetate, pH 5.5. The pellet for each chitin sample was treated with a synthetic enzyme cocktail composed of 0.1 μg each of *Sm*ChiB (chitinase from *Serratia marcescens*) and CSN-174 (chitosanase from *Bacillus* sp. 174) and 0.1 U of chitinase from *Trichoderma viride* (Sigma Aldrich, USA). The enzyme reaction was carried out at 30°C for 48h at 500 rpm shaking. The resulting product (supernatant after centrifuging the reaction mixture) was then freeze dried and resuspended in 100 μL of autoclaved milliQ water. The sample was then filtered using a PES 3 K 500 μL (VWR International, USA) at 14000 g for 30 min and the collected filtrate was then used for quantitative analysis.

Product analysis and quantification of GlcNAc and GlcN in the chitin samples: The filtrate collected for each chitin sample were analyzed by Ultra-High Performance Liquid Chromatography-Electrospray Ionization-Mass Spectrometry (UHPLC-ESI-MS), quantifying the amount of GlcNAc and GlcN units present, to determine the average  $F_A$ . A Dionex Ultimate 3000RS UHPLC system (Thermo Scientific, USA) coupled to an amazon speed ESI-MS<sup>n</sup> detector (Bruker Daltonik, Germany) was used for carrying out the measurements. Product separation was carried out using a VanGuard precolumn (1.7 μm, 2.1×5 mm) and an Acquity UHPLC BEH amide column (1.7 µm, 2.1×150 mm; Waters Corp., USA) through Hydrophilic Liquid Interaction Chromatography (HILIC) with solvent A (80 % acetonitrile and 20 % water) and solvent B (20 % acetonitrile and 80 % water), both containing 10 mM NH<sub>4</sub>HCO<sub>2</sub> and 0.1 % (v/v) HCOOH. The separation was achieved by gradient elution using the solvents as essentially described by Urs et al. (2023), at a scan range of 50-2000 m/z, flow rate of 0.4 mL/min and 35°C column oven temperature. One microlitre of the test sample premixed with a known amount of internal standard R\* ([13C2, 2H3] N-acetylated-Dglucosamine) was injected and the resulting data were analyzed using the respective peak areas with Data Analysis v.4.1 software (Bruker Daltonik, Germany). The absolute concentrations of GlcNAc and GlcN in 1 µL of an injected sample, were determined using the peak area generated by known amount of the internal standard R\*, essentially following the method outlined by Urs et al. (2023).

#### 4.1.4 Enzyme production and chitin substrate hydrolysis

4.1.4.1 Production of the recombinant enzymes: Chi3 and Chi5 from Paenibacillus sp. LS1 were cloned and over-expressed in E. coli system as described earlier in sections 3.1.2 and 3.1.3. On the other hand, StrChiA from Streptomyces sp. UH6, EcLPMO from Enterobacter cloacae MCC 2072 and CaGH18 (catalytic domain only) from Chitinispirillum alkaliphilum

DSM 24539 were cloned into pET-28a(+), pET-22b(+) and pNIC expression vectors, respectively and all of them were expressed in BL21(DE3)plysS cells.

Chi3, Chi5 and *Ec*LPMO were expressed by inoculating an overnight grown pre-culture (1%) into fresh Luria Bertani (LB) broth containing 50 μg/mL kanamycin (for Chi3 and Chi5) or 100 μg/mL ampicillin (for *Ec*LPMO). The cells were grown at 37°C, 180 rpm until OD<sub>600</sub> reached between 0.4-0.6. Afterward, the cells were induced with 0.35 mM (for Chi3) or 0.5 mM (for Chi5 and *Ec*LPMO) IPTG and grown at 18°C for 16 h. In case of *Str*ChiA and *Ca*GH18, 1% pre-culture was inoculated into fresh LB broth containing 50 μg/mL kanamycin and 1X of autoinduction medium (Medium I: 1.25 M Na<sub>2</sub>HPO<sub>4</sub>.2H<sub>2</sub>O, 1.25 M KH<sub>2</sub>PO<sub>4</sub>, 2.5 M NH<sub>4</sub>Cl and 0.25M Na<sub>2</sub>SO<sub>4</sub>; Medium II: 25% glycerol, 2.5% glucose and 10% lactose monohydrate; Both media prepared as 50X stock and sterilised before use). The auto-induced cells were grown at 26°C for 24 h. The culture pellets were harvested at 8000 rpm for 10 min at 4°C.

In case of Chi3, Chi5, CaGH18 and StrChiA, the harvested pellet was resuspended into the lysis buffer and processed through sonication as described earlier in section 3.1.2. EcLPMO, on the other hand, was isolated from the periplasmic fraction (where the signal peptide of the protein will be cleaved off upon export) using a two-step osmotic shock method essentially as described earlier by Madhuprakash et al. (2015). In the first step, the pellet was resuspended in ice-cold spheroplast buffer (PF buffer-I: 100 mM Tris-HCl buffer, pH 8.0, 20% sucrose, 0.5 mM EDTA, pH 8.0 and 1mM PMSF) and incubated at 4°C with gentle mixing up to 15 min. The cell suspension was then centrifuged at 8000 rpm for 20 min at 4°C and the supernatant was discarded. The pellet was further resuspended in ice-cold PF buffer-II containing 5 mM MgSO<sub>4</sub> and incubated at 4°C with gentle mixing up to 15 min. This was followed by centrifugation at 8000 rpm for 20 min at 4°C. The resulting periplasmic fraction (supernatant) was dialyzed against the equilibration buffer, prior to purification.

Purification of the sonicated supernatant or periplasmic fraction was performed by Ni-NTA affinity chromatography, as previously described in section 3.1.3. Highly pure protein fractions were pooled, concentrated, and buffer-exchanged with 50 mM Tris-HCl, pH 8.0 using a Vivaspin<sup>®</sup> Turbo 15, 10 kDa centricon (Sartorius Stedim Lab Ltd., UK). Protein concentration was determined using the Pierce<sup>TM</sup> BCA protein assay kit.

4.1.4.2 Time-dependent hydrolysis of  $\alpha$ -chitin substrates: The hydrolysis of UM  $\alpha$ -chitin and the pre-treated  $\alpha$ -chitin substrates, i.e., UM+BMIA, CM and CM+BMIA (10 mg/mL) was conducted using 1  $\mu$ M of the recombinantly produced chitinases in presence or absence of 1  $\mu$ M EcLPMO. The LPMO containing reactions were supplemented with 1 mM ascorbic acid

as a reducing agent. All reactions were carried out in triplicate under optimal reaction conditions at 1000 rpm in an Eppendorf Thermomixer® C. At various time intervals ranging from 1 to 48 h, aliquots were collected and filtered using a 96-well filter plate (0.45 µm filters; Merck Millipore, USA) operated by a Millipore vacuum manifold. The filtered samples were then mixed with equal volume of 70% acetonitrile and analysed on HPLC essentially as described earlier in the section 3.1.6.

#### 4.2 Results & Discussion

Pre-treatment of highly crystalline and naturally abundant substrates, such as  $\alpha$ -chitin is essential for efficient saccharification into products-of-value such as CHOS. Pre-treatment confers reduction in crystallinity by inducing structural alterations, therefore improving enzyme accessibility to the substrate and in turn, enhance hydrolysis to generate higher yields of CHOS (Duhsaki *et al.*, 2023). The substrate used in this study is a highly crystalline, and crude form of  $\alpha$ -chitin. The substrate used was poorly processed, retained its natural color and comprised of considerable amount of protein (Figure 31), closely resembling its natural state, i.e., arthropod/crustacean shells. Clearly, development of a bioprocess to valorize such close-to-natural substrate for efficient production of higher amounts of CHOS will be a vital step towards waste-to-value conversion. Keeping this in mind, the crude  $\alpha$ -chitin was subjected to mild mechanical and chemical pre-treatment methods as an attempt to bring down the crystallinity of the substrate and in turn improve saccharification.



**Figure 31:** Crude  $\alpha$ -chitin used in the present study.

#### 4.2.1 Cryo-milling didn't affect crystallinity but increased surface area of crude α-chitin

The crude  $\alpha$ -chitin was subjected to cryo-milling with varying parameters of milling speed and time, resulting in the generation of three distinct cryo-milled  $\alpha$ -chitin substrates: CM-1 (milled at 300 rpm for 3 h), CM-2 (milled at 400 rpm for 3 h) and CM-3 (milled at 400 rpm for 4 h) (Mukherjee *et al.*, 2024). pXRD analysis was conducted to probe the changes in the crystalline structure of  $\alpha$ -chitin following cryo-milling. The pXRD diffractograms displayed six prominent peaks corresponding to the crystalline planes of (020), (021), (110), (120), (101) and (130), indicative of a typical  $\alpha$ -chitin crystalline structure. Interestingly, compared to UM  $\alpha$ -chitin, CM-3 exhibited a noticeable yet slight decrease in peak intensities for these crystalline planes, particularly, the most crucial crystalline plane (110), although no such significant changes were observed for CM-1 and CM-2 (Figure 32A). Previously, Shamshina *et al.* (2021)

in their study, also reported reduced peak intensities in crystalline planes of cryo-ground commercial chitin powder, further corroborating the validity of our results. Further, the chitin substrates exhibited a crystallinity index ( $I_{CR}$ ), with CM-1 and CM-2 at 88% crystallinity, CM-3 at 86%, and the UM  $\alpha$ -chitin at 89% (Table 5). This reduction in crystallinity correlated with the decreased peak intensity of the essential crystalline plane (110). However, it is important to note that the decrease in crystallinity observed in our study for the cryo-milled chitin substrates was not as pronounced as reported by Shamshina *et al.* (2021), who used commercial chitin powder. This variation in findings may be attributed to the differences in the substrates used.

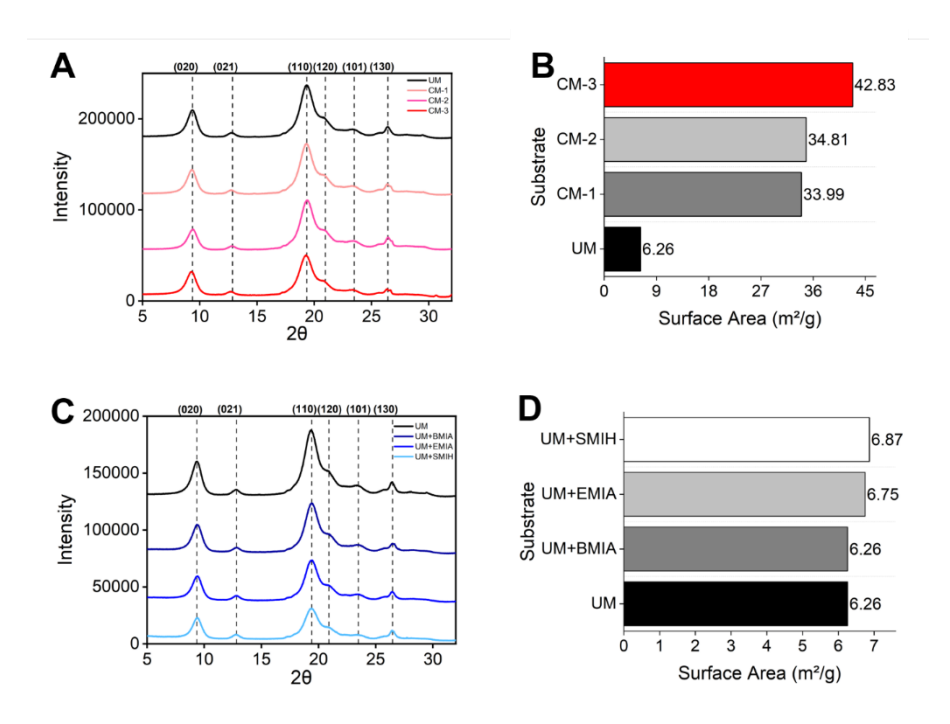


**Figure 32:** Characterization of cryo-milled (CM) and IL-treated un-milled (UM)  $\alpha$ -chitin substrates. A and C represents the pXRD diffractograms and B and D shows the results of BET analysis for the substrates. UM denotes un-milled  $\alpha$ -chitin; CM-1 to CM-3 represents the cryo-milled chitin substrates (A and B); UM+BMIA, UM+EMIA and UM+SMIH represents un-milled  $\alpha$ -chitin substrate treated with three different ionic liquids (C and D).

Of particular interest, a distinct variation in BET surface area ( $S_{BET}$ ) was observed among the chitin substrates, where the cryo-milled chitin substrates showed a 5-7-fold increase in surface area compared to the UM  $\alpha$ -chitin (Figure 32B and Table 6). Among the cryo-milled chitin samples, CM-3 exhibited the highest surface area of 42.8 m²/g (Figure 32B and Table 6). This increase in surface area indicates the relaxation of the compact chitin structure due to the disruption of hydrogen bonds within the chitin polymer induced by cryo-milling. Notably, this is the first report to discuss the impact of cryo-milling on the surface area of chitin.

**Table 5:** Crystallinity Index ( $I_{CR}$ ) of the un-milled and pre-treated  $\alpha$ -chitin substrates determined by pXRD.  $I_{110}$  denotes the maximum intensity of diffraction for the (110) plane at  $2\theta = 20^{\circ}$  and  $I_{am}$  denotes the intensity of the diffraction at the amorphous region at  $2\theta=16^{\circ}$  approximately.

Category	Substrates	I <sub>110</sub> (~20°)	I <sub>am</sub> (16°)	I <sub>CR</sub>
Un-milled α-chitin	UM	63631	7155	89%
Cryo-milled α-chitin	CM-1	62272	7508	88%
	CM-2	60516	7031	88%
	CM-3 (CM)	50444	6972	86%
IL-treated	UM+BMIA	47705	5176	89%
un-milled α-chitin	UM+EMIA	40013	5012	87.5%
a cintin	UM+SMIH	31054	4543	85%
	CM-3+SMIH	22744	5539	75.6%
	CM-3+EMIA	19285	5216	73%
IL-treated cryo-milled	CM-3+BMIA-40min	11670	5309	54.5%
α-chitin	CM-3+BMIA-90min	10803	4983	53.9%
	CM-3+BMIA-180min (CM+BMIA)	10744	5522	48.6%

#### 4.2.2 IL-treatment was effective on CM α-chitin but not on UM α-chitin

Ionic liquids (ILs) have been reported previously as effective pre-treatment agents for chitinous substrates, known to not only make chitin amorphous, but also improve enzymatic hydrolysis rate (Husson *et al.*, 2017; Berton *et al.*, 2018; Xu *et al.*, 2019; Kumar *et al.*, 2020). Imidazolium-based ILs in particular, have gained attention due to their excellent pre-treatment efficiency on chitin substrates (Husson *et al.*, 2017; Berton *et al.*, 2018; Xu *et al.*, 2019). A study by Xu *et al.* (2019) recorded the effect of different imidazolium-based ILs on enzymatic hydrolysis of crab shell particles, among which [BMIm]Ac (BMIA), [EMIm]Ac (EMIA), and [BHSO<sub>3</sub>MIm]HSO<sub>4</sub> (SMIH) were the most effective. Considering the results of the study by Xu *et al.* (2019), the aforementioned ILs were chosen for the pre-treatment of the crude α-chitin in our case. The IL-treatment was conducted for 40 min following the protocol reported by Husson *et al.* (2017) with slight modifications (Section 4.1.2).

**Table 6:** S<sub>BET</sub> analysis of the un-milled and pretreated  $\alpha$ -chitin substrates. The fold change has been calculated compared to UM  $\alpha$ -chitin.

Category	Substrates	S <sub>BET</sub> (m2/g)	Fold change of $S_{BET}$
Un-milled α-chitin	UM	6.2	-
	CM-1	34	5.5
Cryo-milled α-chitin	CM-2	34.8	5.6
	CM-3 (CM)	42.8	6.9
IL-treated	UM+BMIA	6.2	1
un-milled	UM+EMIA	6.7	1.1
α-chitin	UM+SMIH	6.8	1.1
IL-treated cryo-milled α-chitin	CM-3+BMIA-180min (CM+BMIA)	91.7	14.8

Similar to cryo-milling, IL-treatment did not induce any significant reduction to the crystallinity of the crude α-chitin (Figure 32C and Table 5). Only a slight reduction of 4% in  $I_{CR}$  was observed for the SMIH-treated chitin (85%) as compared to the unmilled crude  $\alpha$ -chitin (89%). The poor efficiency of the ILs in amorphization of the substrate could be due to the crude nature of the  $\alpha$ -chitin. Notably, the study by Kumar *et al.* (2020) also showed negligible decrease in  $I_{CR}$  of commercially procured, processed  $\alpha$ -chitin ( $I_{CR}$  reduced from 81% to ~77%) upon treatments with the ILs, EMIA and Trihexyltetradecylphosphonium bis(2,4,4trimethylpentyl)phosphinate. The aforementioned study and our results taken together, clearly confirms that the efficiency of IL-treatment depends upon the IL employed as well as nature of the chitin substrate used. The outcome of BET analysis further ascertained our claims that the ILs were ineffective on the crude  $\alpha$ -chitin as no increase in surface area was observed for any of the IL-treated chitin substrates as compared to the untreated substrate (Figure 32D and Table 6). While, neither cryo-milling nor IL-treatment could reduce crystallinity of the crude  $\alpha$ -chitin substrate, a significant increase in BET surface area was observed for the cryo-milled chitin substrates compared to the UM and UM+IL-treated chitin substrates. This elevated our interest to investigate the possible effects of IL-treatment on cryo-milled chitin during the process of amorphization. Since the cryo-milled substrate, CM-3, showed the highest BET surface area (Figure 32B and Table 6), it was considered as the substrate of choice for the IL-treatments and was referred to as 'CM', henceforth.

Contrary to the UM  $\alpha$ -chitin, the IL treatments were significantly effective on the CM  $\alpha$ -chitin. Upon treatment with the ionic liquids SMIH, EMIA and BMIA, a significant reduction

in I<sub>CR</sub> of CM α-chitin was observed, bringing down the crystallinity from 86% to 75.6%, 73% and 54.5%, respectively (Figure 33A and Table 5). The x-ray diffractograms revealed remarkable reduction in peak intensities of all the crystalline planes for the IL-treated CM αchitin substrates, as compared to UM and CM α-chitin (Figure 33A). This is the first report where a combination of cryo-milling followed by IL treatment have been employed as a pretreatment method. Among the three ILs tested, BMIA showed the best pre-treatment efficiency on CM-3 by a factor of 1.6, reducing the crystallinity up to 54.5% from 86% (Figure 33A and Table 5), therefore indicating the effectiveness of this integrated approach. Our results were in line with the study conducted by Xu et al. (2019), where BMIA showed the best pre-treatment efficiency among eight other ILs tested on crab shell particles. The efficiency of BMIA was higher than EMIA, which is one of the most well-known IL used for amorphization of chitin substrates. This indicates that the n-alkyl group on the imidazolium cation might play an important role in the treatment of chitin. Notably, BMIA has low density (1.05 g/cm<sup>3</sup>) as compared to EMIA (1.1 g/cm<sup>3</sup>) and SMIH (1.47 g/cm<sup>3</sup>) which might favour its operability and its efficiency towards dissolution of chitin (Xu et al., 2019). Interestingly, the resulting substrate upon BMIA treatment of CM-3 was a gel-like form which was in accordance to the observation recorded by Xu et al. (2019). Additionally, variables such as time of IL-treatment may further influence the degree of structural alteration and breakdown of the crude  $\alpha$ -chitin. To investigate this, CM-3 was subjected to BMIA treatment for three different time intervals i.e., 40 min, 90 min and 180 min. On conducting pXRD analysis of the three BMIA-treated CM-3 substrates, no great difference in crystallinity index was observed between 40 min (54.5%) and 90 min (53.9%) treatment time (Figure 33B and Table 5). However, when the treatment time was increased up to 180 min (3 h), a considerable reduction in crystallinity, up to 48.6% was observed (Figure 33B and Table 5). Previously, the study conducted by Xu et al. (2019) also reported 3 h of treatment time with BMIA as ideal for achieving maximum amorphization of crab shell particles, hence confirming the validity of the results obtained in our study. The results collectively indicate that, CM-3 treated with BMIA for 180 min (CM-3+BMIA-180min) is the best pre-treated substrate, considering its low I<sub>CR</sub> value. This substrate was named as CM+BMIA, and the terminology was maintained henceforth.

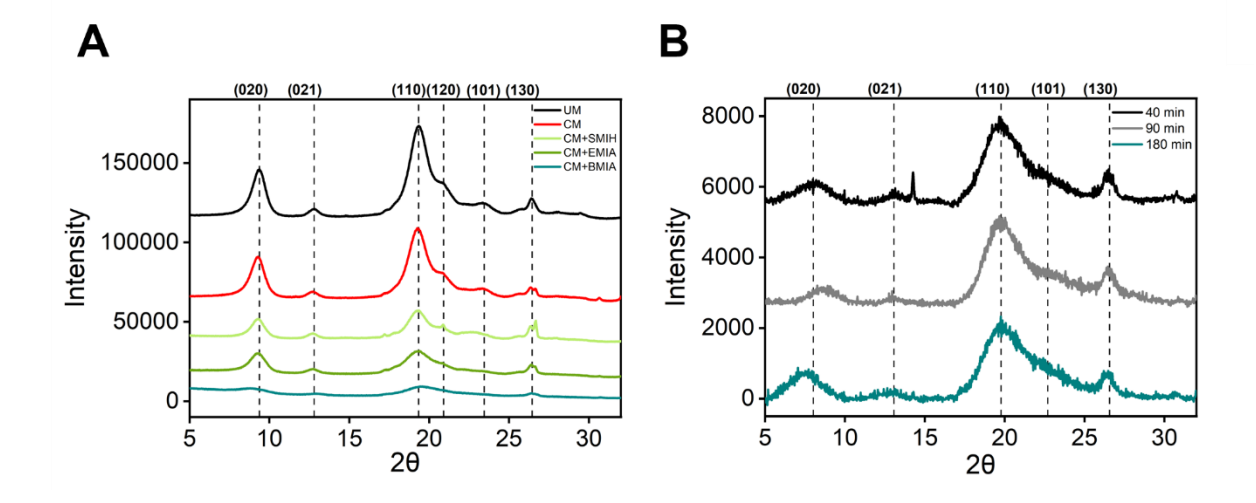


**Figure 33:** pXRD analysis of cryo-milled α-chitin substrates treated with ionic liquids. A represents comparison of the diffractograms recorded for CM α-chitin upon treatment with three different ILs. B – represents pXRD analysis comparing diffractograms of BMIA-treated CM α-chitin for three different treatment times – 40 min, 90 min and 180 min. UM denotes unmilled α-chitin; CM represents cryo-milled chitin; CM+BMIA, CM+EMIA and CM+SMIH represents IL-treated cryo-milled chitin substrates.

In order to understand the extent of structural changes occurred in the crude  $\alpha$ -chitin substrate upon pre-treatment, a comparative analysis representing substrate characterization (FT-IR, pXRD and BET analysis) of the untreated and differentially treated crude α-chitin substrates were recorded in Figure 34. FT-IR spectra was recorded for the substrates - UM, UM+BMIA, CM and CM+BMIA, to gain insights into the impact of cryo-milling on chitin's structural characteristics. Notably, peaks corresponding to the key functional groups, including the amide II band (1558 cm<sup>-1</sup>), amide I single and double bands (1619 and 1654 cm<sup>-1</sup>), N-H stretching band (3259 cm<sup>-1</sup>) and O-H stretching band (3440 cm<sup>-1</sup>) remained unchanged across both UM+BMIA and CM, mirroring the profile observed in UM α-chitin (Figure 34A). This indicated that both cryo-milling and IL-treatment rendered no change in the overall chitin structure of UM α-chitin. Previously, a study by Kumar et al. (2020) reported a similar outcome, wherein no difference in the FT-IR spectral sketches were observed between untreated and IL-treated commercial chitin. Interestingly, FT-IR spectra of CM+BMIA revealed loss of both amide I – single and double bands (1619 cm<sup>-1</sup> and 1654 cm<sup>-1</sup>, respectively) and N-H and O-H stretching bands (3259 cm<sup>-1</sup> and 3440 cm<sup>-1</sup>, respectively) (Figure 34A), suggesting considerable disruption of the chitin structure. Notably, the peak intensity associated with the C-O stretching band (1029-1068 cm<sup>-1</sup>) exhibited no alterations in any of the substrates (Figure 34B), signifying that none of the employed pre-treatment strategies had a discernible impact on the glycosidic bonds within the polymer (Figure 34B).

Furthermore, a comparison of the pXRD diffractograms among the four substrates revealed nearly complete disappearance of all crystalline planes in CM+BMIA, as compared to the other substrates (Figure 34C). This signifies that the proposed process completely disrupted the crystal packing of the crude α-chitin, leading to a great decrease in I<sub>CR</sub> by 1.8 folds (UM vs. CM+BMIA) (Table 5). The achieved fold-decrease in I<sub>CR</sub> is by far the highest as compared to the already known processes involving IL-treatment. Previously, Husson *et al.* (2017) reported 1.5 folds decrease in I<sub>CR</sub> upon treatment of commercial chitin powder with EMIA, while Xu *et al.* (2019) achieved 1.4 folds decrease in I<sub>CR</sub> for both crab shell particles and commercial chitin powder upon treatment with BMIA. It is important to note that the substrate used in our study was a highly crystalline and crude-form of α-chitin, close to its natural state, which makes the proposed process more impactful.

Of distinct interest, a remarkably high BET surface area of 91.67 m<sup>2</sup>/g was observed for CM+BMIA, which was 2 -folds higher than CM and 15 -folds higher than both UM and UM+BMIA (Figure 34D). The high surface area for CM+BMIA suggests further disruption of the hydrogen bonds within the cryo-milled chitin polymer upon IL-treatment, causing relaxation of the compact structure and promoting amorphization. Together, our results show that the CM+IL process effectively disrupts structural attributes of the crude  $\alpha$ -chitin substrate, possibly making it susceptible towards efficient enzymatic degradation.

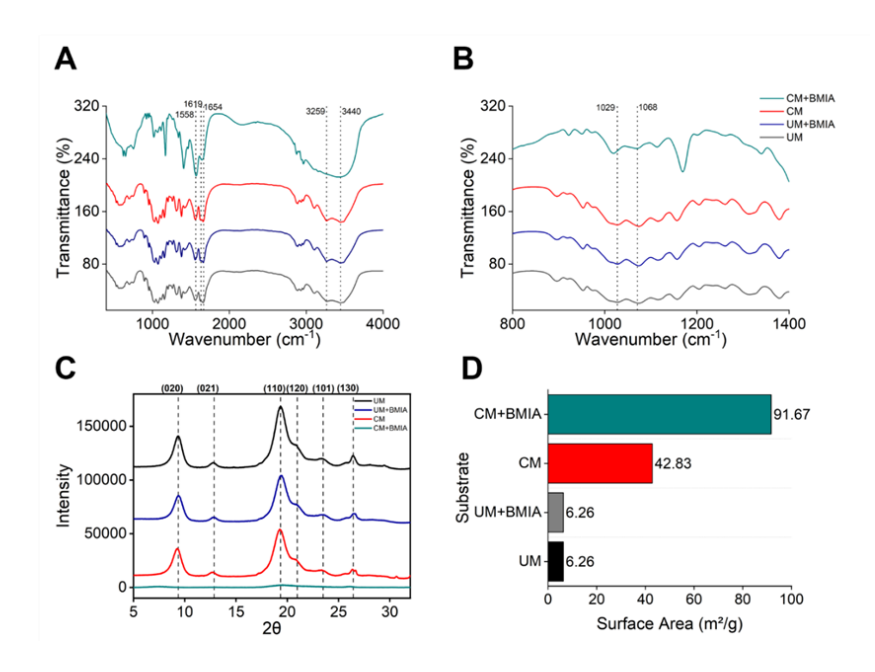


**Figure 34:** Characterization of un-milled (UM) and different pre-treated crude  $\alpha$ -chitin substrate by FTIR (A and B), pXRD (C) and BET analysis (D). UM denotes unmilled  $\alpha$ -chitin, UM+BMIA denotes unmilled  $\alpha$ -chitin treated with BMIA, CM denotes cryo-milled  $\alpha$ -chitin and CM+BMIA denotes cryo-milled  $\alpha$ -chitin treated with BMIA.

#### 4.2.3 The pre-treatment strategies did not affect acetylation of the chitin samples

Average fraction of acetylation ( $\bar{x}$   $F_A$ ) in the unmilled and different pre-treated crude  $\alpha$ -chitin substrates was estimated based on a quantitative enzymatic-mass spectrometric analysis, previously reported by Urs et al. (2023). The method essentially consists of three steps: i) monoisotopic [2H<sub>3</sub>] N-acetylation of GlcN units (if present) in the chitin samples, resulting in isotopically labelled new GlcNAc units and in turn, fully-acetylated chitin; ii) enzymatic hydrolysis of the resulting fully-acetylated chitin using an enzyme cocktail (composition mentioned in section 4.1.3.4); iii) quantification of GlcNAc (denoted as 'A') and [<sup>2</sup>H<sub>3</sub>] GlcNAc (denoted as 'R') for calculation of  $\bar{x}$   $F_A$ . As seen in Figure 35, very high  $\bar{x}$   $F_A$  values were obtained for the UM and different pre-treated crude α-chitin substrates (0.92-0.96), which indicated close to complete acetylation in all the substrates. Further, there was no difference in  $\bar{x}$   $F_A$  values between the samples UM, UM+BMIA and CM, and only a meagre decrease was observed in case of CM+BMIA (Figure 35), suggesting that neither of the pre-treatment strategies induced deacetylation of the crude  $\alpha$ -chitin substrate whatsoever. This observation was further supported by the negligible molar fractions of 'R' (<sup>2</sup>H<sub>3</sub> GlcNAc) found in the chitin samples (ranging between 0.04-0.08) indicating negligible amounts of glucosamine present in the chitin samples. Also, similar to 'A', the molar fraction of 'R' remained unchanged in the samples UM, UM+BMIA and CM, and only a meagre increase was seen for CM+BMIA (Figure 35), further asserting that the different pre-treatment strategies employed did not induce deacetylation of the chitin samples.

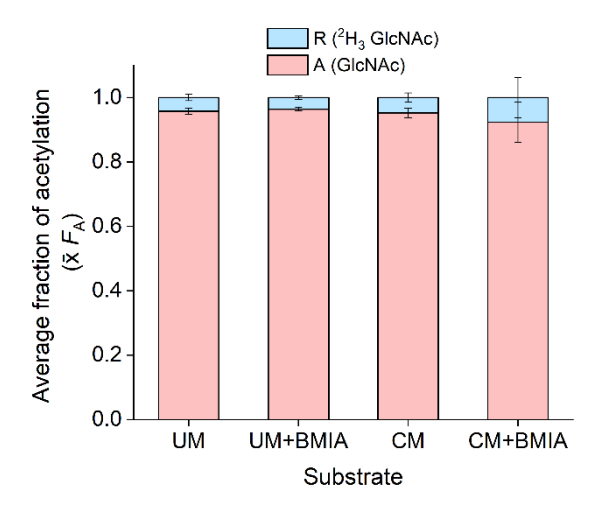


**Figure 35:** Average fraction of acetylation ( $\bar{x}$   $F_A$ ) in the unmilled (UM) and different pretreated crude  $\alpha$ -chitin samples (UM+BMIA, CM and CM+BMIA). A and R were determined using mass spectroscopy after isotopic N-acetylation and complete enzymatic hydrolysis of the chitin samples. The experiment was conducted in biological triplicates, and the error bars represent standard deviation.

## 4.2.4 The mechanochemical pre-treatment improved enzymatic conversion of crude $\alpha$ -chitin to GlcNAc and (GlcNAc)<sub>2</sub>

The impact of the proposed mechanochemical pretreatment method on the enzymatic production of GlcNAc and (GlcNAc)<sub>2</sub> was investigated. A comparative time-course hydrolysis of the unmilled (UM) and the different pre-treated crude α-chitin substrates was performed using the multi-modular chitinase, Chi5 and the uni-modular chitinase, Chi3 from *Paenibacillus* sp. LS1 (Figures 36 and 37). These chitinases as described in Chapters 2 and 3, not only differed in domain architecture, but also in mode-of-action, where Chi5 produced (GlcNAc)<sub>2</sub> as the major product followed by GlcNAc and Chi3 selectively generated only GlcNAc.

The chitin conversion efficiency of Chi5 using CM+BMIA as substrate increased up to 49.4% at 48 h, with a GlcNAc and (GlcNAc)<sub>2</sub> content of  $83 \pm 0.8$  and  $411 \pm 3.2$  mg/g of chitin, respectively (Figure 36 and Table 7). While the conversion efficiency of Chi5 on the substrates, UM, UM+BMIA and CM, was only 2.3%, 2.5% and 5.7%, respectively (Figure 36 and Table 7). The results indicated a significant improvement in conversion efficiency of Chi5 on CM+BMIA by 21.5-, 19.8- and 8.7-folds at 48 h as compared to UM, UM+BMIA and CM  $\alpha$ -chitin substrates, respectively. This showed the efficiency of the CM+IL pre-treatment process in amorphization and subsequent saccharification of the highly crystalline, crude  $\alpha$ -chitin. Further to this, inclusion of *Ec*LPMO in the reaction along with Chi5 only slightly increased conversion efficiency up to 51.2% on the CM+BMIA substrate (Figure 36 and Table 7). This observation was similar to that reported by Nakagawa *et al.* (2013), where addition of *Sm*CBP21 only had a little boosting effect on the activity of the multi-modular *Sm*ChiA on ball-milled chitin substrates.

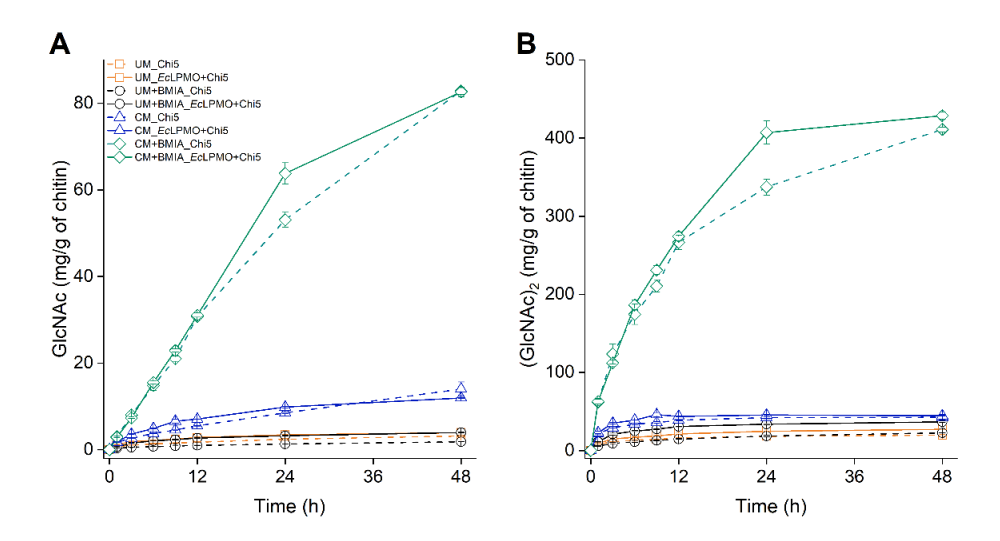


**Figure 36:** Time-course of GlcNAc and (GlcNAc)<sub>2</sub> production from unmilled (UM), BMIA pre-treated UM (UM+BMIA), cryo-milled (CM) and BMIA pre-treated CM (CM+BMIA) crude α-chitin substrates using 1 μM Chi5 from *Paenibacillus* sp. LS1, in presence or absence of 1 μM *Ec*LPMO from *E. cloacae* MCC 2072. The reactions were performed at 40°C and in 50 mM sodium acetate, pH 5.0 (pH optima for Chi5). All LPMO containing reactions were supplemented with 1 mM ascorbic acid. All experiments were performed in biological triplicates and the error bars represent standard deviation.

Surprisingly, Chi3 did not show any significant difference in GlcNAc yield and overall chitin conversion between the untreated and treated substrates (Figure 37 and Table 7). The possible reason behind such outcome could be the weak hydrolytic activity of Chi3 towards crystalline chitin substrates as discussed in Chapter-3. Notably, the rate of hydrolysis of Chi3 on both the IL-treated substrates i.e., UM+BMIA and CM+BMIA was found to be slow but progressive. Interestingly, addition of EcLPMO to the reaction mixture boosted activity of Chi3 on all the four substrates, particularly on CM+BMIA, where the GlcNAc yield at 48 h skyrocketed up to  $28.1 \pm 0.3$  mg/g of chitin, as against  $2.1 \pm 0.01$  mg/g of chitin (in absence of EcLPMO) (Figure 37 and Table 7). Overall, the combination of Chi3 and EcLPMO improved conversion efficiency of CM+BMIA up to 2.8%, which was 8.7-, 14- and 4.7-folds higher than UM, UM+BMIA and CM  $\alpha$ -chitin substrates (Table 7). The results suggest that Chi3 could be better utilized in combination with other chitin-active CAZymes such as an LPMO and/or a multi-modular chitinase for selective and efficient production of GlcNAc, directly from chitin.

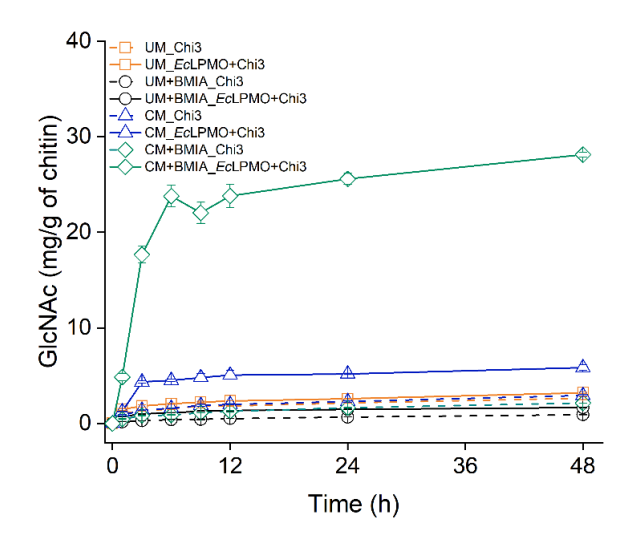


**Figure 37:** Time-course of GlcNAc production from unmilled (UM), BMIA pre-treated UM (UM+BMIA), cryo-milled (CM) and BMIA pre-treated CM (CM+BMIA) crude α-chitin substrates using 1 μM Chi3 from *Paenibacillus* sp. LS1, in presence or absence of 1 μM *Ec*LPMO from *E. cloacae* MCC 2072. The reactions were performed at 40°C and in 50 mM sodium citrate, pH 5.0 (pH optima for Chi3). All LPMO containing reactions were supplemented with 1 mM ascorbic acid. All experiments were performed in biological triplicates and the error bars represent standard deviation.

In order to expand the applicability of our current method beyond *Paenibacillus* chitinases, additional chitin saccharification experiments were performed using unique chitinases from other bacterial sources. *Str*ChiA is a tri-modular chitinase from *Streptomyces* sp. UH6, comprising of an N-terminal CBM4 (sub-family 9) domain, followed by a fnIII and a C-terminal GH18 domain (Duhsaki *et al.*, 2022). Hydrolysis of CM+BMIA using *Str*ChiA generated GlcNAc and (GlcNAc)<sub>2</sub> up to  $7.2 \pm 0.1$  and  $82.5 \pm 2.0$  mg/g of chitin, respectively with an overall conversion efficiency of 9% (Figure 38 and Table 7). The conversion efficiency for *Str*ChiA on CM+BMIA was 37-, 9- and 5.6-folds higher than UM, UM+BMIA and CM  $\alpha$ -chitin substrates (Table 7). The inclusion of *Ec*LPMO with *Str*ChiA further improved GlcNAc and (GlcNAc)<sub>2</sub> yields from CM+BMIA and increased conversion efficiency up to 15% (Figure 38 and Table 7).

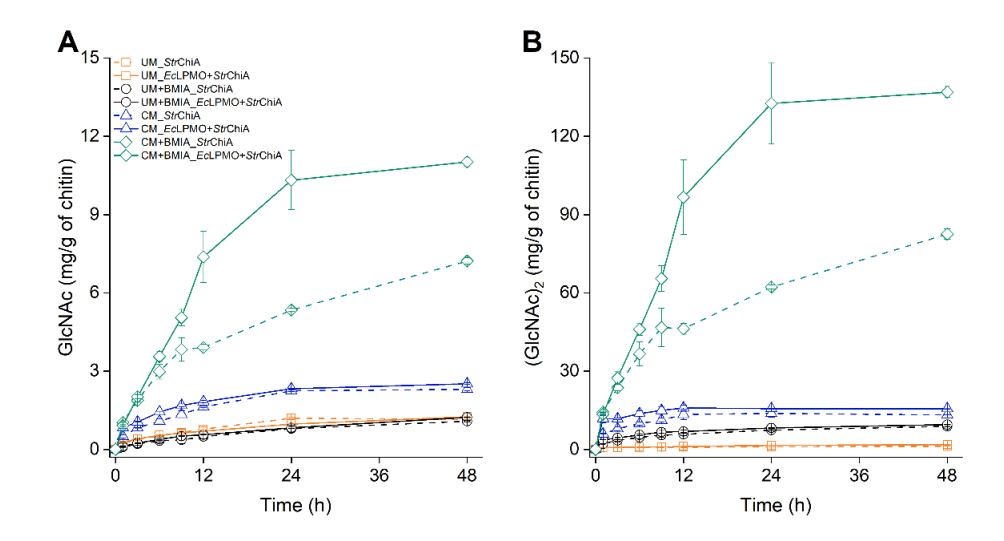


**Figure 38:** Time-course of GlcNAc and (GlcNAc)<sub>2</sub> production from unmilled (UM), BMIA pre-treated UM (UM+BMIA), cryo-milled (CM) and BMIA pre-treated CM (CM+BMIA) crude α-chitin substrates using 1 μM *Str*ChiA from *Streptomyces* sp. UH6, in presence or absence of 1 μM *Ec*LPMO from *E. cloacae* MCC 2072. The reactions were performed at 40°C and in 50 mM sodium citrate, pH 5.0 (pH optima for *Str*ChiA). All LPMO containing reactions were supplemented with 1 mM ascorbic acid. All experiments were performed in biological triplicates and the error bars represent standard deviation.

Furthermore, a unique enzyme, *Ca*GH18 from *Chitinispirillum alkaliphilum* DSM 24539, capable of producing (GlcNAc)<sub>2</sub>, (GlcNAc)<sub>3</sub> and (GlcNAc)<sub>4</sub> directly from crystalline chitin substrates was also tested. Interestingly, hydrolysis of CM+BMIA with *Ca*GH18 generated 12.2 ± 0.8 mg (GlcNAc)<sub>2</sub>, 37.1 ± 2.6 mg (GlcNAc)<sub>3</sub> and 11.3 ± 0.9 mg (GlcNAc)<sub>4</sub> per gram of chitin (Figure 39 and Table 7), with a total chitin conversion efficiency of 6.1%. The conversion efficiency of *Ca*GH18 on CM+BMIA was 15-, 30.5- and 14-folds higher than UM, UM+BMIA and CM α-chitin (Table 7). Furthermore, addition of *Ec*LPMO alongside *Ca*GH18 on CM+BMIA, significantly boosted yield of the individual products and enhanced chitin conversion efficiency up to 15% (Figure 39 and Table 7). The results altogether, indicate that the current process not only enhances GlcNAc and (GlcNAc)<sub>2</sub> production, but also significantly improves production of (GlcNAc)<sub>3</sub> and (GlcNAc)<sub>4</sub>. This is the first study where a mechanochemical-enzymatic method has been reported for direct generation of (GlcNAc)<sub>3</sub> and (GlcNAc)<sub>4</sub> from highly crystalline chitin substrate.

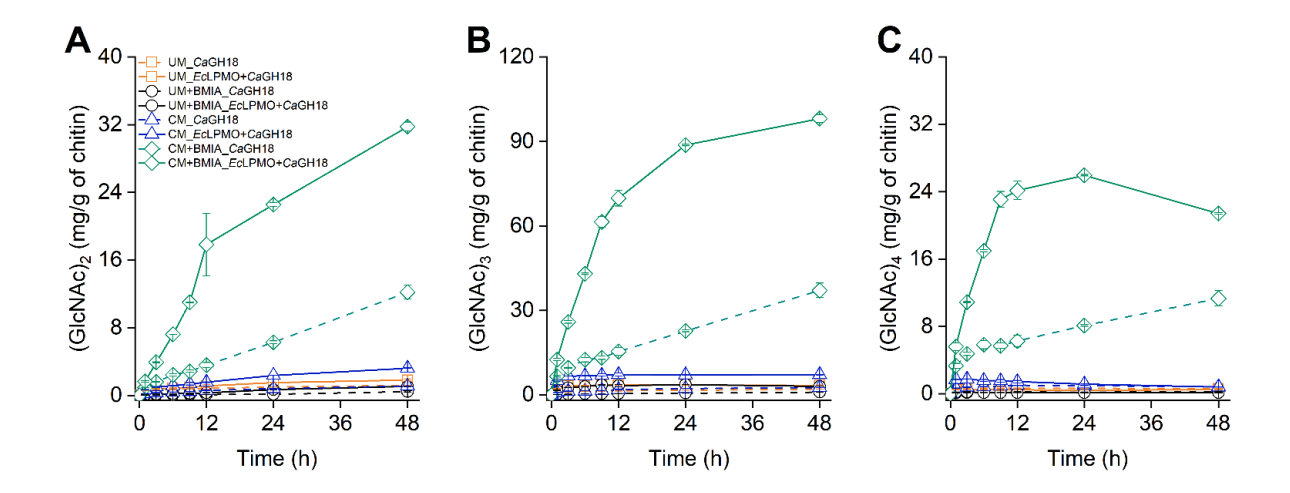


**Figure 39:** Time-course of (GlcNAc)<sub>2</sub>, (GlcNAc)<sub>3</sub> and (GlcNAc)<sub>4</sub> production from unmilled (UM), BMIA pre-treated UM (UM+BMIA), cryo-milled (CM) and BMIA pre-treated CM (CM+BMIA) crude α-chitin substrates using 1 μM *Ca*GH18 from *Chitinispirillum alkaliphilum* DSM 24539, in presence or absence of 1 μM *Ec*LPMO from *E. cloacae* MCC 2072. The reactions were performed at 40°C and in 50 mM Tris-HCl, pH 8.5 (pH optima for *Ca*GH18). All LPMO containing reactions were supplemented with 1 mM ascorbic acid. All experiments were performed in biological triplicates and the error bars represent standard deviation.

Altogether, the results demonstrate that the proposed pre-treatment strategy i.e., CM+IL method is highly effective towards amorphization of highly crystalline chitin substrates and subsequent enzymatic valorization. The proposed bioprocess doesn't involve any harsh chemicals, is energy efficient, avoids loss of CHOS and deacetylation during the process and promotes efficient enzymatic saccharification, making it an eco-friendly process to convert the otherwise chitin waste to value-added products. Another essential highlight of this bioprocess is its versatility and applicability with chitinases of diverse origin and mode-of-action and in turn, supports production of a diverse range of chitooligosaccharides with enhanced yields. For example, the current bioprocess was shown to boost GlcNAc production using Chi3 and EcLPMO (Figure 37 and Table 7). Similarly, it also improved the yields of (GlcNAc)<sub>2-4</sub> in case of CaGH18, both in absence or presence of EcLPMO (Figure 39 and Table 7). The bioprocess also significantly enhanced production of both GlcNAc and (GlcNAc)<sub>2</sub> by multi-modular chitinases such as Chi5 and StrChiA (Figures 36 and 38 and Table 7). Among the chitinases tested, the bioprocess worked remarkably well with the chitinase, Chi5 from Paenibacillus sp. LS1. With a relatively low enzyme load of 1 µM (equivalent to 0.07 mg), Chi5 produced a combined [GlcNAc + (GlcNAc)<sub>2</sub>] yield of 494.0  $\pm$  4.0 and 512.0  $\pm$  6.1 mg/g of chitin, in absence and presence of EcLPMO (also 1  $\mu$ M, equivalent to 0.06 mg), respectively (Table 7).

Previously, CHOS yields of  $547.4 \pm 6.2$  and  $561.0 \pm 10.4$  mg/g of chitin were achieved from 10 mg/mL of IL-treated crab shell particles upon employing the chitinases, chip1 (0.49 mg) and chip2 (0.78 mg) from *P. pasadenensis* CS0611 (Xu *et al.*, 2019). In a different study, 0.1 mg of commercial chitinase preparations from *Trichoderma viride* and *Streptomyces griseus* were employed on 10 mg/mL of IL-treated commercial chitin to selectively produce  $185.0 \pm 4.0$  mg GlcNAc and  $705.0 \pm 5.0$  mg (GlcNAc)<sub>2</sub> per gram of chitin, respectively (Husson *et al.*, 2017). In contrast with these processes, our method achieves similar yields of GlcNAc and/or (GlcNAc)<sub>2</sub> using relatively low enzyme load of Chi5 from *Paenibacillus* sp. LS1. Therefore, considering the mild-nature, versatility and efficiency of the current bioprocess, it can find value in chitin biorefineries.

**Table 7:** Yields of different CHOS products (represented as mg/g of chitin) and chitin conversion efficiency (in %) obtained after 48 h of reaction, over unmilled and different pretreated crude  $\alpha$ -chitin substrates upon hydrolysis with different chitinases in absence or presence of EcLPMO.

Enzymes	Substrates	GlcNAc	(GlcNAc)2	(GlcNAc)3	(GlcNAc)4	Total Yield	% Conversion
Chi3	UM	$2.6 \pm 0.2$	-	-	-	$2.6 \pm 0.2$	0.26
	UM+BMIA	$0.9 \pm 0.03$	-	-	-	$0.9 \pm 0.03$	0.1
	CM	$2.9 \pm 0.1$	-	-	-	$2.9 \pm 0.1$	0.3
	CM+BMIA	$2.1 \pm 0.01$	-	-	-	$2.1 \pm 0.01$	0.2
Chi3+EcLPMO	UM	$3.2 \pm 0.1$	-	-	-	$3.2 \pm 0.1$	0.32
	UM+BMIA	$1.6 \pm 0.02$	-	-	-	$1.6 \pm 0.02$	0.2
	CM	$5.8 \pm 0.3$	-	-	-	$5.8 \pm 0.3$	0.6
	CM+BMIA	$28.1 \pm 0.3$	-	-	-	$28.1 \pm 0.3$	2.8
Chi5	UM	$3.0 \pm 0.2$	$20.0 \pm 0.7$	-	-	$23.0 \pm 0.9$	2.3
	UM+BMIA	$2.0 \pm 0.0$	$23.0 \pm 0.4$	-	-	$25.0 \pm 0.4$	2.5
	CM	$14.0 \pm 1.6$	$43.0 \pm 3.4$	-	-	$57.0 \pm 5.0$	5.7
	CM+BMIA	$83.0 \pm 0.8$	$411.0 \pm 3.2$	-	-	$494.0 \pm 4.0$	49.4
Chi5+EcLPMO	UM	$4.0 \pm 0.1$	$27.0 \pm 0.01$	-	-	$31.0 \pm 0.1$	3.1
	UM+BMIA	$4.0 \pm 0.1$	$37.0 \pm 0.9$	-	-	$41.0 \pm 1.0$	4.1
	CM	$12.0 \pm 0.1$	$45.0 \pm 0.5$	-	-	$57.0 \pm 0.6$	5.7
	CM+BMIA	$83.0 \pm 1.1$	$429.0 \pm 5.0$	-	-	$512.0 \pm 6.1$	51.2
StrChiA	UM	$1.1 \pm 0.0$	$1.2 \pm 0.03$	-	-	$2.4 \pm 0.03$	0.24
	UM+BMIA	$1.1 \pm 0.02$	$8.8 \pm 0.3$	-	-	$9.9 \pm 0.3$	1
	CM	$2.3 \pm 0.1$	$13.8 \pm 0.1$	-	-	$16.1 \pm 0.2$	1.6
	CM+BMIA	$7.2 \pm 0.1$	$82.5 \pm 2.0$	-	-	$89.7 \pm 2.1$	9
StrChiA+EcLPMO	UM	$1.2 \pm 0.0$	$1.8 \pm 0.1$	-	-	$3.0 \pm 0.1$	0.3
	UM+BMIA	$1.2 \pm 0.01$	$9.5 \pm 0.1$	-	-	$10.7 \pm 0.1$	1.1
	CM	$2.5 \pm 0.03$	$15.6 \pm 0.2$	-	-	$18.1 \pm 0.2$	1.8
	CM+BMIA	$11 \pm 0.2$	$136.9 \pm 2.2$	-	-	$147.9 \pm 2.4$	14.8
CaGH18	UM	1	$1.2 \pm 0.03$	$2.1 \pm 0.1$	$0.6 \pm 0.01$	$3.9 \pm 0.1$	0.4
	UM+BMIA	1	$0.5 \pm 0.1$	$0.9 \pm 0.0$	$0.2 \pm 0.03$	$1.6 \pm 0.1$	0.2
	CM	1	$1.1 \pm 0.02$	$2.6 \pm 0.03$	$0.8 \pm 0.02$	$4.5 \pm 0.1$	0.45
	CM+BMIA	-	$12.2 \pm 0.8$	$37.1 \pm 2.6$	$11.3 \pm 0.9$	$60.6 \pm 4.3$	6.1
CaGH18+EcLPMO	UM	-	$1.8 \pm 0.1$	$3.4 \pm 0.2$	$0.5 \pm 0.04$	$5.7 \pm 0.3$	0.6
	UM+BMIA	-	$1.1 \pm 0.03$	$3.1 \pm 0.1$	$0.1 \pm 0.0$	$4.3 \pm 0.1$	0.4
	CM	-	$3.2 \pm 0.03$	$7.2 \pm 0.1$	$0.8 \pm 0.01$	$11.2 \pm 0.1$	1.1
	CM+BMIA	-	$31.8 \pm 0.5$	$98.1 \pm 1.5$	$21.4 \pm 0.1$	$151.3 \pm 2.1$	15.1

Note: chitin conversion efficiency (%) = [(total CHOS released (mg)/1000 mg chitin]  $\times 100$ 

# **Chapter-5**Summary and Conclusion

### 5.1 Insights into the chitinolytic potential of the novel isolate Paenibacillus sp. LS1

Paenibacillus sp. LS1 is a rod-shaped bacterium that produced significant zone of clearance on M9-CC-agar plate. Additionally, the ability to degrade different polymeric chitin substrates has not yet explored for the closest phylogenetic neighbours of the isolate, i.e., *P. amylolyticus*, *P. tundrae* and *P. tylopili*. Therefore, the untapped chitinolytic potential of *Paenibacillus* sp. LS1 was explored in this study.

Growth studies of *Paenibacillus* sp. LS1 on different chitin substrates (as sole carbon source) revealed preference towards  $\beta$ -chitin and CC, as compared to  $\alpha$ -chitin. The same was reflected in the results of time-dependant total cellular protein estimation and extracellular chitinase activity, and zymogram analysis. FE-SEM analysis further confirmed the substrate preference of the isolate, where degradation of α-chitin flake was slow with gradual intensification with time, while degradation of  $\beta$ -chitin flake was rapid and highly intense. Further, Paenibacillus sp. LS1 had a genome size of 7.2 Mb with a 45.5% GC content. ANI and in silico DDH analyses revealed the isolate as a novel species under the genus Paenibacillus. The genome of the isolate encoded CAZymes of different classes and families, of which, six were GH18 family proteins (putative chitinases; Chi1 to Chi6) However, only two of these putative chitinases, i.e., the multi-modular Chi5 and Chi6, were identified in high abundance in the secretome fractions produced by the isolate on  $\alpha$ - and  $\beta$ -chitin. Additionally, a putative (GlcNAc)<sub>2</sub>-specific transporter and a few non-specific transporters with probable affinity towards (GlcNAc)<sub>2</sub> were also identified from the secretome analysis (the isolate was unable to grow on GlcNAc as the sole carbon source, indicating lack of required transport machinery for metabolism). Further, multiple sequence alignment of the six GH18 family proteins with the well-characterized chitinases, SmChiB and BcChiA1 revealed Chi3, Chi5 and Chi6 as true-chitinases. Among these, only Chi3 (a uni-modular chitinase) and Chi5 could be obtained as soluble proteins from heterologous over-expression studies, and hence were taken forward for in-depth biochemical characterization. Both Chi3 and Chi5 showed optimal activity at acidic pH (pH 5.0), but differed in optimal temperature (40°C and 45°C, respectively). Chi3 had a narrow substrate-range, where it showed activity against amorphous chitin substrates, such as CC and chitosan (90% DDA), but not crystalline chitin substrates. On the other hand, Chi5 showed a broad-substrate range, displaying highest activity on the crystalline chitin substrate, β-chitin. Further, both chitinases displayed an exo-acting mode-ofaction. Chi3 was particularly active against different CHOS substrates [ranging from (GlcNAc)<sub>1-6</sub>] and produced GlcNAc as the major end-product. It also produced GlcNAc as the only product from time-dependant CC hydrolysis, confirming β-N-acetylhexosaminidase (chitobiase) activity. On the other hand, Chi5 showed activity on CHOS with longer chain length [ranging from (GlcNAc)<sub>4-6</sub>] and generated (GlcNAc)<sub>2</sub> as the major end-product. It also produced (GlcNAc)<sub>2</sub> followed by GlcNAc from different crystalline chitin substrates with considerably good efficiency. Considering the insights from genomic and proteomic analysis, along with biochemical characterization of Chi3 and Chi5, a pathway showing chitin degradation and metabolism by *Paenibacillus* sp. LS1 has been proposed in Figure 40. This part of the study not only helped in gaining insights into chitinolytic potential of *Paenibacillus* sp. LS1, but also helped in identifying and characterizing two chitinase targets for establishing a bioprocess for efficient chitin valorization to GlcNAc and (GlcNAc)<sub>2</sub>.

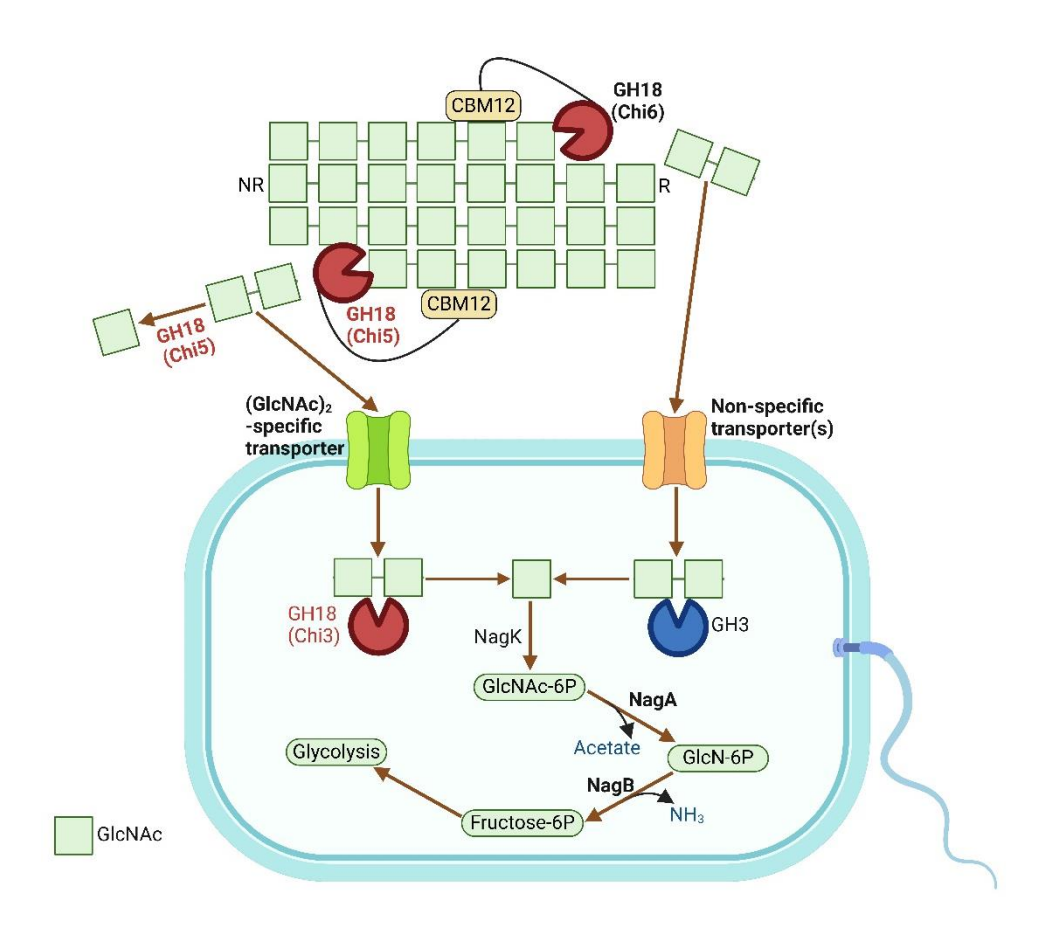


**Figure 40:** Proposed pathway for chitin degradation and metabolism in *Paenibacillus* sp. LS1. The CAZymes involved in chitin degradation are represented as cartoons with different colors as per their CAZyme family: GH18 (red) and GH3 (blue). Labels: black, detected in genome; red, detected in genome and characterized; black with bold, detected in genome and proteome, but not characterized; red with bold, detected in genome and proteome and also characterized; blue, side-products/metabolites. Abbreviations: NR, nonreducing end; R, reducing end; GH, glycoside hydrolase; NagK, N-acetylglucosamine kinase; NagA, N-acetylglucosamine-6-phosphate deacetylase; NagB, glucosamine-6-phosphate deaminase; GlcNAc-6P, N-acetylglucosamine-6-phosphate; GlcN-6P, glucosamine-6-phosphate; Fructose-6P, fructose-6-phospate. Note: NagA (WP\_264934224.1) and NagB (WP\_264934223.1) were detected

among the cytosolic proteins in the proteome analysis. This figure was prepared using BioRender (BioRender.com).

### 5.2 A benign mechanochemical pre-treatment process for production of GlcNAc and (GlcNAc)<sub>2</sub> from highly crystalline crude chitin substrates

The  $\alpha$ -chitin is the most abundant, and also the most crystalline form of chitin existing on Earth. The high degree of crystallinity in  $\alpha$ -chitin is conferred by the tightly packed anti-parallel chains (Figure 2B) due to the presence of both inter- and intra-sheet hydrogen bonds (Figure 2C) (Cao *et al.* 2022; Duhsaki *et al.*, 2023). These characteristics make  $\alpha$ -chitin resistant to efficient enzymatic saccharification for CHOS production [mainly GlcNAc and (GlcNAc)<sub>2</sub>]. In order to overcome this problem, pre-treatment of  $\alpha$ -chitin is necessary to amorphize the substrate prior to enzymatic hydrolysis. In this part of the study, attempts were made to develop a bioprocess (involving chitinases from *Paenibacillus* sp. LS1 and other bacterial sources) for efficient production of GlcNAc and (GlcNAc)<sub>2</sub> directly from a highly crystalline and crude  $\alpha$ -chitin substrate (Figure 31).

Mechanical and chemical pre-treatments of the crude chitin substrate by cryo-milling and IL, respectively, under optimized conditions, were ineffective in reducing crystallinity. Whereas, an integrated mechano-chemical approach, where the chitin was first pre-treated with cryo-milling and then, the resulting cryo-milled substrate was treated with a suitable IL (BMIA) showed remarkable reduction in crystallinity as well as significant increase in BET surface area. While the pre-treatment resulted in loss of few functional groups in the final substrate (CM+BMIA), it had no impact on the glycosidic bonds of the chitin polymer. Additionally, there was no change in average F<sub>A</sub> values among the treated and untreated chitin substrates, suggesting that the mechano-chemical pre-treatment did not induce deacetylation. This substrate, CM+BMIA, was taken forward for enzymatic hydrolysis, involving different chitinases (Chi3 and Chi5 from Paenibacillus sp. LS1, StrChiA from Streptomyces sp. UH6 and CaGH18 from C. alkaliphilum DSM 24539), in presence and absence of an LPMO (from E. cloacae MCC 2072). The proposed bioprocess was versatile and applicable with chitinases of diverse origin and mode-of-action and in turn, supported production of enhanced yields of not only GlcNAc and (GlcNAc)2, but also CHOS such as (GlcNAc)3-4. The enhanced product yields were observed both in presence and absence of LPMO in the reaction mixture. Among the chitinases tested, the process worked remarkably well with the chitinase, Chi5 from Paenibacillus sp. LS1, which showed chitin conversion efficiency of ~50% on CM+BMIA using a very low enzyme load (1 µM). The results taken together demonstrated that the

proposed bioprocess is an efficient strategy for amorphization of highly crystalline chitin substrates and in turn, improvement of enzymatic valorization for efficient production of GlcNAc, (GlcNAc)<sub>2</sub> and CHOS. A schematic representation of the overall bioprocess is shown in Figure 41.

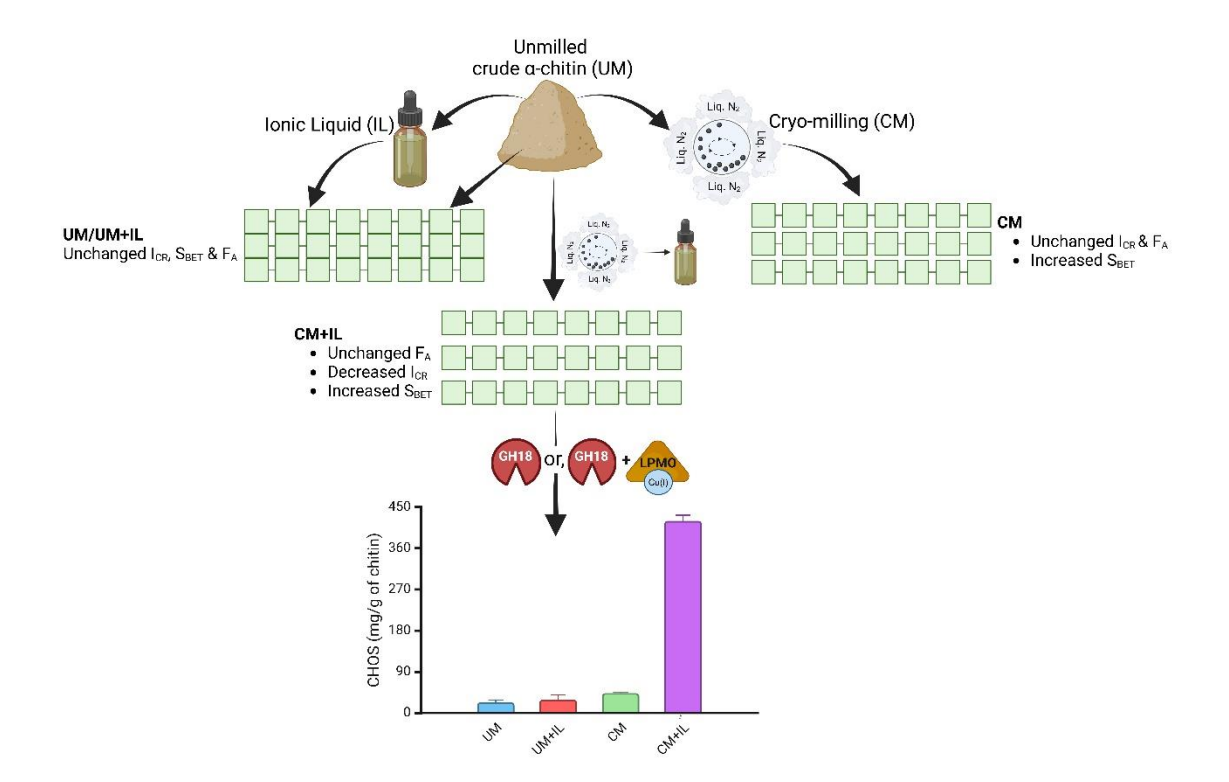


**Figure 41:** Schematic representation of the proposed bioprocess for efficient production of chitooligosaccharides from crude α-chitin.  $I_{CR}$ , crystallinity index;  $S_{BET}$ , BET surface area;  $F_A$ , average fraction of deacetylation; GH18, glycoside hydrolase family 18; LPMO, lytic polysaccharide monooxygenase; CHOS, chitooligosaccharide. This figure was prepared using BioRender (BioRender.com).

In conclusion, the novel isolate, *Paenibacillus* sp. LS1 and the bioprocess proposed in this study can find possible applications in chitin biorefineries for the production of industrially relevant products such as GlcNAc and (GlcNAc)<sub>2</sub>.

- 1) Aam, B.B., Heggset, E.B., Norberg, A.L., Sørlie, M., Vårum, K.M. & Eijsink, V.G. (2010) Production of chitooligosaccharides and their potential applications in medicine, *Marine Drugs.* **8**, 1482-1517. <a href="https://doi.org/10.3390/md8051482">https://doi.org/10.3390/md8051482</a>
- 2) Abidin, M. Z., Kourmentza, K. & Niranjan, K. (2023) Chitin Oligosaccharide *N, N'*-Diacetylchitobiose (GlcNAc<sub>2</sub>) as Antimicrobial Coating against *Listeria monocytogenes* on Ready-to-Eat Shrimp, *Sustainability*. **15**, 1-11. https://doi.org/10.3390/su151310099
- 3) Ash, C., Priest, F. G. & Collins, M. D. (1993) Molecular identification of rRNA group 3 bacilli (Ash, Farrow, Wallbanks and Collins) using a PCR probe test: proposal for the creation of a new genus *Paenibacillus*, *Antonie van Leeuwenhoek*. **64**, 253-260. <a href="https://doi.org/10.1007/BF00873085">https://doi.org/10.1007/BF00873085</a>
- 4) Bai, Y., Eijsink, V. G., Kielak, A. M., van Veen, J. A. & de Boer, W. (2016) Genomic comparison of chitinolytic enzyme systems from terrestrial and aquatic bacteria, *Environmental Microbiology.* **18**, 38-49. <a href="https://doi.org/10.1111/1462-2920.12545">https://doi.org/10.1111/1462-2920.12545</a>
- 5) Barber, M., Bertram, R. & Ride, J. (1989) Chitin oligosaccharides elicit lignification in wounded wheat leaves, *Physiological and Molecular Plant Pathology*. **34**, 3-12. <a href="https://doi.org/10.1016/0885-5765(89)90012-X">https://doi.org/10.1016/0885-5765(89)90012-X</a>
- 6) Berková, V., Berka, M., Štěpánková, L., Kováč, J., Auer, S., Menšíková, S., Ďurkovič, J., Kopřiva, S., Ludwig-Müller, J., Brzobohatý, B. & Černý, M. (2024) The fungus *Acremonium alternatum* enhances salt stress tolerance by regulating host redox homeostasis and phytohormone signaling, *Physiologia Plantarum*. **176**, e14328. https://doi.org/10.1111/ppl.14328
- 7) Berton, P., Shamshina, J. L., Ostadjoo, S., King, C. A. & Rogers, R. D. (2018) Enzymatic hydrolysis of ionic liquid-extracted chitin, *Carbohydrate Polymers*. **199**, 228-235. <a href="https://doi.org/10.1016/j.carbpol.2018.07.014">https://doi.org/10.1016/j.carbpol.2018.07.014</a>
- 8) Bhuvanachandra, B. & Podile, A. R. (2020) A transglycosylating chitinase from *Chitiniphilus shinanonensis* (*CsChiL*) hydrolyzes chitin in a processive manner, *International Journal of Biological Macromolecules*. **145**, 1-10. <a href="https://doi.org/10.1016/j.ijbiomac.2019.12.134">https://doi.org/10.1016/j.ijbiomac.2019.12.134</a>
- 9) Brettin, T., Davis, J. J., Disz, T., Edwards, R. A., Gerdes, S., Olsen, G. J., Olson, R., Overbeek, R., Parrello, B. & Pusch, G. D. (2015) RASTtk: a modular and extensible implementation of the RAST algorithm for building custom annotation pipelines and annotating batches of genomes, *Scientific Reports*. 5, 1-6. <a href="https://doi.org/10.1038/srep08365">https://doi.org/10.1038/srep08365</a>
- 10) Brown, J., Pirrung, M. & McCue, L. A. (2017) FQC Dashboard: integrates FastQC results into a web-based, interactive, and extensible FASTQ quality control tool, *Bioinformatics*. **33**, 3137-3139. https://doi.org/10.1093/bioinformatics/btx373
- 11) Cao, S., Liu, Y., Shi, L., Zhu, W. & Wang, H. (2022) *N*-acetylglucosamine as a platform chemical produced from renewable resources: opportunity, challenge, and future prospects, *Green Chemistry*. **24**, 493-509. <a href="https://doi.org/10.1039/D1GC03725K">https://doi.org/10.1039/D1GC03725K</a>
- 12) Chen, W., Jiang, X. & Yang, Q. (2020) Glycoside hydrolase family 18 chitinases: The known and the unknown, *Biotechnology Advances*. **43**, 107553. <a href="https://doi.org/10.1016/j.biotechadv.2020.107553">https://doi.org/10.1016/j.biotechadv.2020.107553</a>
- 13) Crofton, A. R., Hudson, S. M., Howard, K., Pender, T., Abdelgawad, A., Wolski, D. & Kirsch, W. M. (2016) Formulation and characterization of a plasma sterilized, pharmaceutical grade chitosan powder, *Carbohydrate Polymers*. **146**, 420-426. <a href="https://doi.org/10.1016/j.carbpol.2016.03.003">https://doi.org/10.1016/j.carbpol.2016.03.003</a>
- 14) Dhital, S., Shrestha, A. K., Flanagan, B. M., Hasjim, J. & Gidley, M. J. (2011) Cryomilling of starch granules leads to differential effects on molecular size and

- conformation, *Carbohydrate Polymers*. **84**, 1133-1140. https://doi.org/10.1016/j.carbpol.2011.01.002
- 15) Dhital, S., Shrestha, A. K. & Gidley, M. J. (2010) Effect of cryo-milling on starches: Functionality and digestibility, *Food Hydrocolloids*. **24**, 152-163. <a href="https://doi.org/10.1016/j.foodhyd.2009.08.013">https://doi.org/10.1016/j.foodhyd.2009.08.013</a>
- 16) Dong, W., Tang, J., Cropotova, J., Sun, D.-W. & Tiwari, B. K. (2024) Green Technologies for Bio-refinery in Marine Crustacean Shell Valorisation from Chitin Perspective, *Trends in Food Science & Technology*, 104580. <a href="https://doi.org/10.1016/j.tifs.2024.104580">https://doi.org/10.1016/j.tifs.2024.104580</a>
- 17) Dorfer, V., Pichler, P., Stranzl, T., Stadlmann, J., Taus, T., Winkler, S. & Mechtler, K. (2014) MS Amanda, a universal identification algorithm optimized for high accuracy tandem mass spectra, *Journal of Proteome Research*. **13**, 3679-3684. https://doi.org/10.1021/pr500202e
- 18) Duhsaki, L., Mukherjee, S. & Madhuprakash, J. (2023) Improving the efficiency and sustainability of chitin bioconversion through a combination of *Streptomyces* chitinactive-secretomes and mechanical-milling, *Green Chemistry*. **25**, 6832-6844. https://doi.org/10.1039/D3GC01084H
- 19) Duhsaki, L., Mukherjee, S., Rani, T. S. & Madhuprakash, J. (2022) Genome analysis of *Streptomyces* sp. UH6 revealed the presence of potential chitinolytic machinery crucial for chitosan production, *Environmental Microbiology Reports*. **14**, 431-442. <a href="https://doi.org/10.1111/1758-2229.12986">https://doi.org/10.1111/1758-2229.12986</a>
- 20) Drula, E., Garron, M.-L., Dogan, S., Lombard, V., Henrissat, B. & Terrapon, N. (2022) The carbohydrate-active enzyme database: functions and literature, *Nucleic Acids Research*. **50**, D571-D577. https://doi.org/10.1093/nar/gkab1045
- 21) Felix, G., Regenass, M. & Boller, T. (1993) Specific perception of subnanomolar concentrations of chitin fragments by tomato cells: induction of extracellular alkalinization, changes in protein phosphorylation, and establishment of a refractory state, *The Plant Journal.* **4**, 307-316. <a href="https://doi.org/10.1046/j.1365-313X.1993.04020307.x">https://doi.org/10.1046/j.1365-313X.1993.04020307.x</a>
- 22) Forsberg, Z., Nelson, C. E., Dalhus, B., Mekasha, S., Loose, J. S., Crouch, L. I., Røhr, Å. K., Gardner, J. G., Eijsink, V. G. & Vaaje-Kolstad, G. (2016) Structural and functional analysis of a lytic polysaccharide monooxygenase important for efficient utilization of chitin in *Cellvibrio japonicus*, *Journal of Biological Chemistry*. **291**, 7300-7312. https://doi.org/10.1074/jbc.M115.700161
- 23) Fu, X., Yan, Q., Wang, J., Yang, S. & Jiang, Z. (2016) Purification and biochemical characterization of novel acidic chitinase from *Paenicibacillus barengoltzii*, *International Journal of Biological Macromolecules*. **91**, 973-979. https://doi.org/10.1016/j.ijbiomac.2016.06.050
- 24) Fu, X., Yan, Q., Yang, S., Yang, X., Guo, Y. & Jiang, Z. (2014) An acidic, thermostable exochitinase with β-*N*-acetylglucosaminidase activity from *Paenibacillus barengoltzii* converting chitin to *N*-acetyl glucosamine, *Biotechnology for Biofuels*. **7**, 1-11. https://doi.org/10.1186/s13068-014-0174-y
- 25) Grady, E. N., MacDonald, J., Liu, L., Richman, A. & Yuan, Z.-C. (2016) Current knowledge and perspectives of *Paenibacillus*: a review, *Microbial Cell Factories*. **15**, 1-18. <a href="https://doi.org/10.1186/s12934-016-0603-7">https://doi.org/10.1186/s12934-016-0603-7</a>
- 26) Gurevich, A., Saveliev, V., Vyahhi, N. & Tesler, G. (2013) QUAST: quality assessment tool for genome assemblies, *Bioinformatics*. **29**, 1072-1075. <a href="https://doi.org/10.1093/bioinformatics/btt086">https://doi.org/10.1093/bioinformatics/btt086</a>

- 27) Hamed, I., Özogul, F. & Regenstein, J.M. (2016) Industrial applications of crustacean by-products (chitin, chitosan, and chitooligosaccharides): A review, *Trends in Food Science & Technology*. **48**, 40-50. https://doi.org/10.1016/j.tifs.2015.11.007
- 28) Hessel, V., Tran, N. N., Asrami, M. R., Tran, Q. D., Long, N. V. D., Escribà-Gelonch, M., Tejada, J. O., Linke, S. & Sundmacher, K. (2022) Sustainability of green solvents—review and perspective, *Green Chemistry*. **24**, 410-437. https://doi.org/10.1039/D1GC03662A
- 29) Horn, S. J., Sikorski, P., Cederkvist, J. B., Vaaje-Kolstad, G., Sørlie, M., Synstad, B., Vriend, G., Vårum, K. M. & Eijsink, V. G. (2006b) Costs and benefits of processivity in enzymatic degradation of recalcitrant polysaccharides, *Proceedings of the National Academy of Sciences*. **103**, 18089-18094. <a href="https://doi.org/10.1073/pnas.0608909103">https://doi.org/10.1073/pnas.0608909103</a>
- 30) Horn, S. J., Sørbotten, A., Synstad, B., Sikorski, P., Sørlie, M., Vårum, K. M. & Eijsink, V. G. (2006a) Endo/exo mechanism and processivity of family 18 chitinases produced by *Serratia marcescens*, *The FEBS Journal*. **273**, 491-503. https://doi.org/10.1111/j.1742-4658.2005.05079.x
- 31) Husson, E., Hadad, C., Huet, G., Laclef, S., Lesur, D., Lambertyn, V., Jamali, A., Gottis, S., Sarazin, C. & Van Nhien, A. N. (2017) The effect of room temperature ionic liquids on the selective biocatalytic hydrolysis of chitin via sequential or simultaneous strategies, *Green Chemistry*. **19**, 4122-4131. https://doi.org/10.1039/C7GC01471F
- 32) Ikegami, T., Okada, T., Hashimoto, M., Seino, S., Watanabe, T. & Shirakawa, M. (2000) Solution structure of the chitin-binding domain of *Bacillus circulans* WL-12 chitinase A1, *Journal of Biological Chemistry*. **275**, 13654-13661. <a href="https://doi.org/10.1074/jbc.275.18.13654">https://doi.org/10.1074/jbc.275.18.13654</a>
- 33) Itoh, T., Hibi, T., Suzuki, F., Sugimoto, I., Fujiwara, A., Inaka, K., Tanaka, H., Ohta, K., Fujii, Y. & Taketo, A. (2016) Crystal structure of chitinase ChiW from *Paenibacillus* sp. str. FPU-7 reveals a novel type of bacterial cell-surface-expressed multi-modular enzyme machinery, *PLoS One.* **11**, e0167310. https://doi.org/10.1371/journal.pone.0167310
- 34) Itoh, T., Sugimoto, I., Hibi, T., Suzuki, F., Matsuo, K., Fujii, Y., Taketo, A. & Kimoto, H. (2014) Overexpression, purification, and characterization of Paenibacillus cell surface-expressed chitinase ChiW with two catalytic domains, *Bioscience, Biotechnology, and Biochemistry*. **78**, 624-634. https://doi.org/10.1080/09168451.2014.891935
- 35) Itoh, T., Hibi, T., Fujii, Y., Sugimoto, I., Fujiwara, A., Suzuki, F., Iwasaki, Y., Kim, J.-K., Taketo, A. & Kimoto, H. (2013) Cooperative degradation of chitin by extracellular and cell surface-expressed chitinases from *Paenibacillus* sp. strain FPU-7, *Applied and Environmental Microbiology*. **79**, 7482-7490. https://doi.org/10.1128/AEM.02483-13
- 36) Juarez-Jimenez, B., Rodelas, B., Martinez-Toledo, M. V., Gonzalez-Lopez, J., Crognale, S., Gallo, A. M., Pesciaroli, C. & Fenice, M. (2008) Production of chitinolytic enzymes by a strain (BM17) of *Paenibacillus pabuli* isolated from crab shells samples collected in the east sector of central Tyrrhenian Sea, *International Journal of Biological Macromolecules*. **43**, 27-31. https://doi.org/10.1016/j.ijbiomac.2007.10.022
- 37) Kaczmarek, M. B., Struszczyk-Swita, K., Li, X., Szczęsna-Antczak, M. & Daroch, M. (2019) Enzymatic modifications of chitin, chitosan, and chitooligosaccharides, *Frontiers in Bioengineering and Biotechnology*. **7**, 243. https://doi.org/10.3389/fbioe.2019.00243
- 38) Kobayashi, H., Suzuki, Y., Sagawa, T., Saito, M. & Fukuoka, A. (2023) Selective Synthesis of Oligosaccharides by Mechanochemical Hydrolysis of Chitin over a

- Carbon-Based Catalyst, *Angewandte Chemie*. **135**, e202214229. <a href="https://doi.org/10.1002/ange.202214229">https://doi.org/10.1002/ange.202214229</a>
- 39) Kuisiene, N., Raugalas, J., Spröer, C., Kroppenstedt, R., Stuknyte, M. & Chitavichius, D. (2008) *Paenibacillus tylopili* sp. nov., a chitinolytic bacterium isolated from the mycorhizosphere of *Tylopilus felleus*, *Folia Microbiologica*. **53**, 433-437. https://doi.org/10.1007/s12223-008-0066-2
- 40) Kumar, M., Rajput, M., Soni, T., Vivekanand, V. & Pareek, N. (2020) Chemoenzymatic production and engineering of chitooligosaccharides and *N*-acetyl glucosamine for refining biological activities, *Frontiers in Chemistry*. **8**, 469. https://doi.org/10.3389/fchem.2020.00469
- 41) Kumar, A., Kumar, D., George, N., Sharma, P. & Gupta, N. (2018) A process for complete biodegradation of shrimp waste by a novel marine isolate *Paenibacillus* sp. AD with simultaneous production of chitinase and chitin oligosaccharides, *International Journal of Biological Macromolecules*. **109**, 263-272. <a href="https://doi.org/10.1016/j.ijbiomac.2017.12.024">https://doi.org/10.1016/j.ijbiomac.2017.12.024</a>
- 42) Li, J., Wang, D., Chang, S.-C., Liang, P.-H., Srivastava, V., Guu, S.-Y., Shie, J.-J., Khoo, K.-H., Bulone, V. & Hsieh, Y. S. (2021) Production of structurally defined chitooligosaccharides with a single *n*-acetylation at their reducing end using a newly discovered chitinase from *Paenibacillus pabuli*, *Journal of Agricultural and Food Chemistry*. 69, 3371-3379. https://doi.org/10.1021/acs.jafc.0c06804
- 43) Li, W., O'Neill, K. R., Haft, D. H., DiCuccio, M., Chetvernin, V., Badretdin, A., Coulouris, G., Chitsaz, F., Derbyshire, M. K. & Durkin, A. S. (2021) RefSeq: expanding the Prokaryotic Genome Annotation Pipeline reach with protein family model curation, *Nucleic Acids Research*. **49**, D1020-D1028. <a href="https://doi.org/10.1093/nar/gkaa1105">https://doi.org/10.1093/nar/gkaa1105</a>
- 44) Li, H. & Greene, L. H. (2010) Sequence and structural analysis of the chitinase insertion domain reveals two conserved motifs involved in chitin-binding, *Plos One*. **5**, e8654. <a href="https://doi.org/10.1371/journal.pone.0008654">https://doi.org/10.1371/journal.pone.0008654</a>
- 45) Liao, W., Liu, P., Liao, W. & Miao, L. (2019) Complete genome of the chitin-degrading bacterium, *Paenibacillus xylanilyticus* W4, *Genome Biology and Evolution*. **11**, 3252-3255. https://doi.org/10.1093/gbe/evz241
- 46) Liu, Y., Sun, G., Liu, J., Lou, Y., Zhu, J. & Wang, C. (2024) Enzymatic production of diverse *N*-acetyl chitooligosaccharides employing a novel bifunctional chitinase and its engineered variants, *Food Chemistry*. **453**, 139675. <a href="https://doi.org/10.1016/j.foodchem.2024.139675">https://doi.org/10.1016/j.foodchem.2024.139675</a>
- 47) Liu, Y., Qin, Z., Wang, C. & Jiang, Z. (2023) *N*-acetyl-*d*-glucosamine-based oligosaccharides from chitin: Enzymatic production, characterization and biological activities, *Carbohydrate Polymers*. 121019. <a href="https://doi.org/10.1016/j.carbpol.2023.121019">https://doi.org/10.1016/j.carbpol.2023.121019</a>
- 48) Liu, C., Shen, N., Wu, J., Jiang, M., Shi, S., Wang, J., Wei, Y. & Yang, L. (2020) Cloning, expression and characterization of a chitinase from *Paenibacillus chitinolyticus* strain UMBR 0002, *PeerJ.* **8**, e8964. <a href="https://doi.org/10.7717/peerj.8964">https://doi.org/10.7717/peerj.8964</a>
- 49) Liu, Y., Jiang, Z., Ma, J., Ma, S., Yan, Q. & Yang, S. (2020) Biochemical characterization and structural analysis of a β-N-acetylglucosaminidase from *Paenibacillus barengoltzii* for efficient production of N-acetyl-d-glucosamine, *Journal of Agricultural and Food Chemistry*. 68, 5648-5657. <a href="https://doi.org/10.1021/acs.jafc.9b08085">https://doi.org/10.1021/acs.jafc.9b08085</a>
- 50) Lorentzen, S. B., Arntzen, M. Ø., Hahn, T., Tuveng, T. R., Sørlie, M., Zibek, S., Vaaje-Kolstad, G. & Eijsink, V. G. (2021) Genomic and proteomic study of *Andreprevotia*

- *ripae* isolated from an anthill reveals an extensive repertoire of chitinolytic enzymes, *Journal of Proteome Research*. **20**, 4041-4052. <a href="https://doi.org/10.1021/acs.jproteome.1c00358">https://doi.org/10.1021/acs.jproteome.1c00358</a>
- 51) Madhuprakash, J., El Gueddari, N.E., Moerschbacher, B.M. & Podile, A.R. (2015) Catalytic efficiency of chitinase-D on insoluble chitinous substrates was improved by fusing auxiliary domains, *PLoS One*. **10**, e0116823. https://doi.org/10.1371/journal.pone.0116823
- 52) Madhuprakash, J., Tanneeru, K., Purushotham, P., Guruprasad, L. & Podile, A. R. (2012) Transglycosylation by chitinase D from *Serratia proteamaculans* improved through altered substrate interactions, *Journal of Biological Chemistry*. **287**, 44619-44627. https://doi.org/10.1074/jbc.M112.400879
- 53) Mallakuntla, M. K., Vaikuntapu, P. R., Bhuvanachandra, B., Das, S. N. & Podile, A. R. (2017) Transglycosylation by a chitinase from *Enterobacter cloacae* subsp. *cloacae* generates longer chitin oligosaccharides, *Scientific Reports*. **7**, 5113. <a href="https://doi.org/10.1038/s41598-017-05140-3">https://doi.org/10.1038/s41598-017-05140-3</a>
- 54) Martin, M. (2011) Cutadapt removes adapter sequences from high-throughput sequencing reads, *EMBnet Journal*. **17**, 10-12. <a href="https://doi.org/10.14806/ej.17.1.200">https://doi.org/10.14806/ej.17.1.200</a>
- 55) Margoutidis, G., Parsons, V. H., Bottaro, C. S., Yan, N. & Kerton, F. M. (2018) Mechanochemical amorphization of α-chitin and conversion into oligomers of *N*-acetyl-*d*-glucosamine, *ACS Sustainable Chemistry & Engineering*. **6**, 1662-1669. <a href="https://doi.org/10.1021/acssuschemeng.7b02870">https://doi.org/10.1021/acssuschemeng.7b02870</a>
- 56) Masuda, S., Azuma, K., Kurozumi, S., Kiyose, M., Osaki, T., Tsuka, T., Itoh, N., Imagawa, T., Minami, S. & Sato, K. (2014) Anti-tumor properties of orally administered glucosamine and *N*-acetyl-*D*-glucosamine oligomers in a mouse model, *Carbohydrate Polymers.* **111**, 783-787. <a href="https://doi.org/10.1016/j.carbpol.2014.04.102">https://doi.org/10.1016/j.carbpol.2014.04.102</a>
- 57) Matsumoto, T., Nonaka, T., Hashimoto, M., Watanabe, T. & Mitsui, Y. (1999) Three-dimensional structure of the catalytic domain of chitinase Al from *Bacillus circulars* WL-12 at a very high resolution, *Proceedings of the Japan Academy, Series B.* **75**, 269-274. <a href="https://doi.org/10.2183/pjab.75.269">https://doi.org/10.2183/pjab.75.269</a>
- 58) McLean, J. S., Lombardo, M.-J., Badger, J. H., Edlund, A., Novotny, M., Yee-Greenbaum, J., Vyahhi, N., Hall, A. P., Yang, Y. & Dupont, C. L. (2013) Candidate phylum TM6 genome recovered from a hospital sink biofilm provides genomic insights into this uncultivated phylum, *Proceedings of the National Academy of Sciences*. **110**, E2390-E2399. <a href="https://doi.org/10.1073/pnas.1219809110">https://doi.org/10.1073/pnas.1219809110</a>
- 59) Meier-Kolthoff, J. P., Auch, A. F., Klenk, H.-P. & Göker, M. (2013) Genome sequence-based species delimitation with confidence intervals and improved distance functions, *BMC Bioinformatics*. **14**, 1-14. https://doi.org/10.1186/1471-2105-14-60
- 60) Metsalu, T. & Vilo, J. (2015) ClustVis: a web tool for visualizing clustering of multivariate data using Principal Component Analysis and heatmap, *Nucleic Acids Research*. **43**, W566-W570. <a href="https://doi.org/10.1093/nar/gkv468">https://doi.org/10.1093/nar/gkv468</a>
- 61) Mukherjee, S., Sarma, S. S., Rao, T. N. & Madhuprakash, J. (2024) The first evidence of cryo-milling improving enzymatic production of chitooligosaccharides from chitin biomass, *ChemRxiv*. <a href="https://doi.org/10.26434/chemrxiv-2024-q2g1v">https://doi.org/10.26434/chemrxiv-2024-q2g1v</a> (Pre-print).
- 62) Mukherjee, S., Lodha, T. D. & Madhuprakash, J. (2023) Comprehensive Genome Analysis of Cellulose and Xylan-Active CAZymes from the Genus *Paenibacillus*: Special Emphasis on the Novel Xylanolytic *Paenibacillus* sp. LS1, *Microbiology Spectrum*. 11, e05028-22. <a href="https://doi.org/10.1128/spectrum.05028-22">https://doi.org/10.1128/spectrum.05028-22</a>
- 63) Mukherjee, S., Behera, P. K. & Madhuprakash, J. (2020) Efficient conversion of crystalline chitin to *N*-acetylglucosamine and *N*, *N*'-diacetylchitobiose by the enzyme

- cocktail produced by *Paenibacillus* sp. LS1, *Carbohydrate Polymers*. **250**, 116889. https://doi.org/10.1016/j.carbpol.2020.116889
- 64) Nakagawa, Y. S., Eijsink, V. G., Totani, K. & Vaaje-Kolstad, G. (2013) Conversion of α-chitin substrates with varying particle size and crystallinity reveals substrate preferences of the chitinases and lytic polysaccharide monooxygenase of *Serratia marcescens*, *Journal of Agricultural & Food Chemistry*. **61**, 11061-11066. https://doi.org/10.1021/jf402743e
- 65) Osada, M., Miura, C., Nakagawa, Y. S., Kaihara, M., Nikaido, M. & Totani, K. (2013) Effects of supercritical water and mechanochemical grinding treatments on physicochemical properties of chitin, *Carbohydrate Polymers*. **92**, 1573-1578. <a href="https://doi.org/10.1016/j.carbpol.2012.10.068">https://doi.org/10.1016/j.carbpol.2012.10.068</a>
- 66) Overbeek, R., Olson, R., Pusch, G. D., Olsen, G. J., Davis, J. J., Disz, T., Edwards, R. A., Gerdes, S., Parrello, B. & Shukla, M. (2014) The SEED and the Rapid Annotation of microbial genomes using Subsystems Technology (RAST), *Nucleic Acids Research*. **42**, D206-D214. https://doi.org/10.1093/nar/gkt1226
- 67) Oyeleye, A. & Normi, Y. M. (2018) Chitinase: diversity, limitations, and trends in engineering for suitable applications, *Bioscience Reports*. **38**, BSR2018032300. https://doi.org/10.1042/BSR20180323
- 68) Pang, Z., Chong, J., Zhou, G., de Lima Morais, D. A., Chang, L., Barrette, M., Gauthier, C., Jacques, P.-É., Li, S. & Xia, J. (2021) MetaboAnalyst 5.0: narrowing the gap between raw spectra and functional insights, *Nucleic Acids Research*. **49**, W388-W396. https://doi.org/10.1093/nar/gkab382
- 69) Parks, D. H., Imelfort, M., Skennerton, C. T., Hugenholtz, P. & Tyson, G. W. (2015) CheckM: assessing the quality of microbial genomes recovered from isolates, single cells, and metagenomes, *Genome Research*. **25**, 1043-1055. <a href="https://doi.org/10.1101/gr.186072.114">https://doi.org/10.1101/gr.186072.114</a>
- 70) Pohling, J., Hawboldt, K. & Dave, D. (2022) Comprehensive review on pre-treatment of native, crystalline chitin using non-toxic and mechanical processes in preparation for biomaterial applications, *Green Chemistry*. **24**, 6790-6809. <a href="https://doi.org/10.1039/D2GC01968J">https://doi.org/10.1039/D2GC01968J</a>
- 71) Poshina, D. N., Raik, S. V., Poshin, A. N. & Skorik, Y. A. (2018) Accessibility of chitin and chitosan in enzymatic hydrolysis: A review, *Polymer Degradation and Stability*. **156**, 269-278. https://doi.org/10.1016/j.polymdegradstab.2018.09.005
- 72) Purushotham, P. & Podile, A. R. (2012) Synthesis of long-chain chitooligosaccharides by a hypertransglycosylating processive endochitinase of *Serratia proteamaculans* 568, *Journal of Bacteriology*. **194**, 4260-4271. https://doi.org/10.1128/jb.06473-11
- 73) Purushotham, P., Sarma, P. & Podile, A. R. (2012) Multiple chitinases of an endophytic *Serratia proteamaculans* 568 generate chitin oligomers, *Bioresource Technology*. **112**, 261-269. <a href="https://doi.org/10.1016/j.biortech.2012.02.062">https://doi.org/10.1016/j.biortech.2012.02.062</a>
- 74) Rani, T.S., Madhuprakash, J. & Podile, A.R. (2020) Chitinase-E from *Chitiniphilus shinanonensis* generates chitobiose from chitin flakes, *International Journal of Biological Macromolecules*. **163**, 1037-1043. <a href="https://doi.org/10.1016/j.ijbiomac.2020.07.052">https://doi.org/10.1016/j.ijbiomac.2020.07.052</a>
- 75) Rinaudo, M. (2006) Chitin and chitosan: Properties and applications, *Progress in Polymer Science*. **31**, 603-632. <a href="https://doi.org/10.1016/j.progpolymsci.2006.06.001">https://doi.org/10.1016/j.progpolymsci.2006.06.001</a>
- 76) Schmitz, C., González Auza, L., Koberidze, D., Rasche, S., Fischer, R. & Bortesi, L. (2019) Conversion of chitin to defined chitosan oligomers: current status and future prospects, *Marine Drugs*. **17**, 452. <a href="https://doi.org/10.3390/md17080452">https://doi.org/10.3390/md17080452</a>
- 77) Sivaramakrishna, D., Bhuvanachandra, B., Mallakuntla, M. K., Das, S. N., Ramakrishna, B. & Podile, A. R. (2020) Pretreatment with KOH and KOH-urea

- enhanced hydrolysis of α-chitin by an endo-chitinase from *Enterobacter cloacae* subsp. *cloacae*, *Carbohydrate Polymers*. **235**, 115952. https://doi.org/10.1016/j.carbpol.2020.115952
- 78) Shamshina, J. L., Stein, R. S. & Abidi, N. (2021) Choosing the right strategy: cryogrinding vs. ball milling–comparing apples to apples, *Green Chemistry*. **23**, 9646-9657. <a href="https://doi.org/10.1039/D1GC03128G">https://doi.org/10.1039/D1GC03128G</a>
- 79) Shamshina, J. L. & Berton, P. (2020) Use of ionic liquids in chitin biorefinery: a systematic review, *Frontiers in Bioengineering and Biotechnology*. **8**, 11. https://doi.org/10.3389/fbioe.2020.00011
- 80) Song, Y.-S., Seo, D.-J., Ju, W.-T., Lee, Y.-S. & Jung, W.-J. (2015) Enzymatic properties of chitinase-producing antagonistic bacterium *Paenibacillus chitinolyticus* with various substrates, *Microbial Pathogenesis*. **89**, 195-200. https://doi.org/10.1016/j.micpath.2015.10.025
- 81) Song, Y.-S., Seo, D.-J., Kim, K.-Y., Park, R.-D. & Jung, W.-J. (2012) Expression patterns of chitinase produced from *Paenibacillus chitinolyticus* with different two culture media, *Carbohydrate Polymers*. **90**, 1187-1192. https://doi.org/10.1016/j.carbpol.2012.06.016
- 82) Suma, K. & Podile, A. R. (2013) Chitinase A from *Stenotrophomonas maltophilia* shows transglycosylation and antifungal activities, *Bioresource Technology*. **133**, 213-220. <a href="https://doi.org/10.1016/j.biortech.2013.01.103">https://doi.org/10.1016/j.biortech.2013.01.103</a>
- 83) Synstad, B., Gåseidnes, S., Van Aalten, D. M., Vriend, G., Nielsen, J. E. & Eijsink, V. G. (2004) Mutational and computational analysis of the role of conserved residues in the active site of a family 18 chitinase, *European Journal of Biochemistry*. **271**, 253-262. https://doi.org/10.1046/j.1432-1033.2003.03923.x
- 84) Tran, D. M., Pham, P. T. & Vu, B. T. (2024) Data on annotation and analysis of genome sequence of *Paenibacillus elgii* YSY-1.2, a promising chitinase-producing, plant-growth-promoting, and biocontrol agent, *Data in Brief.* **54**, 110285. https://doi.org/10.1016/j.dib.2024.110285
- 85) Trudel, J. & Asselin, A. (1989) Detection of chitinase activity after polyacrylamide gel electrophoresis, *Analytical Biochemistry*. **178**, 362-366. <a href="https://doi.org/10.1016/0003-2697(89)90653-2">https://doi.org/10.1016/0003-2697(89)90653-2</a>
- 86) Tuveng, T. R., Arntzen, M. Ø., Bengtsson, O., Gardner, J. G., Vaaje-Kolstad, G. & Eijsink, V. G. (2016) Proteomic investigation of the secretome of *Cellvibrio japonicus* during growth on chitin, *Proteomics*. **16**, 1904-1914. <a href="https://doi.org/10.1002/pmic.201500419">https://doi.org/10.1002/pmic.201500419</a>
- 87) Urs, M. J., Moerschbacher, B. M. & Cord-Landwehr, S. (2023) Quantitative enzymatic-mass spectrometric analysis of the chitinous polymers in fungal cell walls, *Carbohydrate Polymers*. **301**, 120304. <a href="https://doi.org/10.1016/j.carbpol.2022.120304">https://doi.org/10.1016/j.carbpol.2022.120304</a>
- 88) Üstok, F. I., Chirgadze, D. Y. & Christie, G. (2015) Structural and functional analysis of SleL, a peptidoglycan lysin involved in germination of *Bacillus* spores, *Proteins: Structure, Function, and Bioinformatics.* 83, 1787-1799. https://doi.org/10.1002/prot.24861
- 89) Vaaje-Kolstad, G., Horn, S. J., Sørlie, M. & Eijsink, V. G. (2013) The chitinolytic machinery of *Serratia marcescens* a model system for enzymatic degradation of recalcitrant polysaccharides, *The FEBS Journal.* **280**, 3028-3049. <a href="https://doi.org/10.1111/febs.12181">https://doi.org/10.1111/febs.12181</a>
- 90) Vaikuntapu, P. R., Rambabu, S., Madhuprakash, J. & Podile, A. R. (2016) A new chitinase-D from a plant growth promoting *Serratia marcescens* GPS5 for enzymatic conversion of chitin, *Bioresource Technology*. **220**, 200-207. https://doi.org/10.1016/j.biortech.2016.08.055

- 91) Watanabe, T., Ariga, Y., Sato, U., Toratani, T., Hashimoto, M., Nikaidou, N., Kezuka, Y., Nonaka, T. & Sugiyama, J. (2003) Aromatic residues within the substrate-binding cleft of *Bacillus circulans* chitinase A1 are essential for hydrolysis of crystalline chitin, *Biochemical Journal*. **376**, 237-244. https://doi.org/10.1042/bj20030419
- 92) Watanabe, T., Oyanagi, W., Suzuki, K. & Tanaka, H. (1990) Chitinase system of *Bacillus circulans* WL-12 and importance of chitinase A1 in chitin degradation, *Journal of Bacteriology*. **172**, 4017-4022. <a href="https://doi.org/10.1128/jb.172.7.4017-4022.1990">https://doi.org/10.1128/jb.172.7.4017-4022.1990</a>
- 93) Wattam, A. R., Abraham, D., Dalay, O., Disz, T. L., Driscoll, T., Gabbard, J. L., Gillespie, J. J., Gough, R., Hix, D. & Kenyon, R. (2014) PATRIC, the bacterial bioinformatics database and analysis resource, *Nucleic Acids Research*. **42**, D581-D591. https://doi.org/10.1093/nar/gkt1099
- 94) Wick, R. R., Judd, L. M., Gorrie, C. L. & Holt, K. E. (2017) Unicycler: resolving bacterial genome assemblies from short and long sequencing reads, *PLoS Computational Biology*. **13**, e1005595. <a href="https://doi.org/10.1371/journal.pcbi.1005595">https://doi.org/10.1371/journal.pcbi.1005595</a>
- 95) Wu, X., Wang, J., Shi, Y., Chen, S., Yan, Q., Jiang, Z. & Jing, H. (2017) *N*-Acetylchitobiose ameliorates metabolism dysfunction through Erk/p38 MAPK and histone H3 phosphorylation in type 2 diabetes mice, *Journal of Functional Foods*. **28**, 96-105. https://doi.org/10.1016/j.jff.2016.11.012
- 96) Xu, P., Wu, X.-L., Guo, X.-X., Tang, J., Zong, M.-H. & Lou, W.-Y. (2018) Double-chitinase hydrolysis of crab shell chitin pretreated by ionic liquid to generate chitooligosaccharide, *ACS Sustainable Chemistry & Engineering*. 7, 1683-1691. https://doi.org/10.1021/acssuschemeng.8b05447
- 97) Yan, N. & Chen, X. (2015) Sustainability: Don't waste seafood waste, *Nature*. **524**, 155-157. <a href="https://doi.org/10.1038/524155a">https://doi.org/10.1038/524155a</a>
- 98) Yang, S., Fu, X., Yan, Q., Guo, Y., Liu, Z. & Jiang, Z. (2016) Cloning, expression, purification and application of a novel chitinase from a thermophilic marine bacterium *Paenibacillus barengoltzii*, *Food Chemistry*. **192**, 1041-1048. <a href="https://doi.org/10.1016/j.foodchem.2015.07.092">https://doi.org/10.1016/j.foodchem.2015.07.092</a>
- 99) Yoon, S.-H., Ha, S.-m., Lim, J., Kwon, S. & Chun, J. (2017) A large-scale evaluation of algorithms to calculate average nucleotide identity, *Antonie Van Leeuwenhoek*. **110**, 1281-1286. https://doi.org/10.1007/s10482-017-0844-4
- 100) Zhang, A., Wang, C., Chen, J., Wei, G., Zhou, N., Li, G., Chen, K. & Ouyang, P. (2021) Efficient enzymatic hydrolysis of chitin into *N*-acetyl glucosamine using alkali as a recyclable pretreatment reagent, *Green Chemistry*. 23, 3081-3089. <a href="https://doi.org/10.1039/D1GC00818H">https://doi.org/10.1039/D1GC00818H</a>
- Thang, W., Ma, J., Yan, Q., Jiang, Z. & Yang, S. (2021) Biochemical characterization of a novel acidic chitinase with antifungal activity from *Paenibacillus xylanexedens* Z2–4, *International Journal of Biological Macromolecules*. **182**, 1528-1536. <a href="https://doi.org/10.1016/j.ijbiomac.2021.05.111">https://doi.org/10.1016/j.ijbiomac.2021.05.111</a>
- Theng, J., Ge, Q., Yan, Y., Zhang, X., Huang, L. & Yin, Y. (2023) dbCAN3: automated carbohydrate-active enzyme and substrate annotation, *Nucleic Acids Research*. **51**, W115-W121. <a href="https://doi.org/10.1093/nar/gkad328">https://doi.org/10.1093/nar/gkad328</a>

1	The first evidence of cryo-milling improving enzymatic production of
2	chitooligosaccharides from chitin biomass
3 4	Saumashish Mukherjee <sup>1</sup> , Sreedhara Sudhakara Sarma <sup>2</sup> , Tata Narsinga Rao <sup>2</sup> and Jogi Madhuprakash <sup>1</sup> *
5	<sup>1</sup> Department of Plant Sciences, School of Life Sciences, University of Hyderabad,
6	Gachibowli, Hyderabad, India.
7	<sup>2</sup> International Advanced Research Centre for Powder Metallurgy and New Materials (ARCI),
8	Balapur, Hyderabad, India.
9	
10	
11	
12	
13	
14	
15	
16	
17	
18	
19	
20	
21	
22	
23	
24	
25	*
26 27 28 29 30 31 32 33 34 35	*Author for correspondence:  Dr. Jogi Madhuprakash  Department of Plant Sciences  School of Life Sciences  University of Hyderabad  Prof. CR Rao Road, Gachibowli,  Hyderabad-500046, India  Tel: +91-40-23134566  Fax: +91-40-23010120  E-mail: jmpsl@uohyd.ac.in



∂ | Host-Microbial Interactions | Full-Length Text

### The *Ustilago maydis* AA10 LPMO is active on fungal cell wall chitin

Roseline Assiah Yao,<sup>1</sup> Jean-Lou Reyre,<sup>1,2</sup> Ketty C. Tamburrini,<sup>1,3</sup> Mireille Haon,<sup>1,4</sup> Olivier Tranquet,<sup>1</sup> Akshay Nalubothula,<sup>5</sup> Saumashish Mukherjee,<sup>5</sup> Sophie Le Gall,<sup>6,7</sup> Sacha Grisel,<sup>1,4</sup> Sonia Longhi,<sup>3</sup> Jogi Madhuprakash,<sup>5</sup> Bastien Bissaro,<sup>1</sup> Jean-Guy Berrin<sup>1,4</sup>

**AUTHOR AFFILIATIONS** See affiliation list on p. 13.

ABSTRACT Lytic polysaccharide monooxygenases (LPMOs) can perform oxidative cleavage of glycosidic bonds in carbohydrate polymers (e.g., cellulose, chitin), making them more accessible to hydrolytic enzymes. While most studies have so far mainly explored the role of LPMOs in a (plant) biomass conversion context, alternative roles and paradigms begin to emerge. The AA10 LPMOs are active on chitin and/or cellulose and mostly found in bacteria and in some viruses and archaea. Interestingly, AA10-encoding genes are also encountered in some pathogenic fungi of the Ustilaginomycetes class, such as *Ustilago maydis*, responsible for corn smut disease. Transcriptomic studies have shown the overexpression of the AA10 gene during the infectious cycle of *U. maydis*. In fact, U. maydis has a unique AA10 gene that codes for a catalytic domain appended with a C-terminal disordered region. To date, there is no public report on fungal AA10 LPMOs. In this study, we successfully produced the catalytic domain of this LPMO (UmAA10\_cd) in Pichia pastoris and carried out its biochemical characterization. Our results show that UmAA10 cd oxidatively cleaves  $\alpha$ - and  $\beta$ -chitin with C1 regionselectivity and boosts chitin hydrolysis by a GH18 chitinase from *U. maydis* (*Um*GH18A). Using a biologically relevant substrate, we show that UmAA10 cd exhibits enzymatic activity on U. maydis fungal cell wall chitin and promotes its hydrolysis by UmGH18A. These results represent an important step toward the understanding of the role of LPMOs in the fungal cell wall remodeling process during the fungal life cycle.

**IMPORTANCE** Lytic polysaccharide monooxygenases (LPMOs) have been mainly studied in a biotechnological context for the efficient degradation of recalcitrant polysaccharides. Only recently, alternative roles and paradigms begin to emerge. In this study, we provide evidence that the AA10 LPMO from the phytopathogen *Ustilago maydis* is active against fungal cell wall chitin. Given that chitin-active LPMOs are commonly found in microbes, it is important to consider fungal cell wall as a potential target for this enigmatic class of enzymes.

**KEYWORDS** filamentous fungi, fungal cell wall, lytic polysaccharide monooxygenase, chitinase, *Ustilago maydis*, plant pathogen, remodeling

Lytic polysaccharide monooxygenases (LPMOs) are monocopper enzymes that catalyze the oxidative cleavage of glycosidic bonds in carbohydrate polymers. Their discovery has been a major breakthrough in the understanding of the microbial enzymatic mechanisms involved in the degradation of natural recalcitrant polymers, including cellulose and chitin (1–3). LPMOs can act at the surface of polysaccharides, in synergy with other oxidoreductases (4) and glycoside hydrolases (GHs), to overcome polymers recalcitrance factors (such as crystallinity), thereby boosting bioconversion yields (5–7). The unique catalytic properties of LPMOs make them of utmost interest for different types of applications, such as the valorization of lignocellulosic biomass for

**Editor** Yvonne Nygård, Chalmers University of Technology, Gothenburg, Sweden

Address correspondence to Bastien Bissaro, bastien.bissaro@inrae.fr, or Jean-Guy Berrin, jean-guy.berrin@inrae.fr.

The authors declare no conflict of interest.

See the funding table on p. 13.

Received 6 April 2023 Accepted 14 July 2023 Published 13 September 2023

Copyright © 2023 Yao et al. This is an open-access article distributed under the terms of the Creative Commons Attribution 4.0 International license.

Downloaded from https://journals.asm.org/journal/aem on 15 September 2023 by 49.37.47.242.





# Comprehensive Genome Analysis of Cellulose and Xylan-Active CAZymes from the Genus *Paenibacillus*: Special Emphasis on the Novel Xylanolytic *Paenibacillus* sp. LS1

Saumashish Mukherjee, Dan Dilipchand Lodha, Dogi Madhuprakash

<sup>a</sup>Department of Plant Sciences, School of Life Sciences, University of Hyderabad, Gachibowli, Hyderabad, India <sup>b</sup>National Centre for Microbial Resource, National Centre for Cell Science, Pune, India

ABSTRACT Xylan is the most abundant hemicellulose in hardwood and graminaceous plants. It is a heteropolysaccharide comprising different moieties appended to the xylose units. Complete degradation of xylan requires an arsenal of xylanolytic enzymes that can remove the substitutions and mediate internal hydrolysis of the xylan backbone. Here, we describe the xylan degradation potential and underlying enzyme machinery of the strain, Paenibacillus sp. LS1. The strain LS1 was able to utilize both beechwood and corncob xylan as the sole source of carbon, with the former being the preferred substrate. Genome analysis revealed an extensive xylan-active CAZyme repertoire capable of mediating efficient degradation of the complex polymer. In addition to this, a putative xylooligosaccharide ABC transporter and homologues of the enzymes involved in the xylose isomerase pathway were identified. Further, we have validated the expression of selected xylan-active CAZymes, transporters, and metabolic enzymes during growth of the LS1 on xylan substrates using qRT-PCR. The genome comparison and genomic index (average nucleotide identity [ANI] and digital DNA-DNA hybridization) values revealed that strain LS1 is a novel species of the genus Paenibacillus. Lastly, comparative genome analysis of 238 genomes revealed the prevalence of xylan-active CAZymes over cellulose across the Paenibacillus genus. Taken together, our results indicate that Paenibacillus sp. LS1 is an efficient degrader of xylan polymers, with potential implications in the production of biofuels and other beneficial by-products from lignocellulosic biomass.

**IMPORTANCE** Xylan is the most abundant hemicellulose in the lignocellulosic (plant) biomass that requires cooperative deconstruction by an arsenal of different xylanolytic enzymes to produce xylose and xylooligosaccharides. Microbial (particularly, bacterial) candidates that encode such enzymes are an asset to the biorefineries to mediate efficient and eco-friendly deconstruction of xylan to generate products of value. Although xylan degradation by a few *Paenibacillus* spp. is reported, a complete genus-wide understanding of the said trait is unavailable till date. Through comparative genome analysis, we showed the prevalence of xylan-active CAZymes across *Paenibacillus* spp., therefore making them an attractive option towards efficient xylan degradation. Additionally, we deciphered the xylan degradation potential of the strain *Paenibacillus* sp. LS1 through genome analysis, expression profiling, and biochemical studies. The ability of *Paenibacillus* sp. LS1 to degrade different xylan types obtained from different plant species, emphasizes its potential implication in lignocellulosic biorefineries.

**KEYWORDS** Paenibacillus spp., xylan, CAZymes, Genome analysis, qRT-PCR

The world is progressing toward natural and renewable resources for generation of energy (as fuels) and chemicals, with the goal of securing a sustainable carbon bioeconomy for the future (1). Potential resources mainly include nonedible biomass,

**Editor** Montarop Yamabhai, Suranaree University of Technology

**Copyright** © 2023 Mukherjee et al. This is an open-access article distributed under the terms of the Creative Commons Attribution 4.0 International license.

Address correspondence to Jogi Madhuprakash, jmpsl@uohyd.ac.in.

The authors declare no conflict of interest.

**Received** 6 December 2022 **Accepted** 24 March 2023

### **Green Chemistry**



**PAPER** 

View Article Online



**Cite this:** *Green Chem.*, 2023, **25**, 6832

# Improving the efficiency and sustainability of chitin bioconversion through a combination of *Streptomyces* chitin-active-secretomes and mechanical-milling†

Lal Duhsaki, Saumashish Mukherjee D and Jogi Madhuprakash D\*

Chitin, particularly  $\alpha$ -chitin, is the most abundant and highly recalcitrant form, fortified by an intricate network of hydrogen bonds. Efficient valorization of α-chitin requires mild pre-treatment and enzymatic hydrolysis. Streptomyces spp. secrete chitin-active CAZymes that can efficiently tackle the recalcitrant problem of chitin biomass. To better understand the potential of Streptomyces spp., a comparative analysis was performed between the novel isolate, Streptomyces sp. UH6 and the well-known chitin degraders, S. coelicolor and S. griseus. Growth studies and FE-SEM analysis revealed that all three Streptomyces spp. could utilize and degrade both  $\alpha$ - and  $\beta$ -chitin. Zymogram analysis showed expression of 5–7 chitinases in the secretomes of Streptomyces strains. The chitin-active-secretomes produced by Streptomyces sp. UH6 and S. griseus were optimally active at acidic pH (pH 4.0 and 5.0) and 50 °C. Timecourse degradation of  $\alpha$ - and  $\beta$ -chitin with the secretomes generated N-acetyl-D-glucosamine (GlcNAc) and N,N-diacetylchitobiose [(GlcNAc)2] as the predominant products. Further, the highly crystalline α-chitin was subjected to pre-treatment by ball-milling, which reduced the crystallinity from 88% to 56.6% and increased the BET surface area by 3-folds. Of note, the activity of all three Streptomyces secretomes was improved by a mild pre-treatment, while Streptomyces sp. UH6 secretome displayed improved GlcNAc and (GlcNAc)<sub>2</sub> yields by 14.4 and 9.6-folds, respectively. Overall, our results suggest that the Streptomyces chitin-active-secretomes, particularly Streptomyces sp. UH6, can be deployed for efficient valorization of chitin biomass and to establish an economically feasible and eco-friendly process for valorizing highly recalcitrant  $\alpha$ -chitin.

Received 3rd April 2023, Accepted 7th August 2023 DOI: 10.1039/d3gc01084h

rsc.li/greenchem

### 1. Introduction

Chitin is a naturally occurring homopolymer consisting of N-acetyl-p-glucosamine (GlcNAc) monomers linked together by  $\beta$ -1,4-glycosidic bonds. It is the second most abundant biopolymer found in nature, surpassed only by cellulose. Chitin plays a crucial structural role in the exoskeleton of arthropods and crustaceans, as well as in the cell wall of fungi. Chitin biomass can be processed through mechanical, chemical or biological means (via microbes or enzymes) to produce chitooligosaccharides (CHOS). CHOS are highly sought-after commercially due to their biodegradable, biocompatible, and nontoxic properties. The monosaccharide GlcNAc and disaccharide, N,N-diacetylchitobiose [(GlcNAc)<sub>2</sub>] are particularly impor-

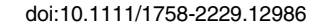
Department of Plant Sciences, School of Life Sciences, University of Hyderabad, Gachibowli, Hyderabad-500046, Telangana, India. E-mail: jmpsl@uohyd.ac.in; Fax: +91-40-23010120

† Electronic supplementary information (ESI) available. See DOI: https://doi.org/10.1039/d3gc01084h

tant among CHOS, owing to their diverse biological applications. GlcNAc is widely used in medicine for its anti-bacterial, anti-oxidant, and anti-tumor properties, and as a clinical drug for rheumatism and rheumatoid arthritis.<sup>3</sup> It can also promote the synthesis of synovial fluid and increase skin hyaluronic acid content.<sup>3</sup> Further, it is also used as food additive and for seed treatments and foliar applications in agriculture.<sup>3</sup> Of note, GlcNAc is also used in the production of various valuable nitrogen-containing chemicals.<sup>3</sup> (GlcNAc)<sub>2</sub> or chitobiose, on the other hand, has been shown to have implications in medicine and therapeutics, such as protection against acute hepatotoxicity induced by CCl<sub>4</sub>,<sup>5</sup> high anti-oxidant and DNA protection activities,<sup>6</sup> amelioration of metabolic dysfunction in type 2 diabetes mice,<sup>7</sup> and alleviation of oleic acid-induced lipid accumulation.<sup>8</sup>

Given the diverse commercial applications of GlcNAc and chitobiose, it is imperative to maximize their production through efficient and sustainable chitin valorization approaches. Apart from CHOS production, the production of advanced materials from chitin has also seen enormous pro-

Environmental Microbiology Reports (2022) 14(3), 431-442





# Genome analysis of *Streptomyces* sp. UH6 revealed the presence of potential chitinolytic machinery crucial for chitosan production

Lal Duhsaki,<sup>1†</sup> Saumashish Mukherjee,<sup>1†</sup> Tirupaati Swaroopa Rani<sup>2</sup> and Jogi Madhuprakash <sup>1</sup>

<sup>1</sup>Department of Plant Sciences, School of Life Sciences, University of Hyderabad, Gachibowli, Hyderabad, Telangana, India.

### **Summary**

Chitosan and its derivatives have numerous applications in wastewater treatment as bio-coagulants, flocculants and bio-adsorbents against both particulate and dissolved pollutants. Chitinolytic bacteria secrete an array of enzymes, which play crucial role in chitin to chitosan conversion. Consequently, there is a growing demand for identification and characterization of novel bacterial isolates with potential implications in chitosan production. We describe genomic features of the new isolate Streptomyces sp. UH6. Analysis of the 6.51 Mb genome revealed the GC content as 71.95% and presence of 6990 coding sequences of which 63% were functionally annotated. Further, we identified two possible chitin-utilization pathways, which employ secreted enzymes like lytic polysaccharide monooxygenases and family-18 glycoside hydrolases (GHs). More importantly, the genome has six family-4 polysaccharide deacetylases with probable role in chitin to chitosan conversion, as well as two chitosanases belonging to GH46 and GH75 families. In addition, the gene clusters, dasABC and ngcEFG coding for transporters, which mediate the uptake of N,N'-diacetylchitobiose and N-acetyl-p-glucosamine were identified. Several genes responsible for hydrolysis of other polysaccharides and fermentation of sugars were also

Received 26 November, 2020; accepted 20 June, 2021. \*For correspondence. E-mail madhuprakash25@gmail.com; Tel. (+91) 40 23134566; Fax (+91) 40 23010120.  $^{\dagger}$ These authors contributed equally to this work.

identified. Taken together, the phylogenetic and genomic analyses suggest that the isolate *Streptomy*ces sp. UH6 secretes potential chitin-active enzymes responsible for chitin to chitosan conversion.

#### Introduction

In the recent times, the demand for seafood has been increasing to meet the food requirements of the ever growing population. Consequently, there has been a rapid growth in the seafood processing industries, which in turn generate huge quantities of shell waste. Close to 70% of the total weight of crustaceans like crabs, shrimps, lobsters and prawns is discarded as shell waste (Hamed et al., 2016). Most of this waste is either burned or dumped in the coastal regions causing water pollution. The chitin-rich crustacean shell waste could instead serve as raw material for chitin production. The development of effective processing protocols will help mitigate the water pollution caused due to improper management of by-products from seafood industries. Approximately, 10 000 tons of chitin waste is being generated every year, which could be transformed into products-of-value (Hamed et al., 2016).

Chitin is an insoluble homopolymer of  $\beta$ -(1, 4) linked Nacetyl-D-glucosamine units. It exists in two polymorphic forms,  $\alpha$ -chitin and  $\beta$ -chitin with the former being the most abundant and crystalline due to anti-parallel arrangement of the polymeric chains (Rinaudo, 2006). Due to its biodegradability, biocompatibility, antimicrobial activity, and non-toxicity, there is a strong growing commercial interest in chitin and chitin-based products, such as the watersoluble chitin variant chitosan, a heteropolymer of N-acetyl-glucosamine and glucosamine and chito-oligosaccharides. Major applications include use in medicine, agriculture and cosmetics (Madhuprakash et al., 2014, 2015; Liagat and Eltem, 2018; Mukherjee et al., 2020; Rani et al., 2020a, 2020b). Chitin and chitosan derivatives were also employed as biosorbents for removal of various metal ions, radionuclides, dyes and phenols from wastewaters due to the high proportion of amino and

<sup>&</sup>lt;sup>2</sup>School of Chemistry, University of Hyderabad, Gachibowli, Hyderabad, Telangana, India.

\$ SUPER

Contents lists available at ScienceDirect

### Carbohydrate Polymers

journal homepage: www.elsevier.com/locate/carbpol





## Efficient conversion of crystalline chitin to N-acetylglucosamine and N, N'-diacetylchitobiose by the enzyme cocktail produced by Paenibacillus sp. LS1

Saumashish Mukherjee, Prashanta Kumar Behera, Jogi Madhuprakash\*

Department of Plant Sciences, School of Life Sciences, University of Hyderabad, Gachibowli, Hyderabad, India

ARTICLE INFO

Keywords:
Chitin
Enzyme-cocktail
Hydrolysis
N-acetylglucosamine
Chitobiose

#### ABSTRACT

Direct conversion of crystalline chitin to N-acetylglucosamine and the related chitooligomers through enzymatic approaches is gaining importance owing to their various biological applications. Here we report the crystalline chitin degradation ability of chitinolytic cocktail produced by the isolate Paenibacillus sp. LS1. Growth studies of the isolate in presence of different chitin substrates revealed preference for  $\beta$ -chitin and colloidal chitin. FE-SEM micrographs showed formation of visible perforations on the crystalline chitin particles by the isolate. Further, zymogram analysis revealed the presence of six potential chitinase isozymes. The enzyme-cocktail produced by the isolate was optimally active at 50 °C in 50 mM sodium acetate, pH-4.0. Time-course hydrolysis of crystalline  $\alpha$ - and  $\beta$ -chitin with the Paenibacillus sp. LS1 enzyme-cocktail produced N-acetylglucosamine and N,N'-diacetylchitobiose as the predominant products. Taken together, our results confirm that the Paenibacillus sp. LS1 enzyme-cocktail would have potential application in eco-friendly enzymatic approaches for efficient saccharification of crystalline chitin.

#### 1. Introduction

Chitin is a linear, insoluble homopolymer made up of  $\beta$ -(1 $\rightarrow$ 4)-linked N-acetylglucosamine (GlcNAc) units. It is the second most abundant polysaccharide in nature next to cellulose and forms the structural backbone of fungal cell walls, exoskeleton of insects and crustaceans (Rinaudo, 2006). Chitin mainly exists in two crystalline polymorphic forms, namely  $\alpha$ - and  $\beta$ -chitin, wherein the former is the most abundant and highly crystalline form due to the anti-parallel arrangement of polymeric chains (Das et al., 2015; Rinaudo, 2006). Chitooligosaccharides, the degradation products of chitin are easily soluble in aqueous solvents and are gaining much attention due to their non-toxic and biocompatible properties. Chitooligosaccharides have numerous applications in the field of agriculture and medicine (Aam et al., 2010; Das et al., 2015; Madhuprakash, El Gueddari, Moerschbacher, & Podile, 2015). Few of the notable medical applications of chitooligosaccharides include antimicrobial activities (Jeon, Park, & Kim, 2001), antitumor and antifungal activities (Wang et al., 2008), and immuno-enhancing effects (Ngo, Kim, & Kim, 2008). Furthermore, the monomeric unit GlcNAc and N,N'-diacetylchitobiose (GlcNAc)2 are known to have diverse biological applications as cosmetic ingredients (Kim, Ravichandran, Khan, & Kim, 2008), dietary supplements (Bak, Lampe, & Sung, 2014) and osteoarthritis therapeutics (Tamai et al., 2003). (GlcNAc)<sub>2</sub> was also reported to alleviate the oleic acid induced lipid accumulation in HepG2 cells (Li et al., 2018). However, the recalcitrant nature of chitin poses a major limitation for the production of GlcNAc and (GlcNAc)<sub>2</sub>

In view of this, valorization of chitin is gaining special interest in the recent past and there are several physicochemical methods available for generation of GlcNAc and (GlcNAc)<sub>2</sub> from chitin (Nakagawa et al., 2011; Osada et al., 2013; Sánchez et al., 2017; Villa-Lerma et al., 2013). But, most of these methods are tedious and typically responsible for accumulation of toxic waste in the environment and are not cost effective. Consequently, search for alternate approaches towards sustainable and eco-friendly methods of chitin degradation is still evolving. Inspite of huge production rates of chitin waste from different sea food industries (around 10,000 tons) (Hamed, Özogul, & Regenstein, 2016), it never accumulates in nature, as it can be hydrolysed by the enzyme cocktails secreted by the chitinolytic microorganisms. This would serve as a potential eco-friendly alternative for depolymerization of chitin and

E-mail address: madhuprakash25@gmail.com (J. Madhuprakash).

<sup>\*</sup> Corresponding author at: Department of Plant Sciences, School of Life Sciences, University of Hyderabad, Prof. CR Rao Road, Gachibowli, Hyderabad 500046, India.

# Understanding the chitinolytic system of Paenibacillus sp. LS1 and advancing chitooligosaccharide bioproduction

by Saumashish Mukherjee

Submission date: 20-Sep-2024 04:24PM (UTC+0530)

Submission ID: 2459904714

File name: Saumashish\_Mukherjee.pdf (5.49M)

Word count: 29709 Character count: 157771 Dr. J. Madhuprakash
Assistant Professor
Dept. of Plant Sciences
School of Life Sciences
University of hyderabad
Hyderabad-500 046, INDIA.

### Understanding the chitinolytic system of Paenibacillus sp. LS1 and advancing chitooligosaccharide bioproduction

ORIGINALITY REPORT

O%

0%

0%

 $\mathbf{O}_{9}$ 

SIMILARITY INDEX INTERNET SOURCES

**PUBLICATIONS** 

STUDENT PAPERS

**PRIMARY SOURCES** 

Lal Duhsaki, Saumashish Mukherjee, Jogi Madhuprakash. "Improving the efficiency and sustainability of chitin bioconversion through a combination of Streptomyces chitin-active-secretomes and mechanical-milling", Green Chemistry, 2023

Publication

Saumashish Mukherjee, Sreedhara Sudhakara Sarma, Tata Narsinga Rao, Jogi Madhuprakash. "The first evidence of cryomilling improving enzymatic production of chitooligosaccharides from chitin biomass", American Chemical Society (ACS), 2024

<1%

www.ncbi.nlm.nih.gov

<1%

Saumashish Mukherjee, Prashanta Kumar Behera, Jogi Madhuprakash. "Efficient conversion of crystalline chitin to Nacetylglucosamine and N,N'-

<1%

Dr. J. Madhuprakash
Assistant Professor
Dept. of Plant Sciences
School of Life Sciences
University of hyderabad
Hyderabad-500 046, INDIA.

### diacetylchitobiose by the enzyme cocktail produced by Paenibacillus sp. LS1", Carbohydrate Polymers, 2020

Publication

edoc.unibas.ch

Internet Source

Exclude quotes

Exclude bibliography On

Exclude matches

< 14 words

Dr. J. Madhuprakash Assistant Professor
Dept. of Plant Sciences
School of Life Sciences
University of hyderabad
Hyderabad-500 046, INDIA.